TYRAMINE SUBSTITUTED-HYALURONAN ENRICHED FASCIA FOR ROTATOR CUFF TENDON REPAIR

by

LIKANG CHIN, MS

Submitted in partial fulfillment of the requirements

For the degree of Doctor of Philosophy

Dissertation Advisor: Kathleen Derwin, PhD

Department of Biomedical Engineering

CASE WESTERN RESERVE UNIVERSITY

January 2011

Print out two copies of this form, as it will accompany your thesis or dissertation. (This notice will not show up on printouts).

CASE WESTERN RESERVE UNIVERSITY

SCHOOL OF GRADUATE STUDIES

We hereby approve the thesis/dissertation of

LiKang Chin

candidate for the Doctor of Philosophy degree *.

(signed) Roger Marchant, PhD
(chair of the committee)

Kathleen Derwin, PhD

Eben Alsberg, PhD

Thomas Bauer, MD, PhD

Vince Hascall, PhD

(date) November 16, 2010

*We also certify that written approval has been obtained for any proprietary material contained therein.

DEDICATION

To Mama and Baba,

for your many sacrifices

… and to Gohgoh, too.

Table of Contents

List of Tables

List of Figures

Acknowledgements

"The trail is the thing, not the end of the trail. Travel too fast and you miss all you are traveling for." –Louis L'Amour

First and foremost, I am indebted to my research advisor Kathleen Derwin, PhD for her mentorship, support, and for the opportunity to train in her laboratory at the Cleveland Clinic. Dr. Derwin expected nothing short of my best, which encouraged me to become a better researcher. I would like to acknowledge the rest of my PhD Guidance and Examination Committee members – Roger Marchant, PhD, Eben Alsberg, PhD, Thomas Bauer, MD, PhD, and Vince Hascall, PhD – for their guidance throughout the PhD process. The scientific expertise of Anthony Calabro, PhD and Joseph Iannotti, MD, PhD helped shape some of the work presented in this dissertation. I am grateful for their mentorship.

Many thanks to the past and present members of the Derwin Laboratory for their camaraderie and support, especially Amit Aurora, MS (my graduate student confidante, who offered many ice cream cones in times of need), Andrew Baker, MS, Prakash Chandrasekaran, PhD, Diane Leigh, MS, Ryan Milks, MS, Sambit Sahoo, MBBS, PhD, and Steve Vilt, BS.

I would like to acknowledge E Rene Rodriguez, MD, Carmela Tan, MD, and Thomas Bauer, MD, PhD for their contributions to the histologic studies; Esteban Walker, PhD for statistical support; Maria Siemionow, MD, PhD and the Microsurgery Laboratory (Michal Molski, MD, Lukasz Krokowicz, MD, and Jen Mule, BS) for the use of their surgical facilities and surgical advice.

I am thankful for many wonderful friends. Several individuals in particular have been extremely supportive during the PhD process: Tonya Caralla, MS, Caren Chang, MS, David Chang, MD, PhD, Maria Gatica, BS, Anny Hsu, MS, Mychi Nguyen, MD, Demin Wen, DEng, and Zhong Wang, PhD.

Most importantly, I would like to thank my family. My motivation and desire to do my best stem from the love and support of my Mom, Dad, and brother Albert. I hope that I have made them proud. Lastly, I would like to thank my best friend and companion Jamal Derakhshan, PhD. Jamal's love for science has been inspirational, and I am grateful that we journeyed through the ups and downs of graduate school together.

Over the past seven years, I've learned more than what can be encompassed in this dissertation. I've learned that the difficult and long trail to the PhD is fraught with many unexpected twists and turns and that a life in science is accompanied with many obstacles and sacrifices. However, I also learned how to think more deeply and how to be a successful researcher. Overall, I have appreciated my experience as a graduate student. This journey has challenged me to become a stronger scientist and person.

Funding for this work was provided by R01 AR056633, F31AR057305, and T32 AR50959 from the National Institute of Arthritis and Musculoskeletal and Skin Diseases (NIAMS) as well as the Ohio Biomedical Research and Technology Transfer Partnership. The content is solely the responsibility of the authors and does not necessarily represent the official views of NIAMS or the National Institutes of Health.

Tyramine Substituted-Hyaluronan Enriched Fascia
for Rotator Cuff Tendon Repair

Abstract

by

LIKANG CHIN, MS

Rotator cuff tendon injury is a debilitating health concern that affects more than 40% of the aging population. Despite advances in surgical treatment, the failure rate of rotator cuff repairs ranges 20-90%. Naturally-occurring extracellular matrices (ECMs) have been recently investigated as augmentation scaffolds, but none has yet demonstrated both the appropriate biological and mechanical properties.

This dissertation proposes to enrich fascia ECM with high molecular weight tyramine substituted-hyaluronan (TS-HA) for rotator cuff repair. The central hypothesis is that TS-HA treatment will decrease chronic inflammation without decreasing the time-zero or post-implantation mechanical properties of fascia. The specific aims are to develop a TS-HA treatment method and to evaluate the host response and concomitant mechanical properties of treated fascia in a rat abdominal wall model.

TS-HA treatment increased the HA content of fascia by an order of magnitude to ~1% tissue weight. The incorporated HA was distributed throughout the ECM and, upon cross-linking, was retained as a hydrogel network. Cross-linked TS-HA treated fascia exhibited an increased macrophage and giant cell

response and a lower density of fibroblast-like cells than water treated controls. Treated fascia, with or without cross-linking, exhibited a predominantly M2 pro-remodeling macrophage profile similar to water controls, which is suggestive of constructive tissue remodeling. All grafts exhibited a chronic lymphocytic response that is suggestive of an immune response to the fascia xenograft. Fascia samples in all groups demonstrated time-dependent decreases in mechanical properties. Cross-linked TS-HA treated fascia exhibited a lower toe-region elastic modulus and trended towards a higher transition strain than water treated controls not only after implantation, but also at time zero.

These findings demonstrate that HA augmentation can alter both the host response and the mechanical properties of fascia ECM. Contrary to the hypothesis, the particular TS-HA treatment (at the concentration, molecular weight, and tyramine substitution rate) employed in this dissertation elicited a heightened macrophage and giant cell response and a decrease in low-load elastic mechanical properties compared to water treated fascia. This work provides a starting point and guidance for the ongoing development of TS-HA enriched fascia ECM as an augmentation scaffold for rotator cuff repair.

.

Chapter 1

Introduction

Tears of the Rotator Cuff Tendons

Rotator cuff injuries are a common cause of shoulder pain and debilitation. About 75,000 rotator cuff surgeries are performed annually in the United States (1,2), the treatment, evaluation, and management of which costs the US economy $7 billion dollars per year (3). Tears of the rotator cuff tendons can afflict a wide range of the population, but the elderly and those who engage in physically demanding occupations (i.e., athletes and manual laborers) are more prone to injury.

Because rotator cuff tears are often asymptomatic, the number of documented shoulder cases may not be an accurate indication of how common the disorder truly is. Radiological studies of asymptomatic patients or cadavers may provide a better measure of prevalence. In a prospective clinical study of

over 400 asymptomatic patients, 23% demonstrated evidence of a cuff tear as detected by ultrasonography (4). The prevalence of injury was age-dependent, and patients aged 80 years and older had the highest rate of occurrence (51%). Reilly et al. surveyed all radiological studies of cadavers published in peer-reviewed literature and determined an overall tear rate of 30% for the general population (5). Hence, the reported 1-2% of the population who complain of shoulder pain is likely an underestimation of the prevalence of rotator cuff tears (6).

The exact etiology of rotator cuff disorders is not completely known, but is believed to involve a combination of intrinsic, extrinsic, and traumatic factors (6-9). Intrinsic mechanisms are initiated by disease, age-related changes to metabolism, or changes to vascularity that result in tendon degeneration (6-9). Extrinsic mechanisms are caused by instability of the glenohumeral joint or impingement of the supraspinatus tendon of the rotator cuff by surrounding bony structures or soft tissue (6-9). Tendon lesions can also originate from mechanical overloading from a single traumatic event or from repetitive microdamage (6-9).

Current Treatment for Rotator Cuff Tears

Because rotator cuff tears are caused by a number of contributing factors, a standardized treatment program has yet to be established. Initial treatment is often conservative and may include the administration of non-steroidal anti-inflammatory medication or corticosteroid injections, heat or massage therapy, and some degree of immobilization to prevent overhead reaching or motions that

may cause impingement. As pain subsides and the patient's range of motion increases, treatment continues with physical rehabilitation that focuses on improving shoulder strength. However, no reliable, long-term study evaluating patient outcomes following nonsurgical treatment exists in the published literature, and the lack of a standardized treatment protocol among studies makes comparisons challenging.

When conservative treatments fail or when the tears are large and chronic, surgical intervention may be indicated, followed by extensive physical rehabilitation. Surgical management may involve debridement of poor quality tissue; debridement with acromioplasty to plane down the coracoacromial arch, the bony structure that can compress the supraspinatus tendon; or primary repair of the torn tendon(s) with or without acromioplasty.

Despite advances in surgical treatment options, however, the failure rate of rotator cuff repairs ranges from 20 to 90% and depends on factors such as patient age, tear size and chronicity, tendon tissue quality, muscle atrophy and degeneration, the healing ability of the involved tissues, repair technique, the immediacy of repair after injury, and the post-operative rehabilitation protocol (10-18).

Hence, there remains a critical need for a repair strategy that provides effective mechanical reinforcement and stimulates tendon healing.

Augmentation Scaffolds for Rotator Cuff Repair

The most common cause of failed rotator cuff repairs is believed to be suture pull-through as a result of excessive repair tension (19-21). To address the critical need for a repair strategy that provides mechanical support, naturally-occurring and synthetic augmentation scaffolds have been investigated for the reinforcement of rotator cuff repairs with the goal to foster the formation of a functional tendon-bone bridge. As depicted in Figure 1.1, an augmentation device would be placed over the primary repair using sutures or suture anchors. Augmentation devices may provide some degree of load sharing across the tendon repair site, thereby decreasing the likelihood of tendon re-tear. The ideal augmentation scaffold would serve as an inductive template with the appropriate mechanical properties to prevent or limit tissue re-tear during the course of remodeling and would facilitate downstream integration/reconstruction of functional musculotendinous tissue (22,23). Over the past decade, polyurethaneurea (24), polyglycolic acid (25), poly(lactide-co-gycolide) (26), polylactic acid (27-30), polytetrafluoroethylene (31), chitin (32), chitosan-hyaluronan (33), and naturally-occurring extracellular matrices (ECMs) (19,34-43) have been investigated as augmentation devices. Of these, devices made of poly-L-lactide, polyurethaneurea as well as dermis, small intestinal submucosa (SIS), and pericardium ECMs are currently FDA cleared for rotator cuff repair (44).

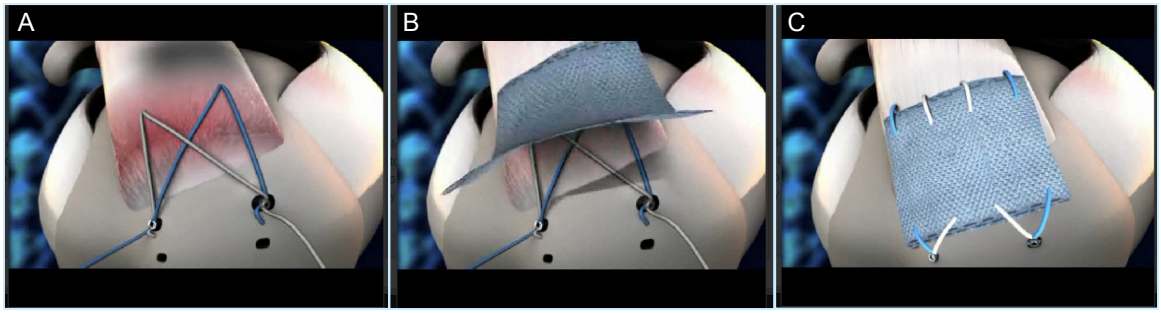

Figure 1.1 Schematic demonstrating the application of an augmentation device for rotator cuff repair. (A) The torn tendon is sutured back to bone. (B) The augmentation device is placed over the primary repair and (C) secured with sutures or suture anchors (45).

ECM Scaffolds for Rotator Cuff Repair

Scaffolds derived from ECM have been the topic of recent investigation in the context of rotator cuff tendon repair. These naturally-occurring biomaterials are particularly attractive due to their native three-dimensional architecture that is a composite of structural and functional proteins, including but not limited to collagen, elastin, proteoglycans, and glycosaminoglycans (GAGs) (22,46). Perhaps more important for regenerative medicine, macromolecules intrinsic to the ECM (e.g., vascular endothelial growth factor, fibroblast growth factor 2, and transforming growth factor β1) may mediate inflammation as well as direct host functions, such as cell migration and proliferation, collagen deposition, and angiogenesis (22,46-51). As bioactive environments that can potentially enhance and accelerate tissue healing, ECM scaffolds have great promise in the field of tendon repair.

Several commercially-available ECM scaffolds, derived from a variety of tissue types and animal sources, are marketed for rotator cuff repair augmentation (Table 1.1).

Table 1.1 Commercially-available ECM scaffold devices available for rotator cuff repair (44)

Product Name	ECM Type	ECM Source	Marketed by
Restore®	SIS	Porcine	DePuy Orthopaedics
CuffPatch™	SIS (cross-linked)	Porcine	Organogenesis
GraftJacket®	Dermis	Human	Wright Medical Technology
Conexa™	Dermis	Porcine	Tornier
TissueMend®	Dermis (fetal)	Bovine	Stryker Orthopaedics
Zimmer® Collagen Repair Patch	Dermis (cross-linked)	Porcine	Zimmer
Bio-Blanket™	Dermis (cross-linked)	Bovine	Kensey Nash
OrthADAPT™ Bioimplant	Pericardium (cross-linked)	Equine	Pegasus Biologics

Clinical Studies of ECM Scaffolds for Rotator Cuff Repair

To date, few clinical studies have been published in peer-reviewed literature that investigate ECM scaffolds for rotator cuff repair. Furthermore, these studies are limited to porcine SIS (Restore), human dermis (GraftJacket), and cross-linked porcine dermis (Zimmer Collagen Repair Patch).

Restore (porcine SIS ECM)

Metcalf et al. conducted one of the first follow-up studies evaluating Restore as an augmentation scaffold for massive, chronic rotator cuff tears (52). After two years, thickening of the tendon and incorporation of the graft was reported based on postoperative magnetic resonance imaging (MRI) in 11 of the 12 patients. The graft failed clinically in only one patient within 12 weeks.

Postoperative functional scores were significantly improved over preoperative scores, but were still lower than normal. The lack of a non-augmented control group complicates interpretation of these results.

Despite the overall positive outcomes of the Metcalf study, several other investigators have shown less favorable results following the use of Restore for cuff repair. A six-month follow-up study demonstrated postoperative failure for 10 of the 11 patients who received SIS as an augmentation or interpositional graft for large or massive rotator cuff tears (53). Iannotti et al. conducted the only prospective, randomized, controlled clinical trial using Restore for rotator cuff repair (54). Patients with repairable, large 2-tendon tears were 7% more likely to heal following an unaugmented repair than after a repair augmented with Restore as measured by postoperative functional scores. Additionally, a sterile inflammatory reaction was observed for three of the 15 patients in the Restore group. A study conducted by Walton et al. reported that four of the 10 patients required open debridement after experiencing a severe inflammatory reaction from the use of Restore as an augmentation device (55). Noninfectious edema, swelling, pain, and increased skin temperature around the wound have also been noted in ~40% of patients receiving SIS for cuff repair (53-56). Hence, the Restore device in its current form is not considered suitable for rotator cuff augmentation (55).

GraftJacket (human dermis ECM)

A retrospective study with a follow-up period of 12-38 months conducted by Dopirak et al. reported significantly higher postoperative functional scores than preoperative scores for 16 patients who received GraftJacket as an interpositional graft for massive, irreparable cuff tears (57). However, three patients experienced failure of the graft as detected by MRI, two at three months and one (associated with the patient falling) at four months.

Burkhead et al. evaluated 17 patients who received GraftJacket as an augmentation device and reported that postoperative functional scores were significantly greater than preoperative scores (58). Although postoperative MRI detected small recurrent tears, some connection between native tissue and the humeral tuberosity through the graft was observed in all cases. Mean follow-up was 1.2 years.

The most recent study of GraftJacket evaluated its use as an interpositional graft for massive cuff tears (59). After a mean follow-up period of 26.8 months, 15 of 16 patients were satisfied with their surgery, and postoperative functional scores were significantly improved over preoperative scores. Thirteen patients exhibited full incorporation of the graft as determined by MRI, but three patients experienced failure at one year. Although a non-augmented control group was lacking from each of these GraftJacket clinical studies, the overall outcomes were positive and support the continued investigation of GraftJacket for rotator cuff repair.

Zimmer Collagen Repair Patch (cross-linked porcine dermis ECM)

Results from short-term follow-up studies of Zimmer® Collagen Repair Patch for the repair of massive tendon tears have been mixed. An improvement in clinical outcomes was reported for a cohort of ten patients 4.5 years after receiving the Zimmer Collagen Repair Patch as an augmentation device (60). Ultrasound and MRI identified intact repairs for eight patients and failure in only two patients. However, another study in which Collagen Repair Patch was used as an interpositional graft for massive tears reported graft failure between three and six months in all four patients (61). Interpretation of these studies is limited by their small sample size and the lack of proper controls.

Fascia ECM

Augmentation scaffolds derived from human fascia lata – a tendinous structure procured from the deep fascia of the thigh at a region that corresponds to the iliotibial band – may be appropriate for tendon repair, because fascia ECM has material, chemical, and structural properties similar to tendon (62). The Derwin Laboratory previously investigated the mechanical properties of fascia and several commercially-available ECM scaffolds available for rotator cuff repair augmentation (21). When pulled to failure under uniaxial tension, fascia exhibited an elastic modulus (532 ± 106 MPa) (62) similar to canine infraspinatus tendon (405 ± 86 MPa) (21), while all commercially-available ECM scaffolds had elastic moduli that were an order of magnitude lower than tendon. While fascia stretched only ~3% before stiffening and bearing any significant load, all other scaffolds

derived from SIS and dermis required higher strains of 10-30% before bearing load (Figure 1.2). The difference in material properties between SIS, dermis, and tendon suggests that SIS and dermis ECM scaffolds may offset only a small amount of load from the repair and/or would stretch appreciably under physiologic forces. However, mechanical augmentation of rotator cuff repairs might be possible with fascia ECM, which has mechanical properties similar to tendon.

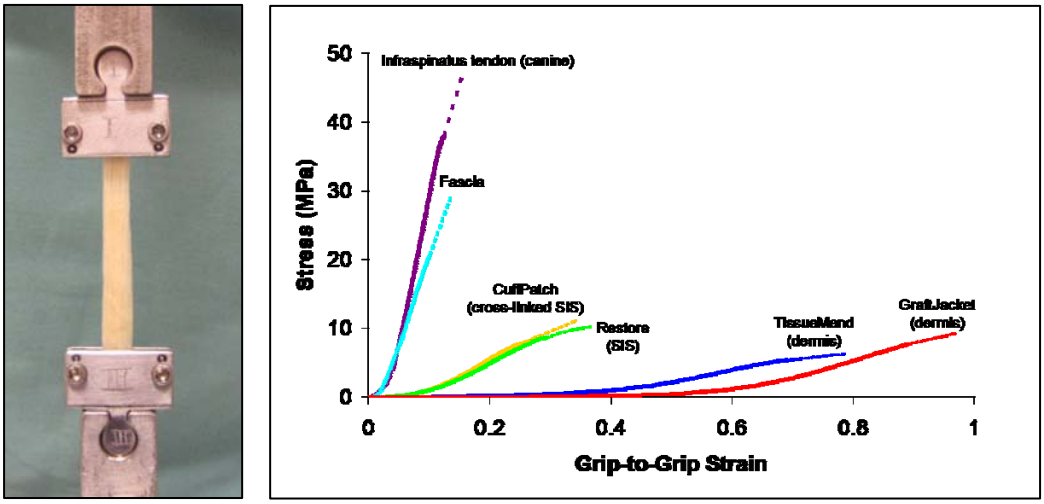

Figure 1.2 Representative stress versus grip-to-grip strain curves for 4 mm wide ECM strips as compared to normal canine infraspinatus tendon. The dotted lines were added to demonstrate that the failure point is underrepresented in all curves because all failures occurred at the grip (adapted from (63)).

In addition to its tendon-like mechanical properties, fascia ECM has a biochemical composition and histologic structure similar to tendon (62). The hydroxyproline and chondroitin sulfate/dermatin sulfate GAG concentrations in fascia are similar to canine flexor tendon (Table 1.2) (62).

Table 1.2 Mean ± SD hydroxyproline and chondroitin sulfate/dermatin sulfate glycosaminoglycans (CS/DS GAG) content of fascia ECM and tendon (62)

Content	Fascia ECM	Canine Flexor Tendon
Hydroxyproline (mg/mg)	0.114 ± 0.014	0.104 ± 0.004
CS/DS GAG (μg/mg)	0.61 ± 0.30	0.84 ± 0.24

Furthermore, fascia ECM is a bilayer of collagen fascicles that are orthogonally-oriented (Figure 1.3A), and tendon is essentially a bundle of collagen fascicles that are arranged in parallel. As seen in the stereomicrograph, the deep layer of fascia resembles a flat sheet of tendon with fascicles that are easily distinguished (Figure 1.3B).

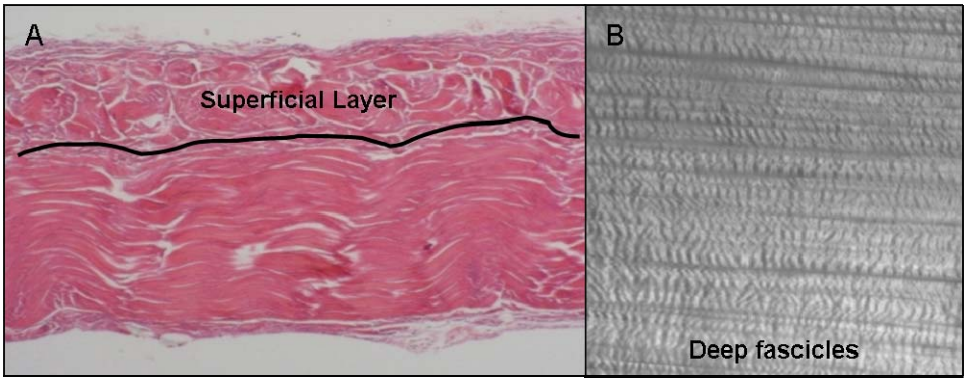

Figure 1.3 (A) Image of H&E stained section of unmodified fascia ECM, demonstrating the bilayer of collagen fascicles that are orthogonally-oriented and (B) stereomicrograph of the deep layer of fascia, which resembles a flat sheet of tendon

Although fascia ECM has not been previously evaluated as a tendon augmentation scaffold in a formal clinical study, nor is it currently marketed as an ECM device for rotator cuff repair, human fascia lata has been successfully employed as an autograft or allograft in the reconstruction of various soft tissues,

including pectoralis major tendon (64), hallucis longus tendon (65), and Achilles tendon (66).

The tendon-like mechanical, chemical, and structural properties of fascia make it an attractive option for tendon repair and provide the rationale for the investigation of fascia ECM as an augmentation scaffold for rotator cuff repair.

Furthermore, this dissertation proposes that fascia ECM enriched with high molecular weight hyaluronan (HA) – a molecule well-known for its anti-inflammatory and wound healing properties – may foster the formation of a functional tendon-bone bridge by minimizing chronic inflammation within the scaffold and enhancing fibroblast infiltration.

The human fascia lata used in the experiments described in this dissertation was procured by the Musculoskeletal Transplant Foundation (MTF, Edison, NJ) from donors aged 18-55 years old. Fascia lata was harvested aseptically from cadavers and further processed at MTF facilities. After the fascia was cleaned of superficial connective tissue and underlying muscle, it was cut into 5x5 cm patches, and subjected to an antibiotic/antifungal soak treatment in a PBS solution containing 1.6 µg/ml of amphotericin B, 30 µg/ml of imipenem cilastatin, and 6 µg/ml gentamicin sulfate for 24 hours at 37°C on a shaker (67). After the 24 hours, fascia was rinsed two times in PBS for 20 minutes each at room temperature on a shaker. Subsequently, individual fascia patches were sterilely packaged, frozen, and sent to the Derwin laboratory.

Hyaluronan

HA is a ubiquitously-present, non-sulfated GAG molecule composed of repeating disaccharide units of N-acetylglucosamine and β-glucuronic acid (Figure 1.4). The highest concentrations of HA in normal physiologic tissue are found in joint synovial fluid (1.4-3.6 μg/mg wet weight (68)), vitreous humor (0.14-0.34 μg/mg wet weight (68)), dermis (~0.2 μg/mg wet weight (68)), and cartilage (0.2-2 μg/mg wet weight (69)). Well-known for its roles in development, wound healing, and inflammation, HA has a myriad of properties that are highly dependent on molecular weight (70-73). This dissertation focuses on the use of high molecular weight HA.

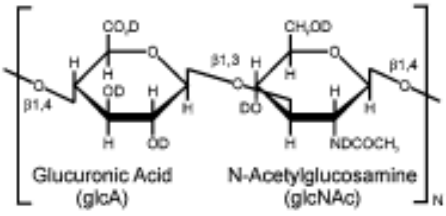

Figure 1.4 Chemical structure of the HA repeating disaccharide units (74)

High molecular weight HA (> 250 kDa molecular weight (75)) is most often recognized for its anti-inflammatory properties. Numerous studies have demonstrated that exogenous HA can inhibit the infiltration, proliferation, and cytokine production of various inflammatory cells (75-80). As demonstrated in cell culture and *in vivo* model systems, HA can decrease the expression and production of inflammatory and catabolic genes, such as prostaglandin E_2, interleukin (IL)-6, matrix metalloproteinase (MMP)-3, tumor necrosis factor (TNF)-alpha, interferon-gamma (IFN-γ), macrophage inflammatory protein-2, and IL-4,

while simultaneously increasing the expression of anti-inflammatory and anabolic genes (75,76,81,82). By physically blocking the binding of low molecular weight HA to the cell surface receptor CD44, an interaction that is associated with inflammation, high molecular weight HA can inhibit the recruitment and activation of lymphocytes, macrophages, and natural killer cells (76). As well, the viscous nature of an HA-rich environment can limit inflammatory cell migration and the diffusion of cytokines (72).

Yet another property that may be beneficial for tissue repair is the ability of HA to modulate cell migration by binding to the receptor for hyaluronan-mediated motility (RHAMM), expressed on a wide variety of motile cells (83-85). I*n vitro* studies have demonstrated the ability of HA to promote the migration of fibroblasts (84,86-89).

It has been well-established that HA is a main component of a fetal wound milieu that is conducive to scarless healing. In both fetal and adult wounds, HA levels increase following injury (90). While the concentration of HA returns to normal after the acute inflammatory phase in adult wounds, the fetal wound environment maintains an elevated amount of HA for at least 21 days post injury (90). This phenomenon, in combination with the presence of HA stimulating activity factor and the absence of hyaluronidase, is believed to promote scarless wound healing (90).

HA in Orthopaedic Applications

These favorable properties of HA have prompted its use for tissue repair strategies. HA in various configurations – injectables (91-94), hydrogels (95,96), composite scaffolds (33,97) – has been evaluated for a variety of clinical needs, including the orthopaedic, pharmacologic, cardiovascular, and dermatologic fields.

The short half-life of HA, which ranges from minutes to hours depending on the physiologic tissue (68,98), has been a challenge for tissue engineering applications and has driven the development of chemically-modified cross-linkable forms – such as thiol-modified, carbodiimide cross-linked, and esterified HA – as a means to stabilize the molecule (98). Hydrazide chemistry has been used to convert the carboxylate groups of HA to pendant thiol groups, which can be oxidatively cross-linked (99,100). The resulting disulfide cross-links are reversible, and these HA hydrogels have been used as cell-seeded three-dimensional hydrogels for cartilage tissue repair (100). Also, HA has been incorporated with collagen slurry to form a collagen-based scaffold that was subsequently cross-linked with carbodiimide (101). After a two-week culture with adult canine chondrocytes, the HA-collagen scaffold exhibited cartilaginous-like tissue. Another form of chemically-modified, cross-linkable HA involves esterification of the molecule. Hyaloglide^{TM} is a commercially-available HA ester that is marketed for the prevention of post surgical adhesions following tendon and peripheral nerve surgery. Rabbit digital flexor tendons, that were injured and subsequently repaired, exhibited increased tensile strength after receiving

injections of Hyaloglide™ at the repair site compared to saline treated controls (102). These aforementioned studies demonstrate the utility and potential of chemically-modified HA as a tissue engineering strategy, particularly in orthopaedic applications.

To the best of the author's knowledge, only two other studies reported the augmentation of a naturally-occurring ECM scaffold with HA. Brown et al. incorporated thiol-modified HA into bladder ECM using a diffusion-based protocol and oxidatively cross-linked the HA to achieve a disulfide-containing HA hydrogel within the bladder scaffold (103). Although the *in vivo* host response to HA treated bladder ECM was not evaluated, a cell culture study demonstrated that the addition of the thiol-modified HA facilitated and expedited the infiltration of bladder smooth muscle cells into bladder ECM. Previous use of unmodified bladder ECM for bladder augmentation in a porcine model resulted in undesirable outcomes such as scar formation and graft contracture (103,104). A modified bladder ECM, in particular one that is augmented with HA, may be effective in improving organ regeneration.

More recently, Roth et al. reported the use of porcine SIS augmented with HA-poly(lactic-co-glycolic-acid) nanoparticles (HA-PLGA-SIS) for bladder regeneration in a canine model (105). Animals were subjected to a 40% partial cystectomy, followed by bladder augmentation with either unmodified SIS or HA-PLGA-SIS. Following a 10 week implantation, urodynamic bladder capacity was determined, and the repair was histologically assessed for neovascularization, smooth muscle ingrowth, smooth muscle bundle formation, and calcification. All

dogs demonstrated full-thickness bladder regeneration, and there was no difference between the two treatment groups with respect to bladder capacity (a 40% reduction for both groups) or histologic scoring. This study demonstrated a modification of SIS with HA-PLGA nanoparticles, but additional research into the benefits of HA on bladder regeneration is needed.

Tyramine-Substituted Hyaluronan

The work described in this dissertation investigates the use of tyramine substituted-hyaluronan (TS-HA), a novel modification of HA that has tyramine adducts coupled to the carboxyl groups of the glucuronic acid residues along 5% of the molecule (Figure 1.5) (74). Through a free radical reaction initiated by a small amount of hydrogen peroxide and horseradish peroxidase, neighboring tyramine adducts cross-link to form a dityramine bridge (Figure 1.6). The resulting hydrogel is not susceptible to hydrolysis and has a concentration-dependent resistance to hyaluronidase degradation (74).

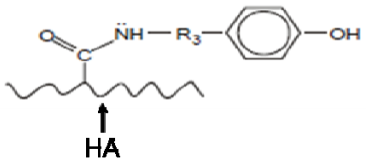

Figure 1.5 Chemical structure of TS-HA (adapted from (74))

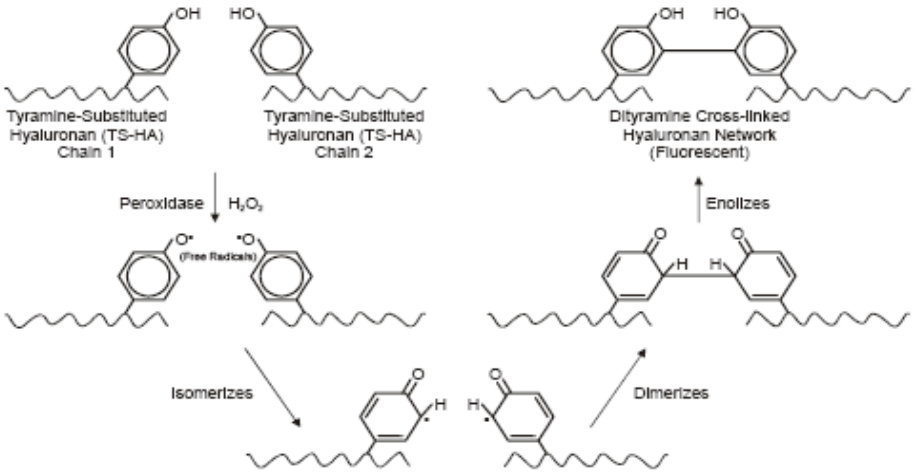

Figure 1.6 Schematic representation of the proposed mechanism for peroxidase catalyzed oxidation of tyramine on TS-HA to form di-tyramine cross-links (74)

The host response to TS-HA hydrogel plugs following implantation in a rat subcutaneous dorsal model was previously investigated in a pilot study (106). TS-HA hydrogels were harvested at 1, 3, 6, and 12 months post implantation, and qualitative assessment of histologic sections showed no cellular infiltration into the plugs, an absence of multinucleated giant cells, and minimal inflammation of the surrounding tissue. As well, the number of inflammatory cells decreased over the 12 month time course.

Herein, this dissertation proposes to immobilize high molecular weight HA within fascia ECM by means of tyramine cross-linking, thus providing a sustained concentration of HA.

Host Response to ECM Scaffolds

The host inflammatory response, including the macrophage component, appears to be a critical determinant, and perhaps predictor, of successful and

constructive remodeling of an implanted biomaterial (107,108). Implantation of a biomaterial scaffold, or any foreign body for that matter, triggers a host response that is classically described by several stages, each of which is associated with and identified by the predominant inflammatory cell type(s) and/or wound healing process(es) (109,110):

acute inflammation – transient stage characterized by edema and neutrophils, associated with the surgical procedure (109,110)

chronic inflammation – characterized by monocytes, macrophages, lymphocytes, and plasma cell; can persist as a result of an unresolved, constant inflammatory stimulus (109,110)

granulation tissue formation – characterized by the deposition of collagen types I and III by fibroblasts, wound contracture by myofibroblasts, and blood vessel formation (109,110)

foreign body reaction to a non-degradable material – characterized by macrophages and giant cells; giant cells form from the fusion of macrophages and function to break down the material by producing reactive oxygen species, arachidonic acid, and MMPs; may also be characterized by the presence of lymphocytes (109,110)

fibrous capsule formation – functions to isolate non-degradable material (109,110).

Although ECM scaffolds wholly comprised of collagen do not tend to evoke a foreign body reaction or fibrous encapsulation (109,110), chemical modifications to the scaffold may do so. It is generally accepted that an ECM scaffold should

facilitate host cell repopulation, tissue ingrowth, vascularization, organization of newly formed collagenous tissue, and elicit a minimal inflammatory response to successfully function as a soft-tissue augmentation graft (111).

Valentin et al. previously evaluated the host response to ECM devices available for rotator cuff repair in a rat abdominal wall study (112). Although all scaffolds elicited an acute inflammatory response that consisted primarily of neutrophils and some mononuclear cells, each eventually presented a distinct cellular and morphologic reaction that differed with respect to temporal occurrence of inflammatory events, cellularity, spatial distribution of cells, cell population, the presence or absence of a foreign body reaction, vascularity, and organization of newly remodeled tissue. Restore (noncross-linked porcine SIS) and GraftJacket (noncross-linked human dermis) evoked different responses that were representative of fast- and slow-degrading materials, respectively. Initially, implanted Restore was densely infiltrated by monocytes, macrophages, lymphocytes, and plasma cells throughout the entire graft. By four months, the scaffold was completely degraded and replaced by skeletal muscle, vascularized collagenous connective tissue, and adipose tissue. In contrast, implanted GraftJacket was characterized by a mononuclear cell population localized at the graft periphery that diminished by two months. At four months, GraftJacket was only partially degraded and replaced by a moderate degree of organized, dense, collagenous connective tissue.

Factors that contribute to the host response to an ECM scaffold include the species of origin, tissue source, the graft recipient, and the mechanical

loading environment (44). As well, processing methods, such as acellularization, cross-linking, terminal sterilization, and post sterilization rinsing, may be the most influential factors in determining the host inflammatory response (113). For example, cross-linked ECM scaffolds, such as Permacol (cross-linked porcine dermis), exhibit minimal degradation, minimal cellular infiltration, no evidence of tissue remodeling, and are associated with giant cells and fibrous capsule formation (112). This significantly differs from the host response to GraftJacket (noncross-linked human dermis). Thus, extensive cross-linking of matrix components might inhibit the infiltration of host cells, angiogenesis, and scaffold remodeling, thus contributing to graft failure (113).

Macrophage Polarization

Macrophages, one of the predominant cell types of the chronic inflammatory reaction, function to phagocytose an implanted biomaterial (109,110). Capable of secreting reactive oxygen intermediates, arachidonic acid, and MMPs, macrophages are long-lasting and can reside on an implanted biomaterial for months, even years (110).

The classification of macrophage polarization has recently been used as a means to predict the remodeling outcome of an implanted biomaterial (107,108). Based on microenvironmental cues from cytokines or microbial products, macrophages demonstrate their plasticity by exhibiting certain phenotypic markers, expression profiles, and cellular functions (44,107,114-119). Consequently, macrophage phenotypes span a continuous spectrum, the two

extremes of which are represented by the M1 pro-inflammatory and M2 pro-remodeling activated forms (117). Induced by IFN-γ alone or with lipopolysaccharide, TNF, or granulocyte macrophage colony stimulating factor, M1 macrophages exhibit an IL-12^{high}, IL-23^{high}, IL-10^{low}, inducible nitric oxide synthase^{high} expression profile; produce large amounts of reactive oxygen species and inflammatory cytokines; express chemokine (C-C motif) receptor type 7 (CCR7) as a cell surface marker; and are associated with tissue destruction and inflammation (107,117). Macrophages of the M2 phenotype are inducible by IL-4, IL-13, and IL-10; exhibit an IL-12^{low}, IL-23^{low}, IL-10^{high}, arginase-1^{high}, TNF^{low} expression profile; are characterized by cluster of differentiation 163 (CD163) as a cell surface marker; and are associated with angiogenesis as well as tissue repair and remodeling (107,117). This dissertation evaluates macrophage phenotype as a means to predict the remodeling outcome of implanted TS-HA treated fascia.

Rodent Model to Study Host Response

Abdominal (112,120-124), subcutaneous (125,126), and tissue cage (127,128) rodent models are well-established tools for studying the host inflammatory response to an implanted biomaterial. Although the material of interest is not evaluated at the intended site of clinical application, these models serve as affordable preclinical means to investigate *in vivo* material-tissue interactions and inflammation for a large number of samples. The rat abdominal wall defect model, in particular, is a well-accepted *in vivo* system for assessing host response in a musculoskeletal environment (112,120,121). Characterization of the host response can be accomplished through semi-quantitative scoring of the various inflammatory cell types at various time points following implantation. Previous studies employ scoring systems based on qualitative descriptors (i.e., 0=none, 1=mild, 2=moderate, 3=severe (129)) as well as those based on a quantitative range of cell densities (i.e., 0=between 0-50 cells per high powered field (hpf), 1=51-100 cells per hpf, 2=101-150 cells per hpf, 3=more than 150 cells per hpf (112)). In addition, ISO 10993-6 entitled “Biological evaluation of medical devices – Tests for local effects after implantation” describes a semi-quantitative scoring system to evaluate biocompatibility that has been published as an international standard by the Association for the Advancement of Medical Instrumentation (130). In this dissertation, a partial-thickness rat abdominal wall defect model in conjunction with a semi-quantitative scoring system adapted from ISO 10993-6 is used to evaluate the host response to fascia ECM with or without TS-HA treatment.

Mechanical Property Decreases as a Result of Inflammation

The success of an ECM augmentation scaffold for rotator cuff repair is not only dependent on the host response to the material, but also on the mechanical properties at implantation and over the time course of remodeling. While rapid degradation of an ECM scaffold is associated with a decrease in mechanical properties, fibroblast infiltration along with new matrix deposition is associated with an increase in mechanical properties (44). Hence, a balance between matrix degradation and deposition must be reached to ensure continued mechanical reinforcement throughout the time course of healing (44). In normal remodeling, this balance is achieved in part by the homeostatic equilibrium of MMPs and their inhibitors (131). MMPs are produced by a number of cell types, including macrophages and giant cells (132-134) and target various components of the ECM. Thus, increased MMP activity (a possible consequence of persistent, chronic inflammation) can excessively degrade the ECM and reduce its mechanical properties (131).

Because the high-strain elastic behavior of fascia ECM is governed by load-bearing collagen fibers (135-137), an increase in collagenase activity (e.g., MMP-1, -2, and -9, which are secreted by macrophages and giant cells (132-134)) could decrease linear-region elastic properties (131). At low-strains, the mechanical behavior of fascia is dictated mainly by elastin and other non-collagenous ECM proteins (138). Hence, a reduction in toe-region elastic properties after implantation could be a consequence of increased activity of elastase MMP-12 and/or the broad spectrum MMP-14 (138), both of which are

produced by macrophages and giant cells (132-134). As well, postoperative swelling or edema could physically disrupt the interaction between collagen and other ECM proteins, thus interrupting force transmission through the ground substance and lowering toe-region elastic properties (139,140).

The viscoelastic behavior of fascia is believed to arise from the proteoglycan and water content of the ECM (141). Thus, postoperative swelling and edema as well as the natural accumulation of proteoglycans that occurs following injury (142,143) could contribute to an increase in the rate or amount of stress relaxation of implanted fascia ECM (144).

TS-HA enriched fascia is expected to elicit minimal chronic inflammation and facilitate fibroblast infiltration. As a result, it is logical to expect a reduction in MMP activity. The elastic mechanical properties of TS-HA treated fascia should decrease to no greater extent than water treated fascia, and HA treatment may even prove to mitigate the expected loss of elastic properties following implantation. As well, TS-HA treatment is expected to influence the viscoelastic behavior of fascia ECM. Because water is highly attracted to HA, the added TS-HA may increase tissue water content, thereby increasing the rate or amount of stress relaxation of fascia ECM.

Significance and Specific Aims

Rotator cuff injury is a debilitating health concern that affects more than 40% of the aging population. Seventy-five thousand rotator cuff surgeries are performed annually in the United States, placing a financial burden of $3 billion on the US economy. For large, chronic tears, surgical intervention can improve clinical outcomes, but re-tear rates are reportedly as high as 90%. Several ECM devices are commercially available for the augmentation of rotator cuff repairs, but none have yet demonstrated both the appropriate biological milieu and the sufficient mechanical strength for tendon augmentation. An ECM scaffold that elicits minimal chronic inflammation and has mechanical properties similar to tendon may be effective in facilitating the regeneration of a functional tendon-bone bridge. To address the critical need for such a scaffold, the Derwin Laboratory seeks to develop fascia ECM for rotator cuff augmentation, since it has mechanical, chemical, and structural properties similar to tendon.

This dissertation proposes to enrich fascia with high molecular weight HA , a molecule well-known for its roles in wound healing and modulating inflammation. The successful development of TS-HA enriched fascia would provide an augmentation scaffold that has both the appropriate time-zero mechanical properties for tendon repair and a biological milieu that minimizes chronic inflammation within the scaffold and enhances fibroblast infiltration. It is expected that decreased inflammation would decelerate and to some extent mitigate resorption of the scaffold. As a result, the mechanical properties of treated fascia would be maintained to some degree so as to prevent or limit re-

tear over the course of tendon healing and tissue deposition. However, the host inflammatory response to fascia enriched with HA has not been previously characterized, and the effect of HA treatment on the time-zero and post-implantation mechanical properties of fascia are unknown.

Hence, the *objective* of this work was to develop fascia ECM for rotator cuff repair augmentation by incorporating HA to minimize chronic inflammation within the scaffold and by maintaining fascia's tendon-like mechanical properties. The *central hypothesis* was that HA treatment will decrease chronic inflammation within the scaffold and enhance fibroblast infiltration without decreasing the time-zero or post-implantation mechanical properties of fascia ECM. The work described herein investigates the use of high molecular weight TS-HA to enrich fascia ECM. TS-HA, developed by Anthony Calabro, PhD (Department of Biomedical Engineering, Cleveland Clinic), is a novel modification of HA that enables the cross-linking of neighboring HA chains. The central hypothesis was tested through the following specific aims:

Specific Aim 1: Develop an HA treatment of fascia ECM using TS-HA (Chapters 2 and 4)

The approach was to incorporate TS-HA into fascia ECM using diffusion- or convection-based methods with subsequent cross-linking. Time-zero HA content was quantified, and the treatment protocol that achieved an average content of 5-10 micrograms of HA per milligram of dry weight tissue was selected for further characterization, including HA staining and an *in vitro* retention experiment. TS-

HA treated fascia with cross-linking was hypothesized to retain more incorporated TS-HA than treated fascia without cross-linking.

Specific Aim 2: Evaluate the extent to which TS-HA treatment minimizes chronic inflammation within fascia ECM (Chapters 3 and 4)

The approach was to evaluate the host response to TS-HA treated fascia when implanted in a rat abdominal wall defect model at one and three months. TS-HA treated fascia with cross-linking was hypothesized to exhibit lower lymphocyte, plasma cell, macrophage, and giant cell densities, a higher fibroblast-like cell density, and a greater proportion of M2 pro-remodeling macrophages than M1 pro-inflammatory macrophages than water treated controls and TS-HA treated fascia without cross-linking.

Specific Aim 3: Evaluate the extent to which TS-HA treatment decreases the mechanical properties of fascia ECM (Chapter 5)

The approach was to evaluate the mechanical properties of TS-HA treated fascia at time zero and at one and three months post-implantation in a rat abdominal wall defect model. TS-HA treated fascia with cross-linking was hypothesized to exhibit similar time-zero and post-implantation mechanical properties as water treated controls and TS-HA treated fascia without cross-linking.

This work is innovative in that it proposes to develop an HA enriched fascia ECM scaffold and to evaluate both its biological and mechanical suitability

for musculoskeletal soft tissue repair. Development of an HA treated fascia ECM scaffold could fulfill the critical need for an augmentation scaffold that has both the appropriate mechanical and biological properties for tendon repair. Use of such a scaffold for rotator cuff augmentation could restore function of the tendon, alleviate pain, and consequently improve patient quality of life.

Chapter 2

Development and Characterization of Tyramine Substituted-Hyaluronan Enriched Fascia

Introduction

Several naturally-occurring, extracellular matrix (ECM) devices are commercially available for rotator cuff repair augmentation, but none has yet demonstrated the appropriate biological and mechanical properties for tendon healing. It is hypothesized that augmentation of fascia ECM with high molecular weight hyaluronan (HA), a molecule well-known for its anti-inflammatory and wound healing properties, may improve fascia's ability to foster the formation of a functional tendon-bone bridge. More specifically, this work uses tyramine-substituted hyaluronan (TS-HA), a chemically-modified HA that can be cross-linked through covalently-bonded dityramine bridges to form a hydrogel that is resistant to hydrolytic degradation (74).

Only two other studies have reported on the augmentation of a naturally-occurring ECM with HA, and both employed diffusion-based treatment methods (103,105). Because examples of HA enrichment are limited, several approaches to incorporate up to 5 micrograms of TS-HA per milligram of dry weight tissue (μg/mg) into fascia ECM were evaluated and included diffusion and vacuum treatments. Further, lacking any guiding precedent, the design criterion of ~5 μg/mg (~1 μg/mg wet weight) for these initial studies was based on the HA content of hyaline cartilage (0.2-2 μg/mg wet weight (69)), the maximum concentration found in any musculoskeletal tissue. Furthermore, a method to treat fascia with TS-HA has not been previously established nor characterized, and the effectiveness of tyramine cross-linking in immobilizing HA in fascia is unknown.

This chapter describes two pilot studies that were conducted to establish the development and characterization of TS-HA treated fascia. The objective of the first pilot study was to determine a method to incorporate and immobilize up to 5 μg/mg of TS-HA within fascia ECM and to visualize the distribution of the incorporated TS-HA. A number of treatment approaches were explored, and the concentrations of the TS-HA solutions used were also varied. Time-zero HA content was quantified, and the treatment protocol (diffusion or vacuum) that achieved up to 5 μg/mg with the least number of man-hours was selected for further evaluation. The objective of the second pilot study was to validate the cross-linking efficiency of TS-HA treated fascia through an *in vitro* release

experiment. TS-HA treated fascia with cross-linking was hypothesized to retain more incorporated HA than TS-HA treated fascia without cross-linking.

Pilot Study #1: Development and Characterization of TS-HA Treated Fascia

Materials and Methods

Experimental Design

Decellularized, lyophilized human fascia lata derived from the iliotibial tract of donors aged 18-55 years was obtained from the Musculoskeletal Transplant Foundation (MTF, Edison, NJ). Fascia pieces were treated with TS-HA using either the diffusion or vacuum method, and HA content was quantified immediately after treatment (i.e., time zero). The treatment protocol (diffusion or vacuum) that achieved up to 5 μg/mg and required the least number of man-hours was chosen for further evaluation. HA distribution was visualized by HA staining of fascia treated according to the chosen protocol. Detailed methods are described below.

TS-HA Treatment of Fascia

Diffusion: Lyophilized fascia pieces (1x1 cm) were individually rehydrated in 1.5 ml of 0.5, 0.75, or 1% aqueous TS-HA (0.9-1 M Da molecular weight, Lifecore Biomedical, Chaska, MN) or by increasing concentrations (0.05→0.1→0.2→0.5%) over a 24 hr period at 37ºC on a shaker. For the increasing concentrations protocol, fascia pieces were rehydrated in 0.05% TS-HA for 2 hr and sequentially equilibrated in 0.1 and 0.2% TS-HA for 2 hr each, followed by an 18 hr equilibration in 0.5% TS-HA. TS-HA solutions also contained 10 U/ml horseradish peroxidase (Sigma, St. Louis, MO), which was required for the cross-linking reaction.

Vacuum: Fascia pieces (3 cm diameter) were rehydrated in ultrapure water for approximately 10 min and then individually mounted onto the platform of a modified Steriflip filtration system (Millipore, Billerica, MA). The top conical tube was filled with approximately 10 ml of TS-HA solution with 10 U/ml of horseradish peroxidase and secured to the filtration system. Vacuum was applied and the TS-HA solution was pulled through the fascia. This step was repeated to increase the number of passes. TS-HA concentrations evaluated were 0.5, 0.75, 1%, and increasing concentrations.

After treatment, all fascia pieces were rinsed in ultrapure water for 30 sec and blotted two times per side on a towel to remove excess surface TS-HA. Fascia pieces were submerged into 0.3% hydrogen peroxide solution (Fisher, Pittsburgh, PA) in ultrapure water for 30 sec at room temperature with slight agitation and then allowed to sit covered on a glass dish at 4ºC for the reaction to continue overnight. Following overnight incubation, all TS-HA treated fascia pieces were then rinsed with ultrapure water for 30 sec to remove excess hydrogen peroxide. All treated fascia pieces were subsequently lyophilized. Lyophilized, untreated fascia served as control.

HA Content of Treated Fascia

HA content was quantified using fluorophore-assisted carbohydrate electrophoresis (FACE) according to previously described methods (21,145). Lyophilized tissue samples of a known weight were rehydrated in 100 mM ammonium acetate, pH 7.0, overnight at 4°C. Next day, samples were boiled for

5 min and digested with 0.25 mg/ml proteinase K (PK, Fisher) for 3 hr at 60°C. The PK digestion was repeated once more, followed by an overnight digestion. Samples were boiled for 10 min to deactivate the PK and centrifuged at 10.5 krpm for 30 min to separate the undigested tissue residue. An aliquot of the supernatant was dried in a speed-vac and ethanol precipitated overnight at -20°C by the addition of 1.3 ml of 77% ethanol in 160 mM ammonium acetate to isolate the glycosaminoglycans (GAGs). Next day, samples were centrifuged at 13 krpm for 15 min at 4°C to pellet the macromolecular material. Pellets were resuspended in 200 µl of 100 mM ammonium acetate and digested with 100 mU/ml hyaluronidase SD for 1 hr at 37°C, followed by a 2 hr digestion at 37°C with 100 mU/ml chondroitinase ABC (both from Seikagaku America, Falmouth, MA). Samples were dried with a speed-vac and fluorotagged by the addition of 40 µl of 12.5 mM 2-aminoacridone (AMAC, Molecular Probes, Eugene, OR) in 85% DMSO/15% acetic acid and 40 µl of 1.25 M sodium cyanoborohydride (Sigma) in ultrapure water, followed by 16 hr incubation at 37°C. After fluorotagging, samples were mixed with 20 µl glycerol, mixed 1:1 with an AMAC-derivatized trisaccharide standard (maltotriose), and then mixed 1:1 with 0.5 M 4-morpholinoethanesulfonic acid (pH = 7.0, Acros Organics, Geel, Belgium).

The FACE gels were run using a customized electrophoresis apparatus and a customized gel formulation. A 25 µl aliquot of 10% ammonium persulfate (Bio-Rad Laboratories, Hercules, CA) and 7.5 µl of TEMED (Bio-Rad Laboratories) were added to 5 ml of gel solution comprising 20% acrylamide-bis, 37.4:1 (Bio-Rad Laboratories), 45 mM Tris-acetate, pH 7.0, and 2.25% glycerol.

A resolving gel was poured between 10x10 cm glass plates using a 0.5 mm spacer. A stacking gel was then poured using the same solution composition. The gels were run using standard 1x Tris Borate EDTA buffer for 80 min at 500 V. Gels were imaged under UV light (365 nm) and peak areas for HA disaccharides were quantified with Gel Pro software (Media Cybernetics, Silver Spring, MD).

Distribution of HA in Treated Fascia

Fascia pieces were treated with TS-HA with cross-linking and HA without cross-linking following the diffusion-based protocol using increasing concentrations as previously described (n=3 per group), and HA distribution was evaluated by staining for HA. Both untreated and water treated fascia served as controls. Water treated fascia was prepared by incubation in ultrapure water for 24 hr at 37ºC on a shaker.

Samples were embedded in Tissue-Tek OCT compound (Sakura Finetek, Torrance, CA). Five-micron longitudinal frozen sections were cut and fixed in a 10% neutral buffered formalin for 1 hr, followed by a 1 min rinse in distilled water and two 1 min washes in Hank's buffered saline solution (HBSS). Sections were blocked in 1% bovine serum albumin in HBSS for 30 min and incubated with biotinylated HA binding protein (bHABP, Calbiochem, San Diego, CA) diluted 1:100 in PBS in a humidified chamber for 50 min. Sections were rinsed in HBSS three times for 1 min each, incubated with Alexa Fluor 488-conjugated streptavidin (Molecular Probes, Carlsbad, CA) diluted 1:500 in PBS for 45 min,

and rinsed three times in HBSS for 1 min each. All steps were performed at room temperature. Porcine cartilage served as a positive control, and sections incubated with HBSS in place of bHABP served as negative controls. All slides were mounted with Vectashield mounting media (Vector Labs, Burlingame, CA).

Results

HA Content of Treated Fascia

The average HA content of treated fascia varied from 1.5 – 16 μg/mg, depending on the treatment method (Table 2.1). Thus the incorporated HA constituted up to ~1.6% of the tissue weight in treated fascia, which is an order of magnitude higher than the HA content in untreated controls (0.41 ± 0.13 μg/mg). Increasing the concentration of the TS-HA solution as well as the number of passes with vacuum treatment increased the amount of incorporated HA. The coefficient of variability of HA content for all groups ranged from 30 – 60%, which was relatively high compared to 20 – 30% variability of endogenous HA content in untreated fascia.

Table 2.1 Mean ± SD HA content of TS-HA treated fascia using diffusion or vacuum methods

	TS-HA concentration/ number of passes	Mean ± SD HA content (µg/mg)	Sample size
Untreated	**NA**	0.41 ± 0.13	10
Diffusion 1x1 cm	**0.5%**	2.45 ± 1.42	15
	0.75%	6.90 ± 2.96	11
	1%	12.08 ± 4.10	5
	Increasing concentrations	3.56 ± 0.97	5
Vacuum 3 cm diameter	**0.5% 8 passes**	1.94 ± 0.52	3 grafts, 2 samples from each graft
	0.75% 1 pass	2.98 ± 0.98	6
	1% 2 passes	12.56 ± 5.07	3
	1% 8 passes	16.01 ± 8.39	3
	Increasing concentrations 8 passes total	1.43 ± 0.77	3 grafts, 2 samples from each graft

Distribution of HA in Treated Fascia

HA staining of TS-HA treated fascia, with or without cross-linking, demonstrated that the incorporated TS-HA was distributed throughout the fascia matrix, primarily around large fascicle bundles (Figure 2.1C-D). The autofluorescence from untreated fascia (Figure 2.1.A) was noticeably reduced following incubation in water (Figure 2.1.B).

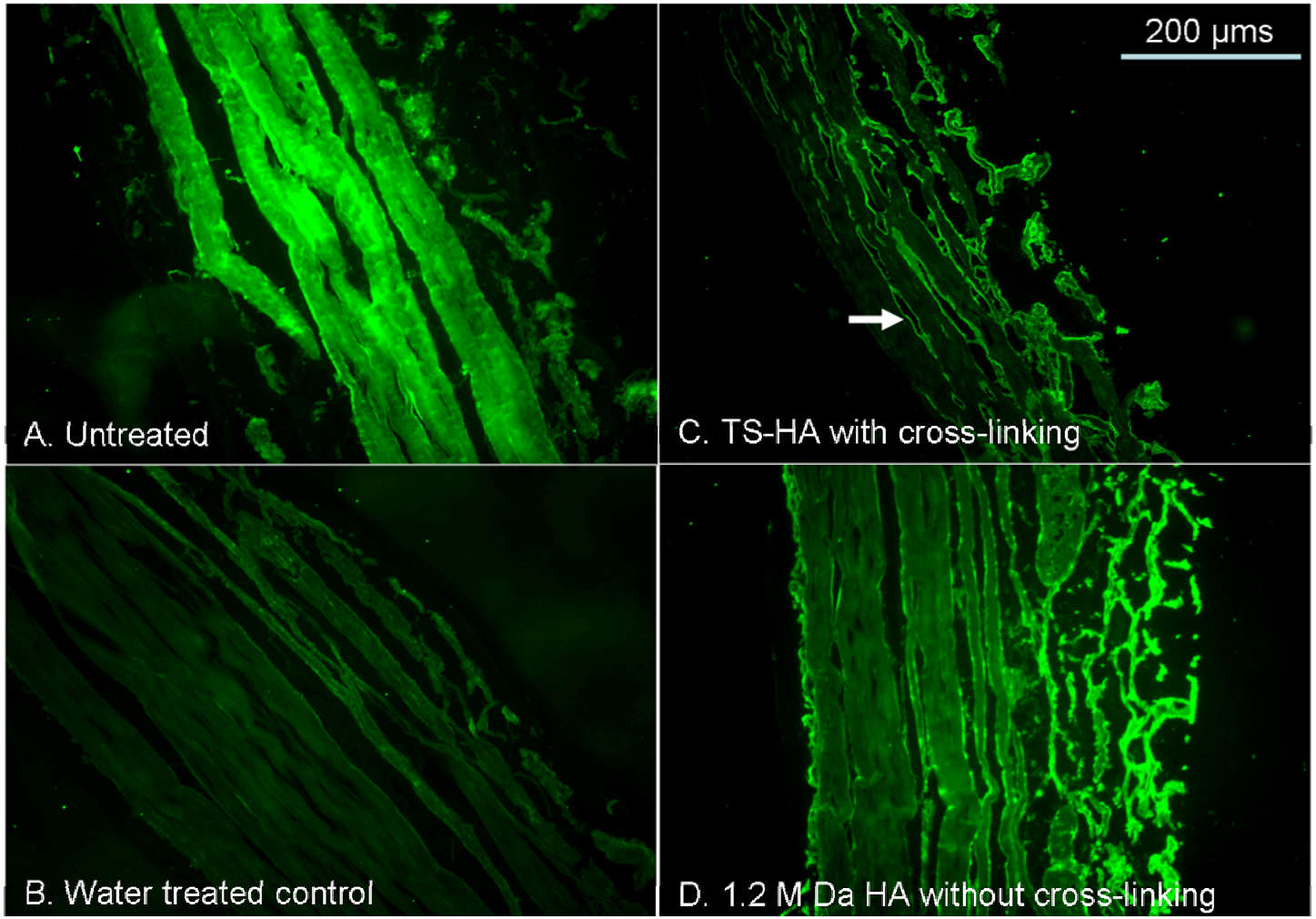

Figure 2.1 Representative HA staining of (A) untreated fascia, (B) water treated control, (C) TS-HA with cross-linking, and (D) 1.2 M Da HA without cross-linking treated fascia. The incorporated HA was localized throughout the depth of the scaffold, primarily around large fascicle bundles. Arrow denotes HA staining. 100x.

Pilot Study #2: *In vitro* Release of HA from Treated Fascia

Materials and Methods

Experimental Design

Fascia pieces (0.8x1 cm) were distributed into three treatment groups: TS-HA with cross-linking, 1.2 M Da HA without cross-linking, and untreated controls (n=10 per group). After treatment, pieces were cut in half. Time-zero HA content was quantified from one half, and the other half was subjected to an *in vitro* release experiment. Detailed methods are described below.

TS-HA Treatment of Fascia

For the TS-HA and HA treatment groups, fascia pieces (0.8x1 cm) were individually rehydrated in 1.5 ml of increasing concentrations (0.05→0.1→0.2→0.5%) of aqueous TS-HA or HA solution over a 24 hr period at 37ºC on a shaker as described previously. Both HA preparations had a molecular weight of 1.2 M Da. TS-HA was obtained from the Calabro Laboratory (Department of Biomedical Engineering, Cleveland Clinic), and HA was obtained from Acros Organics (Geel, Belgium). TS-HA solutions also contained 10 U/ml of horseradish peroxidase. After treatment, fascia pieces were rinsed with 3 ml of ultrapure water per side and blotted two times per side on a sterile towel to remove excess surface HA. Fascia pieces in the cross-linked group were submerged into 0.3% hydrogen peroxide solution in ultrapure water for 30 sec at room temperature with slight agitation and then allowed to sit covered on a glass dish at 4ºC for the reaction to continue overnight. Fascia pieces in the uncross-

linked group were submerged in water for 30 sec (instead of hydrogen peroxide) and also allowed to sit at 4ºC overnight. Following overnight incubation, all TS-HA treated fascia pieces were rinsed with 3 ml per side of ultrapure water to remove excess hydrogen peroxide. All treated fascia pieces were subsequently lyophilized. Lyophilized, untreated fascia served as control.

In Vitro Release of HA

After treatment, fascia pieces were cut in half. Time-zero HA content was quantified from the first half with HABP enzyme-linked immunosorbent assay (ELISA, Corgenix, Westminster, CO). The second half was incubated in 7 ml of PBS for 48 hr at 37°C on a shaker. Aliquots of 50 µl were taken from the PBS release solution at 1, 6, 24, and 48 hr and assayed with HABP ELISA.

HABP ELISA

Time-zero fascia pieces were digested with 5 mg/ml PK for approximately 24 hr at 60°C prior to ELISA quantification. The digested tissue samples, PBS release solutions, and HA reference solutions were processed according to the manufacturer's instructions. Briefly, samples were diluted 1:10 with reaction buffer and 100 µl was incubated in HABP-coated microwells for 1 hr. After four PBS washes, 100 µl of horseradish peroxidase-conjugated HABP was added to the wells for 30 min. After a second round of PBS washes, 100 µl of tetramethylbenzidine/hydrogen peroxide chromagen substrate was added for 30 min. Finally, 100 µl of stopping solution was added to the wells, and the optical

density at 450 nm of the resulting solution was read using a SpectraMax spectrophotometer (Molecular Devices, Sunnyvale, CA). HA concentrations of the samples were determined using a linear standard curve constructed from the reference solutions, and the mass of HA in the time-zero fascia samples and PBS release solutions was calculated.

Results

Previous experiments conducted in the Derwin Laboratory showed that the concentrations of cross-linked TS-HA solutions were underestimated by a factor of 5.5 with HABP ELISA (Appendix A). Consequently, a correction factor of 5.5 was applied to adjust the data to the correct HA concentration for cross-linked TS-HA treated fascia or solution samples.

On average, only 8% of the HA in TS-HA treated fascia with cross-linking was released by the end of the 48 hour incubation, while 77% of HA was released from HA treated fascia without cross-linking (Table 2.2). Nine percent of endogenous HA was released from untreated fascia during the *in vitro* release experiment.

Table 2.2 Mean ± SD time-zero HA amount as well as the amount and percent released after the 48 hour *in vitro* release experiment

	Untreated control	TS-HA with cross-linking	1.2 M Da HA without cross-linking
Time-zero HA amount (µg)	3.9 ± 0.9	153.1 ± 38.6	90.3 ± 10.3
HA amount released after IVR (µg)	0.4 ± 0.1	12.1 ± 5.2[†]	69.3 ± 21.3
Mean percent released after IVR	9%	8%	77%

[†]Includes 5X correction factor for cross-linked TS-HA
n=10 per group

At all time points, the amount of HA released from treated fascia without cross-linking was greater than the amount released by treated fascia with cross-linking or untreated controls, by as much as 100-fold at the one hour time point (Figure 2.2). A bolus of HA was released from treated fascia without cross-linking during the first hour, followed by relatively a small amount over the remaining 47 hours.

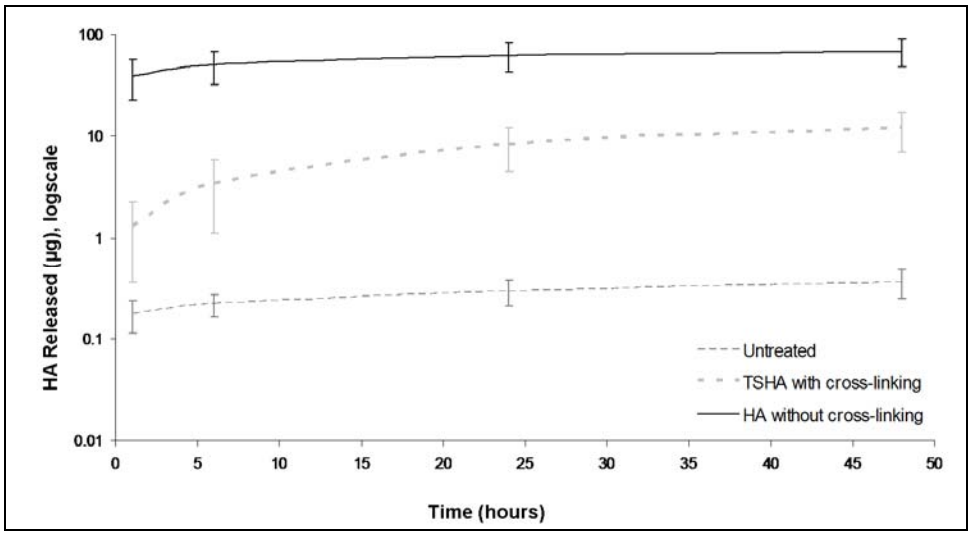

Figure 2.2 *In vitro* release profiles of untreated controls, TS-HA with cross-linking, and 1.2 M Da HA without cross-linking

Discussion

In these pilot experiments, several methods of TS-HA treatment were able to increase the amount of HA in fascia by at least an order of magnitude. The design criteria of up to 5 μg/mg TS-HA content could be achieved through the diffusion- and vacuum-based protocols. Furthermore, the incorporated HA was distributed throughout the tissue and, upon cross-linking of the TS-HA, was retained as a hydrogel network. It is also important to note that binding of bHABP to cross-linked TS-HA demonstrated that the structure of the HA molecule is maintained after tyramine substitution (74). The effectiveness of tyramine cross-linking in immobilizing HA within fascia was validated through an *in vitro* release experiment.

The results suggest that treatment methods can be tailored – by selecting either the diffusion or vacuum approach, increasing TS-HA solution concentrations, or increasing the number of passes – to achieve TS-HA concentrations that average up to 16 μg/mg in the tissue. Solution concentrations greater than 1% were assessed, but their increased viscosity made handling difficult and would be impractical for commercial manufacturing. Other means to enrich fascia with TS-HA were explored, but proved less effective and more tedious than diffusion or vacuum. For example, TS-HA solution was “centrifuged” into fascia ECM, similar in concept to vacuum treatment. Although HA staining of centrifugation treated fascia showed incorporation of HA into the tissue (data not shown), it was impractical to run the equipment for the lengths of time required for the TS-HA to infiltrate the tissue. Another delivery approach that was

investigated involved the injection of small volumes of TS-HA solution into various locations within a fascia piece. HA staining of injection-treated fascia was poor (data not shown), so further development of the method was not pursued.

Interestingly, untreated fascia sections exhibited autofluorescence, which was markedly diminished with water treatment. The fluorescent material may have been residual antibiotic (146) from the standard soak treatment performed at MTF and was presumably removed during the 24 hour incubation in water.

While treated fascia without cross-linking released a bolus of HA within the first hour of the release experiment, tyramine cross-linking was effective in immobilizing HA within fascia. This suggests that treated fascia, only when cross-linked, can be used to deliver a sustained concentration of HA to an injury site.

The diffusion-based treatment and characterization methods described here are not without limitations. Large variability in HA content from one treated piece to another (30-60% coefficient of variability) is one shortcoming and may be largely dictated by the inherent variability of fascia ECM, specifically with respect to physical properties such as surface smoothness, porosity of the matrix, and the amount of inter-fascicular space. Additionally, surface smoothness could be influenced by the extent to which the loose connective tissue, fat, and muscle were removed during processing at MTF. While these characteristics cannot be easily manipulated, the treatment method could be altered to achieve a uniform HA content across a treated fascia patch. One such improvement could involve the use of vacuum methods to impregnate fascia with HA, as opposed to the more passive diffusion method. From a manufacturing

standpoint, significant inter- or intra-sample variability in HA content is unfavorable, and future iterations of TS-HA treated fascia will need to address this issue. Secondly, samples from the release experiment were analyzed with HABP ELISA, an assay that indirectly quantifies HA concentration by measuring the intensity of colorimetrically-labeled HABP that binds to uninterrupted oligosaccharides of the HA chain. However, the formation of dityramine bridges upon cross-linking of the TS-HA could inhibit HABP from binding to large segments of the HA chain, thereby underestimating the HA concentration. This was confirmed in a previous experiment (Appendix A). Hence, the use of HABP ELISA to quantify HA content will be discontinued. Instead, future work will continue to use FACE, an electrophoretic-based method that allows individual disaccharide units to be measured with a picomole resolution (145). Lastly, HA treated fascia demonstrated weaker staining than cross-linked TS-HA treated fascia, which could be due to leaching of HA during fixation in aqueous formalin or during other steps of the staining process involving aqueous solutions (147). To resolve this issue for future experiments, HA staining will only be performed on cross-linked TS-HA sections, which should be representative of the localization of HA for all treated fascia. As well, an alcohol-based fixative will be used in lieu of formalin to prevent leaching of HA from histologic sections (147).

In summary, these preliminary studies demonstrate that diffusion-based methods are effective in enriching fascia ECM with up to 5 μg/mg of TS-HA and that the incorporated TS-HA is distributed throughout the tissue as a hydrogel network. Furthermore, dityramine cross-linking is effective in immobilizing HA

within fascia ECM. Collectively, these preliminary data provide guidance for the treatment and characterization of TS-HA enriched fascia ECM in subsequent experiments.

Chapter 3

Pilot Study: Host Response to Tyramine Substituted-Hyaluronan Enriched Fascia

Introduction

Characterization of the host response may predict the tissue remodeling outcome of an implanted extracellular matrix (ECM) scaffold (107,108). Successful and constructive remodeling is more likely to result when the scaffold exhibits host cell repopulation, tissue ingrowth, vascularization, organized collagenous tissue, and minimal inflammation (111).

The rat abdominal wall defect model is a well-established tool for studying the host inflammatory response to an implanted biomaterial (112,120,121). Although the material of interest is not evaluated at the intended site of clinical application, the rodent model serves as an affordable preclinical means to

investigate *in vivo* material-tissue interactions and inflammation for a large number of samples. The presence of inflammatory cells (such as neutrophils, lymphocytes, macrophages, and giant cells) can be semi-quantitatively scored at various time points following implantation.

The anti-inflammatory properties of high molecular weight hyaluronan (HA) are well-established, and numerous studies in both cell culture and *in vivo* model systems demonstrate that HA can inhibit the infiltration, proliferation, and cytokine production of various inflammatory cells (75-80). Hence, HA augmentation of fascia ECM scaffold may be effective in modulating chronic inflammation within the scaffold. However, characterization of the host inflammatory response to HA treated fascia has not been previously reported.

The objective of this pilot study was to evaluate the host response to tyramine substituted-hyaluronan (TS-HA) enriched fascia in a rat abdominal wall defect model. Total cell density was quantified with image processing techniques, and the presence of various inflammatory cells, vascularity, and overall inflammation were scored by a board-certified pathologist. TS-HA treated fascia with cross-linking was hypothesized to exhibit an increase in total cell density, a decrease in lymphocyte, macrophage, and giant cell densities, as well as a decrease in overall inflammation compared to water treated controls and HA treated fascia without cross-linking.

Materials and Methods

Experimental Design

Decellularized, lyophilized, sterile human fascia lata derived from the iliotibial tract of donors aged 18-55 years was obtained from the Musculoskeletal Transplant Foundation (Edison, NJ). Fascia pieces (0.8x1 cm) were distributed into three treatment groups: untreated controls, TS-HA with cross-linking, and HA without cross-linking (n=4 per group). Twelve rats were used for rat abdominal wall implantation at two time points. Rats were sacrificed at 1 and 4 weeks (n=2 per treatment group per time point), and the implants were harvested for histologic analysis of cell types, vascularity, and inflammation. Detailed methods are described below.

TS-HA Treatment of Fascia

For the TS-HA and HA treatment groups, fascia pieces (0.8x1 cm) were individually rehydrated in 1.5 ml of 0.5% aqueous TS-HA or HA over a 24 hr period at 37ºC on a shaker. Both HA preparations had an average molecular weight of 1.2 M Da. TS-HA was obtained from the Calabro Laboratory (Department of Biomedical Engineering, Cleveland Clinic), and HA was obtained from Acros Organics (Geel, Belgium). TS-HA solutions also contained 10 U/ml of horseradish peroxidase (Sigma, St. Louis, MO). After treatment, fascia pieces were rinsed with 3 ml of ultrapure water per side and blotted two times per side on a sterile towel to remove excess surface HA. Fascia pieces in the cross-linked group were submerged into 0.3% hydrogen peroxide solution (Fisher, Pittsburgh,

PA) in ultrapure water for 30 sec at room temperature with slight agitation and then allowed to sit covered on a glass dish at 4ºC for the reaction to continue overnight. Fascia pieces in the uncross-linked group were submerged in water for 30 sec (instead of hydrogen peroxide) and also allowed to sit at 4ºC overnight. Following overnight incubation, all TS-HA treated fascia pieces were then rinsed with 3 ml of ultrapure water per side to remove excess hydrogen peroxide. All treated fascia pieces were subsequently lyophilized. Lyophilized, untreated fascia served as control.

Rat Abdominal Wall Defect Model

All procedures were performed in accordance with the National Institutes of Health guidelines for care and use of laboratory animals and were approved by the Institutional Animal Care and Use Committee at the Cleveland Clinic.

Twelve adult, male Lewis rats were used for this study (450-600 g, Harlan, Indianapolis, IN). Each rat was anesthetized with an intramuscular injection of ketamine, xylazine, and acepromazine (30/6/1 mg/kg), and the abdomen was prepared for aseptic surgery. Via a ventral midline incision, a 0.8x1 cm partial-thickness defect was created in the anterior sheath adjacent to the linea alba. The anterior sheath was removed, and the underlying rectus muscle, transversalis fascia, and peritoneum were left intact. One 0.8x1 cm fascia piece from each patch was wetted in saline for 10 min, and secured into the defect using four corner sutures of 5-0 Prolene. The skin incision was closed using 4-0 chromic gut suture, and the rat was allowed to recover from anesthesia under a

heating lamp. For analgesia, each rat received of 0.15 mg/kg buprenorphine post-operatively, 12 hours later, and thereafter as needed for breakthrough pain. For prophylactic treatment of bacterial infection, rats were given tetracycline supplemented drinking water (1 mg/ml) post-operatively and for roughly three days afterwards. Rats were also given tetracycline supplemented water for up to two days prior to surgery to allow acclimation to taste. Rats were housed individually for the duration of the study.

Euthanasia and Histologic Processing

At 1 and 4 wk, rats were sacrificed via carbon dioxide asphyxiation and cervical dislocation (n=2 per treatment group per time point). The fascia graft and underlying muscle were harvested, fixed in 4% paraformaldehyde for 8 hr, and routinely processed for paraffin embedding. Five-micron thick longitudinal sections were cut and stained with hematoxylin and eosin (H&E).

Cell Density within Fascia Grafts

RBG images of the H&E sections were acquired using a Retiga 2000R CCD digital camera (1600x1200 pixel, Q-Imaging, Burnaby, B.C., Canada) attached to a Leica DM 4000 upright microscope (Heidelberg, Germany). Image acquisition was fully automated using an X, Y, Z-motorized stage (Prior Scientific, Rockland, MA) managed by Objective Imaging Oasis 4i controller (Kansasville, MI) and Image-Pro 6.0 software (Media Cybernetics, Silver Spring, MD). Images (100x) of the entire section were captured and knitted into a single montage.

Image-Pro software (Media Cybernetics, Bethesda, MD) was used to count hematoxylin-stained nuclei by converting the image to grayscale, inverting the image, manually selecting the fascia scaffold as the region of interest by tracing the perimeter of the graft, and counting the number of nuclei above a threshold intensity. Respective tissue area was determined by counting the number of pixels in the region of interest and converting to square area. Total cell density within the graft was calculated for three sections per rat.

Semi-quantitative Histologic Analysis

One representative H&E stained section from each rat was semi-quantitatively scored by a blinded, board-certified pathologist (Thomas Bauer, MD, PhD, Anatomic Pathology, Cleveland Clinic). Sections were scored for the presence of inflammatory cells – neutrophils, lymphocytes, macrophages, and giant cells – as well as vascularity, using a scale from 0 (no cellular response) to 3 (intense/severe presence).

In addition, chronic inflammation (defined largely by the persistent presence of lymphocytes) at four weeks was qualitatively ranked by the same pathologist (TB) on two occasions, separated by a two-month time period.

Statistical Analysis

Given the low sample size and pilot nature of the study, the total cell densities from all six slides (three slides from two rats) were averaged for each group at each time point. Significant differences in total cell density between

untreated fascia, TS-HA with cross-linking, and HA without cross-linking were assessed with two-way ANOVA. Exploratory one-way ANOVA at both time points with experimental group as the factor was performed. Multiple comparisons were completed with Holm-Sidak test where untreated fascia served as the control. A p value ≤ 0.05 was considered significant.

Results

All animals survived the length of the study period. The histologic results from one rat, implanted with a TS-HA graft with cross-linking for one week, were excluded from the study due to a bacterial infection as determined by the pathologist from the H&E stained sections.

Descriptive Histology

Fascia grafts of all experimental groups were still visible and discernable from the underlying muscle at one (Figure 3.1A-C) and four weeks (Figure 3.2A-C). At both time points, fascia in all groups elicited a chronic inflammatory host response predominantly seen at the periphery of the grafts with fewer cells in the central region (Figure 3.1D-F, 3.2D-F). The cellular infiltrate was composed of lymphocytes, macrophages, and a mild to moderate degree of giant cells. Remnant fascia architecture was identified as acellular bundles of dense collagen (Figure 3.1D-F, 3.2D-F). At one week, cells were most prominent around the grafts, and visual differences in total cell density within the grafts were not apparent between the three groups (Figure 3.1D-F). At four weeks, cross-linked TS-HA treated fascia appeared to have the greatest cellularity *within the graft* of the three groups, and tracks of cells between large fascicle bundles were evident (Figure 3.2E). At four weeks, the central region of all grafts showed variable cellularity ranging from completely acellular regions to regions with a low density cells to tracks or pockets of dense cellular infiltrate (Figure 3.2D-F). A

variable degree of vascularity was observed within grafts of all groups at both time points.

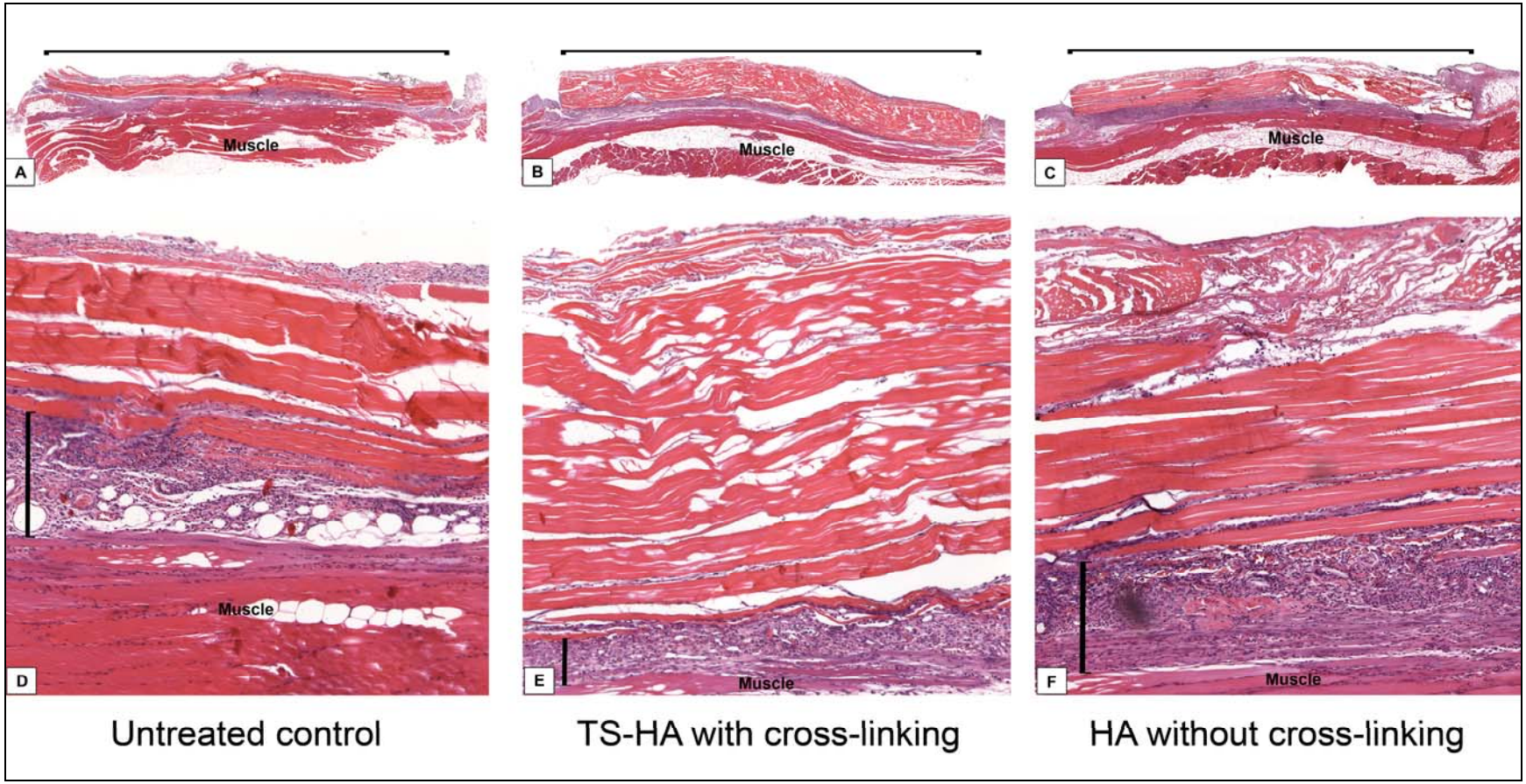

Figure 3.1 Representative H&E images at one week of (A, D) untreated control, (B, E) TS-HA with cross-linking, and (C, F) 1.2 M Da HA without cross-linking treated fascia. (A-C, 10x) Fascia grafts of all experimental groups (horizontal brackets) were still visible and discernable from the underlying muscle. (D-F, 100x) Fascia in all groups elicited a chronic inflammatory host response predominantly seen at the periphery of the grafts (vertical brackets) with fewer cells in the central region. Remnant fascia architecture was identified as acellular bundles of dense collagen. Visual differences in total cell density within the fascia grafts were not apparent among the three groups.

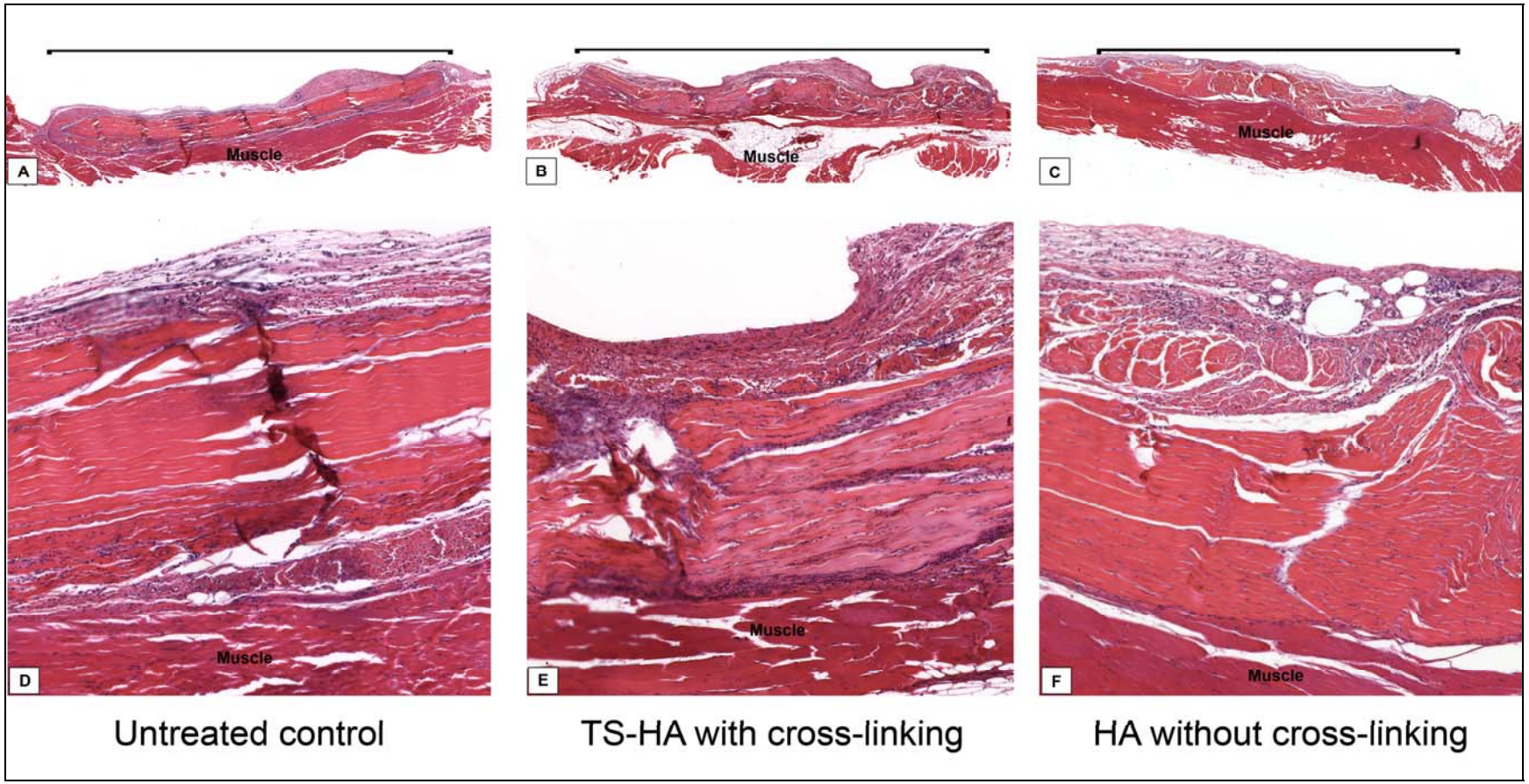

Figure 3.2 Representative H&E images at four weeks of (A, D) untreated control, (B, E) TS-HA with cross-linking, and (C, F) 1.2 M Da HA without cross-linking treated fascia (A-C, 10x). Fascia grafts of all experimental groups (horizontal brackets) were still visible and discernable from the underlying muscle. (D-F, 100x) Fascia in all groups elicited a chronic inflammatory host response, predominantly seen at the periphery of the grafts with fewer cells in the central region. Remnant fascia architecture was identified as acellular bundles of dense collagen. Cross-linked TS-HA treated fascia grafts had visibly increased cellularity of the three groups, and tracks of cells between large fascicle bundles were evident (E). The central region of all grafts showed variable cellularity ranging from completely acellular regions to regions with a low density of cells to tracks or pockets of dense cellular infiltrate.

Cell Density within Fascia Grafts

The average total cell densities for each group at both time points are presented in Table 3.1. Based on the two-way ANOVA model, there were no statistical differences in total cell density between untreated control, TS-HA with cross-linking, and HA without cross-linking at either time point, but total cell density increased significantly from one week to four weeks post-implantation ($p<0.001$).

Table 3.1 Mean ± SD total cell density at implantation time points

Time point	Untreated Control (cells/mm^2)	TS-HA with cross-linking (cells/mm^2)	HA without cross-linking (cells/mm^2)
1 week	1230 ± 520	1080 ± 110*	1330 ± 540
4 week	2100 ± 550†,‡	2860 ± 300†	2720 ± 660‡

† p=0.02 by exploratory one-way ANOVA
‡ p=0.06 by exploratory one-way ANOVA.
n=6 per group per time point (triplicate measurements from two rats)
* n=3 (triplicate measurements from one rat)

As detected by exploratory one-way ANOVA, total cell density within cross-linked TS-HA treated fascia grafts was significantly greater than untreated controls at four weeks (p=0.02). HA treated grafts without cross-linking demonstrated a trend towards an increase in total cell density compared to untreated controls (p=0.06).

Semi-quantitative Histologic Analysis

The histologic scores for the presence of neutrophils, lymphocytes, macrophages, giant cells, and vascularity for each group at both time points are presented in Table 3.2. Statistics were not performed because of the low-sample size of this pilot study, but the following observations were made. At one week, a mild infiltrate of neutrophils was present in TS-HA with cross-linking and HA without cross-linking treated grafts, which decreased by the four week time point. At one week, TS-HA with cross-linking treated fascia had fewer lymphocytes and macrophages and a similar number of giant cells as untreated and HA without cross-linking treated fascia. At one week, a greater degree of vascularity was present in TS-HA with cross-linking and HA without cross-linking treated grafts than untreated controls. At four weeks, grafts from all groups exhibited an absence of neutrophils, a moderate to severe infiltrate of lymphocytes and macrophages, a mild to moderate infiltrate of giant cells, and a mild degree of vascularity.

Table 3.2 Histologic scores of untreated control, TS-HA treated fascia with cross-linking, and HA treated fascia without cross-linking

Time Point	Group	Histologic Outcomes				
		Neutrophils	Lymphocytes	Macrophages	Giant Cells	Vascularity
1 week	Untreated control	0, 0	2, 2	3, 3	1, 1	2, 2
	TS-HA with cross-linking†	1	1	2	1	3
	HA without cross-linking	1, 0	3, 2	3, 3	2, 1	3, 3
4 week	Untreated control	0, 0	3, 3	3, 2	2, 1	1, 1
	TS-HA with cross-linking	0, 0	3, 2	2, 3	1, 2	2, 1
	HA without cross-linking	0, 0	3, 3	3, 3	2, 1	1, 1

Scale: 0=none, 1=mild, 2=moderate, 3=severe
Individual scores from two rats per group per time point are listed for each histologic outcome.
†One rat excluded from study due to bacterial infection

The inflammatory rankings of the four week histologic sections are shown in Table 3.3. The rank of a given section did not change by more than one position between the two reviews by the same pathologist. The data may suggest that TS-HA treatment with cross-linking is associated with the least amount of chronic inflammation of the three groups.

Table 3.3 Ranking of chronic inflammation for untreated control, TS-HA treated fascia with cross-linking, and HA treated fascia without cross-linking at four weeks

Treatment Group	Rat Number	Inflammation Ranking (2 repeats)
Water control	1	5, 6
	2	4, 3
TS-HA with cross-linking	3	3, 4
	4	1, 1
HA without cross-linking	5	6, 5
	6	2, 2

Scale: 1=least, 6=most
Individual scores from one rat per group at the four week implantation time point evaluated on two separate occasions by the same reviewer are listed.

Discussion

In this study, the host response to TS-HA treated fascia with cross-linking was evaluated in a rat abdominal wall defect model with the hypothesis that treated fascia would exhibit an increase in total cell density, a decrease in lymphocyte, macrophage, and giant cell densities, and less chronic inflammation than untreated controls and HA treated fascia without cross-linking. At four weeks, TS-HA treated fascia with cross-linking exhibited an increase in total cell density compared to untreated controls. Semi-quantitative evaluation of histologic sections demonstrated that TS-HA treated fascia with cross-linking exhibited a moderate to severe infiltrate of lymphocytes and macrophages and a mild to moderate infiltrate of giant cells, similar to untreated controls and HA treated fascia without cross-linking. However, cross-linked treated fascia demonstrated possibly lower rankings for overall chronic inflammation compared to untreated controls.

The untreated controls in this study demonstrate the host response to unmodified, decellularized, xenogenic fascia ECM. At four weeks, untreated fascia supported a high density of cells, consisting largely of lymphocytes and macrophages and, to a lesser extent, giant cells. The lymphocytic response may be a consequence of an immune reaction to the xenograft and may be specifically attributed to remnant cellular components (43,62,148) or antibiotic (149,150) that remains in the fascia even after processing. Host recognition of the slight molecular differences in the proteoglycans and glycoproteins in tissue from a different species (151,152) or changes in protein structure after

processing (153) may have also triggered the adaptive immune system. Whether or not the lymphocyte aggregation clears has yet to be determined with longer implantation time points.

Although untreated fascia was highly infiltrated by macrophages, the predominant phenotype was not identified, because immunostaining for the cell surface markers of M1 pro-inflammatory or M2 pro-remodeling macrophages was not performed. Because macrophages are involved in both remodeling and inflammatory processes, classification of macrophage polarization may be useful in predicting downstream outcomes following graft implantation (107,108). Characterization of macrophage polarization will be explored in future studies. In addition, although the presence of giant cells – the hallmark of the foreign body response – was noted, no fibrous capsule was observed at four weeks.

HA treatment appeared to have no effect on lymphocyte, macrophage, or giant cell density within fascia ECM according to the semi-quantitative scoring data. However, when the slides were ranked for chronic inflammation, the rankings suggest that cross-linked TS-HA treated fascia had less chronic inflammation than untreated controls. This discrepancy could be a reflection of the limitations of the scoring system used to assess histologic outcomes. With only four discrete levels, each of which represents a qualitative descriptor of cell density rather than a quantitative range, the scoring system employed herein would not allow for modest differences between groups to be detected. For future semi-quantitative histologic evaluations, a scoring system adapted from ISO

10993-6, which has five discrete levels that are associated with a qualitative range of cell densities per high powered field, will be used.

Taken together, the increase in total cell density and lower chronic inflammatory ranking of cross-linked TS-HA treated fascia suggest that there are more *non-inflammatory* cells within cross-linked treated grafts than untreated controls. Thus, the presence of immobilized HA within fascia ECM may promote the infiltration, adhesion, and/or proliferation of non-inflammatory cells (i.e., fibroblasts). This hypothesis is supported by several *in vitro* cell culture studies which demonstrate that HA facilitates fibroblast migration and proliferation (84,86-89).

At one week, a thick cellular periphery surrounding the fascia graft could be seen in H&E stained sections for all groups. The cellular periphery was markedly diminished by four weeks, presumably as a result of cell infiltration into the graft over time. This hypothesis is supported by the significant increase in total cell density within fascia grafts from one to four weeks for all groups.

This pilot study has several limitations. A larger sample size is necessary to properly determine statistically significant differences in total cell density, histologic scoring, and chronic inflammatory ranking. The data are too preliminary to be conclusive, but do provide some indication of the host response to untreated fascia, TS-HA treated fascia with cross-linking, and HA treated fascia without cross-linking. Second, the latest implantation time point investigated in this study was four weeks. To determine whether or not the lymphocyte aggregation clears and to observe end-stage remodeling, longer

implantation times are necessary and will be evaluated in future experiments. Third, the uncross-linked fascia group in this study was treated with unmodified HA rather than uncross-linked TS-HA. However, the same unmodified HA (with respect to molecular weight and manufacturer) served as the base material from which the TS-HA was synthesized.

Although preliminary, these findings suggest that TS-HA treated fascia with cross-linking was associated with a greater total cell density and possibly less chronic inflammation than untreated controls, thus providing the rationale for the continued investigation of TS-HA treated fascia in this dissertation. Furthermore, this study demonstrates and gives guidance on the use of a rat abdominal wall defect model in conjunction with a semi-quantitative scoring system to assess host response. Future work described in this dissertation will include longer implantation time points, phenotyping of the M1 pro-inflammatory and M2 pro-remodeling macrophages, use of a modified version of ISO-10993 for semi-quantitative histologic evaluation, larger sample sizes, and the use of only TS-HA for all treatment groups.

Chapter 4

Characterization and Host Response to Tyramine Substituted-Hyaluronan Enriched Fascia

Introduction

Several naturally-occurring, extracellular matrix (ECM) devices are commercially available for rotator cuff repair augmentation, but none has yet demonstrated the appropriate biological and mechanical properties for tendon healing. Enriching fascia ECM with exogenous high molecular weight hyaluronan (HA) – a molecule known to play a critical role in morphogenesis, wound repair and inflammation (71,73,90,154) – may foster the formation of a functional tendon-bone bridge by minimizing chronic inflammation within the scaffold and enhancing fibroblast infiltration. The current study investigates the use of tyramine substituted-hyaluronan (TS-HA) to immobilize high molecular weight HA within fascia ECM by means of tyramine cross-linking, thus providing a sustained presence of HA to the augmented repair site. However, the extent to which high

molecular weight HA can modulate the host response to fascia ECM, particularly in a manner which would promote a constructive remodeling outcome, has not been previously investigated.

The host inflammatory response, including the macrophage component, appears to be a critical determinant, and perhaps predictor, of successful and constructive remodeling of an implanted biomaterial (107,108). Macrophage phenotypes span a continuous spectrum, the two extremes of which are represented by the M1 pro-inflammatory and M2 pro-remodeling activated forms (117). M1 macrophages produce large amounts of reactive oxygen species and inflammatory cytokines, express CCR7 as a cell surface marker, and are associated with tissue destruction and inflammation (107,117). Macrophages of the M2 phenotype are characterized by CD163 as a cell surface marker and are associated with angiogenesis as well as tissue repair and remodeling (107,117).

The objective of this study was to build upon the pilot studies outlined in Chapters 2 and 3 and to characterize the host inflammatory response as well as the macrophage polarization to HA enriched fascia ECM. Fascia was treated with TS-HA, with or without cross-linking, using a diffusion-based protocol, and the resulting TS-HA content, distribution, and retention was characterized. The host response to fascia enriched with 5-10 micrograms of HA per milligram of dry weight tissue (μg/mg) was investigated in a rat abdominal wall defect model. The presence of various inflammatory cells, non-inflammatory cells, total cellularity, vascularity, and macrophage polarization into the M1 and M2 phenotypes were scored. TS-HA treated fascia with cross-linking was hypothesized to exhibit lower

lymphocyte, plasma cell, macrophage, and giant cell densities, a higher fibroblast-like cell density, and a greater proportion of M2 macrophages than M1 macrophages in comparison to water treated controls and treated fascia without cross-linking.

Materials and Methods

Experimental Design

Decellularized, lyophilized, sterile human fascia lata derived from the iliotibial tract of donors aged 18-55 years was obtained from the Musculoskeletal Transplant Foundation (Edison, NJ). Fascia patches (5x5 cm) were distributed into three treatment groups: water treated control, TS-HA with cross-linking, and TS-HA without cross-linking (n=8-20 patches per group, Figure 4.1). After treatment, HA content was quantified. TS-HA treated fascia patches with a mean concentration of 5-10 μg/mg were selected for subsequent experiments (n=8 per group). Each fascia patch was then divided into samples that were used for an *in vitro* retention experiment, HA staining, and rat abdominal wall implantation at two time points. Forty-eight rats were used for the host response study (n=16 per treatment group). Rats were sacrificed at one and three months (n=8 per group per time point), and the implants were harvested for histologic analysis of cell types and vascularity. Detailed methods are described below.

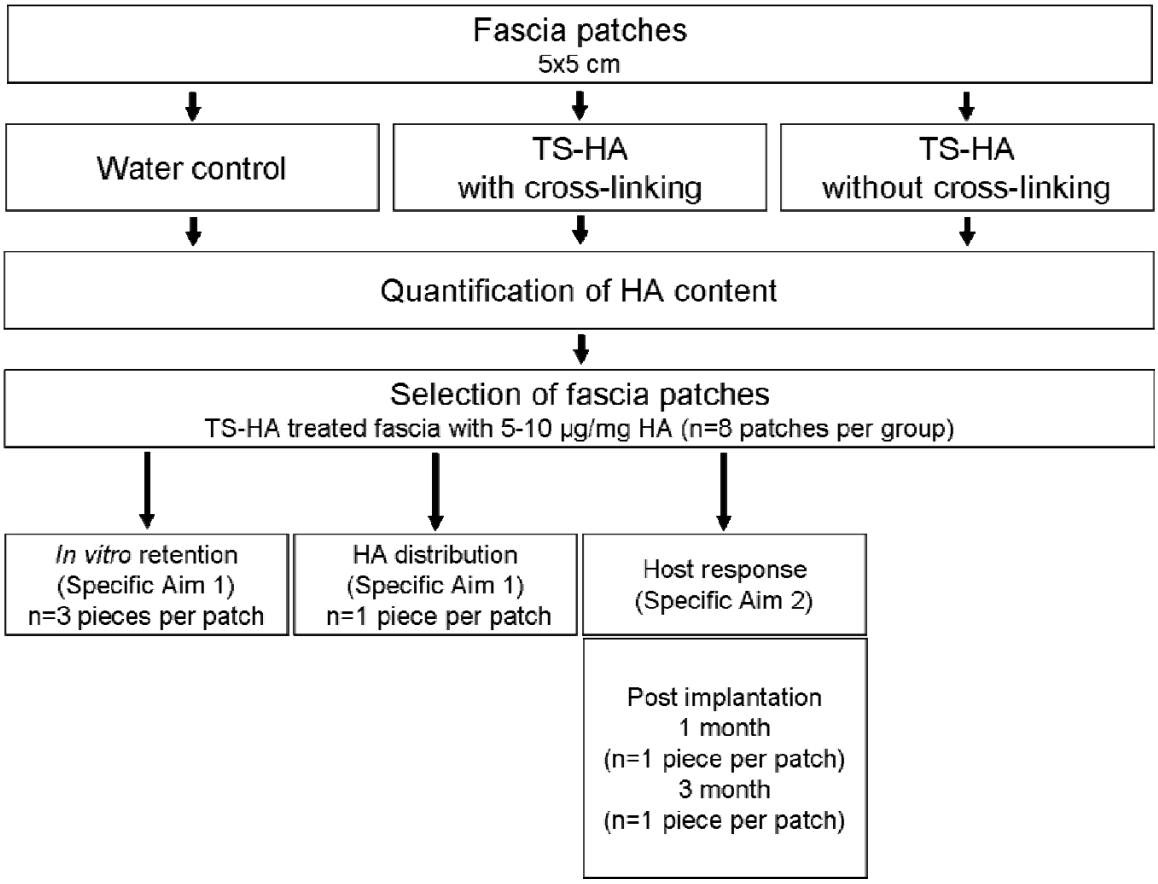

Figure 4.1 Experimental design for TS-HA treatment of fascia, the *in vitro* retention experiment, HA staining, and the rat abdominal wall implantation study

TS-HA Treatment of Fascia

For the two TS-HA treatment groups, each fascia patch (5x5 cm) was rehydrated in 30 ml of 0.75% TS-HA solution (0.9-1 M Da MW, Lifecore Biomedical, Chaska, MN) in ultrapure water for 24 hr at 37ºC on a shaker. The solutions used to treat cross-linked patches also contained 10 U/ml of horseradish peroxidase (Sigma, St. Louis, MO). After treatment, the patches were rinsed once in 30 ml of ultrapure water for 30 sec and blotted two times per side on a sterile towel to remove excess surface TS-HA. Treated patches in the uncross-linked group were then rinsed in 125 ml of ultrapure water for 5-20 min

at 37ºC on a shaker. Patches in the cross-linked group were submerged in 30 ml of a 0.3% hydrogen peroxide solution (Fisher, Pittsburgh, PA) in ultrapure water for 30 sec at room temperature with slight agitation and then allowed to sit covered on a glass dish at 4ºC for the reaction to continue overnight. Cross-linked patches were subsequently rinsed with 125 ml of ultrapure water for 24 hr at 37ºC on a shaker to remove excess horseradish peroxidase, hydrogen peroxide, and any uncross-linked TS-HA. Fascia patches rehydrated in 30 ml of ultrapure water for 24 hr at 37ºC served as controls. All fascia patches were subsequently lyophilized. A diagram outlining the treatment methods for the three experimental groups is shown in Figure 4.2.

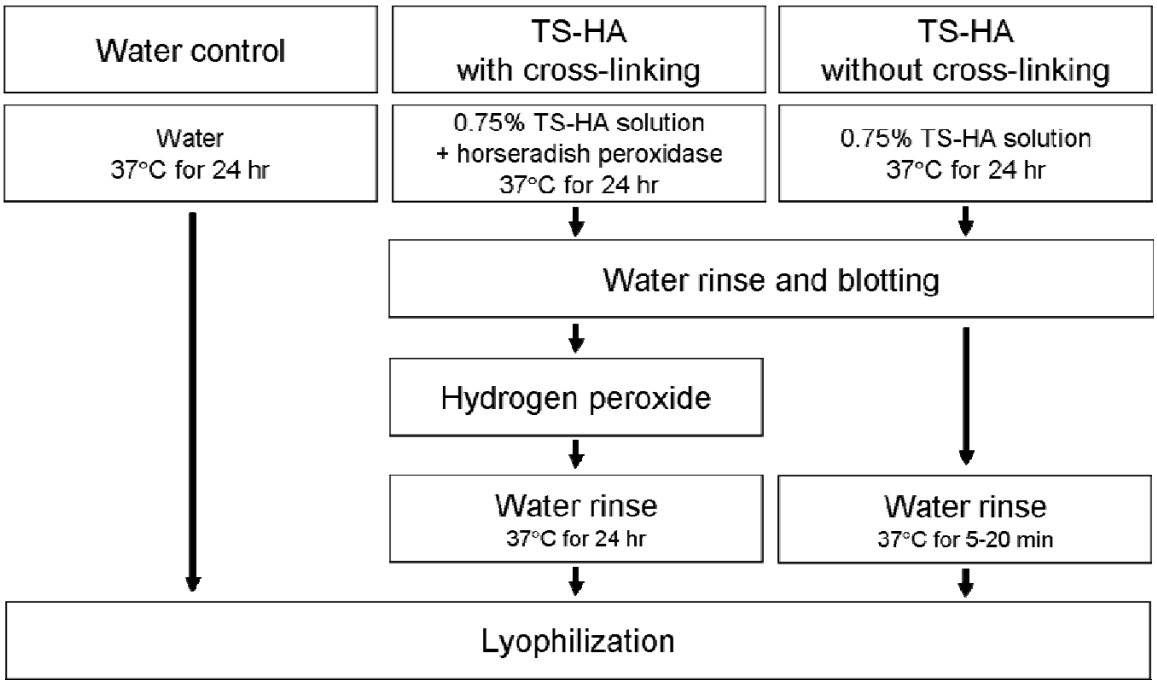

Figure 4.2 Treatment methods for water, TS-HA with cross-linking, and TS-HA without cross-linking treated fascia

HA Content of Treated Fascia

From each 5x5 cm patch, triplicate pieces that together represented ~10% of total patch volume were used to estimate the mean HA content of the entire patch. HA content was quantified using fluorophore-assisted carbohydrate electrophoresis (FACE) according to the previously described methods in Chapter 2 (62,145). Briefly, tissue samples were rehydrated, digested with proteinase K (PK, Fisher Biotech, Fair Lawn, NJ), and centrifuged to remove undigested tissue residue. The glycosaminoglycans (GAG) released into the supernatant fraction were isolated by ethanol precipitation. After extensive digestion of the resuspended ethanol pellet with hyaluronidase SD and chondroitinase ABC (both from Seikagaku America, Falmouth, MA), the resulting GAG disaccharides were tagged with the fluorophore 2-aminoacridone (AMAC, Molecular Probes, Eugene, OR), separated by electrophoresis, and the HA disaccharides were quantified using ultraviolet imaging and analysis.

All of the HA in water treated and uncross-linked TS-HA treated samples was recovered in the ethanol precipitate fraction of the PK supernatant. However, the cross-linked TS-HA treated samples required additional processing for FACE analysis, since the TS-HA hydrogel generated within the fascia by the cross-linking reaction was not solubilized by digestion with PK alone. Thus, both the PK pellet and supernatant fractions were processed for FACE analysis. The PK supernatant fraction was incubated with 18 U/ml of testicular hyaluronidase (Sigma) overnight at 37°C to solubilize cross-linked TS-HA hydrogel. After 5 min boiling to deactivate the PK, a 400 µl aliquot was dried in a speed-vac and

precipitated in 77% ethanol as previously described (Chapter 2). Both the ethanol precipitate and the aspirate were dried, resuspended in 200 µl of 100 mM ammonium acetate, digested with hyaluronidase SD and chondroitinase ABC, fluorotagged with AMAC, and electrophoresed according to the standard protocol. The PK pellet fraction was resuspended in 200 µl of 1 M ammonium acetate, pH 7.0, and then precipitated in 77% ethanol following previously described methods (Chapter 2). The precipitate was resuspended in 200 µl of 100 mM ammonium acetate, digested with 5 U/ml testicular hyaluronidase for 48 hr at 37°C, and the hyaluronidase digest was centrifuged at 10.5 krpm for 15 min. The resulting supernatant (a 10 µl aliquot was resuspended in 190 µl of 100 mM ammonium acetate) and pellet (resuspended in 200 µl of 100 mM ammonium acetate) fractions were further digested with hyaluronidase SD and chondroitinase ABC, fluorotagged with AMAC, and electrophoresed according to the standard protocol. Treated fascia patches, with or without cross-linking, that had a mean TS-HA content of 5-10 µg/mg were selected for all subsequent experiments (n=8 patches per group).

In Vitro Retention of HA

From each 5x5 cm TS-HA treated patch, with or without cross-linking, triplicate 0.8x1 cm pieces that together represented ~10% of the total patch volume were obtained. Each piece was rehydrated in 1.2 ml of PBS and incubated for 72 hr at 37ºC on a shaker, after which the TS-HA content in the fascia was measured with FACE according to methods described above.

Distribution of HA in Treated Fascia

Representative ~0.4x1 cm pieces from the TS-HA with cross-linking and water control groups (n=6 per group) were rehydrated in 100 µl of ultrapure water for 6 hr at room temperature and embedded in Tissue-Tek OCT compound (Sakura Finetek, Torrance, CA). Five-micron longitudinal frozen sections were cut and fixed in a 4% paraformaldehyde/6% glacial acetic acid/82% ethanol aqueous solution (147) for 10 min, followed by three 1 min PBS rinses. Sections were blocked in 3% normal goat serum (Jackson ImmunoResearch Labs, Inc., West Grove, PA) for 30 min and incubated with biotinylated HA binding protein (bHABP, Calbiochem, San Diego, CA) diluted 1:100 in PBS in a humidified chamber at 4°C overnight. Sections were then rinsed in PBS three times for 5 min each, incubated with Alexa Fluor 488-conjugated streptavidin (Molecular Probes, Carlsbad, CA) diluted 1:500 in PBS for 45 min, and rinsed again in PBS. All steps were performed at room temperature, unless otherwise specified. Porcine cartilage served as a positive control and sections incubated with PBS in place of bHABP served as negative controls. All slides were mounted with Vectashield mounting media (Vector Labs, Burlingame, CA).

Rat Abdominal Wall Defect Model

All procedures were performed in accordance with the National Institutes of Health guidelines for care and use of laboratory animals and were approved by the Institutional Animal Care and Use Committee at the Cleveland Clinic.

Forty-eight adult, male Lewis rats were used for this study (450-600 g, Harlan, Indianapolis, IN). Each rat was anesthetized with an intramuscular injection of ketamine, xylazine, and acepromazine (30/6/1 mg/kg). The abdomen was prepared for aseptic surgery. Via a ventral midline incision, a partial-thickness 0.8x1 cm defect was created in the anterior sheath adjacent to the linea alba. The anterior sheath was removed and the underlying rectus muscle, transversalis fascia, and peritoneum were left intact. One 0.8x1 cm fascia piece from each patch was wetted in saline for 10 min, and secured into the defect using four corner sutures of 5-0 Prolene (Figure 4.3). On the contralateral side of the linea alba, a second defect (0.4x4.5 cm) was created and replaced with a 0.4x4.5 cm fascia piece, wetted as above, from the same patch for mechanical property analysis (mechanical properties data presented in Chapter 5). The skin incision was closed using 4-0 chromic gut suture, and the rat was allowed to recover from anesthesia under a heating lamp. For analgesia, each rat received 0.15 mg/kg buprenorphine post-operatively, 12 hours later, and thereafter as needed. Rats were housed individually for the duration of the study.

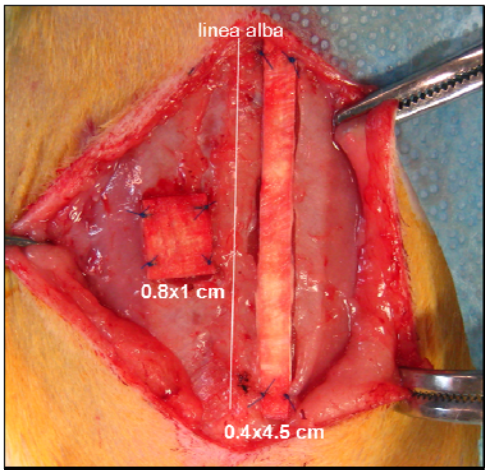

Figure 4.3 The rat abdominal wall defect model. One fascia piece from each patch was secured into a 0.8x1 cm defect. On the contralateral side of the linea alba, a second defect (0.4x4.5 cm) was created and replaced with a fascia piece from the same patch for mechanical property analysis (mechanical properties data presented in Chapter 5).

Euthanasia and Tissue Harvest

At one and three months, rats were sacrificed via carbon dioxide asphyxiation (n=8 per group per time point). The fascia graft and underlying muscle were harvested. Half of the graft was fixed in 10% neutral buffered formalin for 24 hr and routinely processed for paraffin embedding. The second half was embedded in OCT compound.

Histology and Immunohistochemistry

The formalin-fixed, paraffin-embedded samples were cut into five-micron-thick longitudinal sections and stained with hematoxylin and eosin (H&E). A subset of the OCT embedded samples (n=4 per group per time point) were immunostained for CCR7 (a pro-inflammatory M1 macrophage maker), CD163 (a pro-remodeling M2 macrophage marker), and CD31 (an endothelial cell marker for neovascularization). Five-micron-thick, serial frozen sections were cut and

fixed in acetone for 2 min. Following three 5 min PBS rinses, sections were then incubated with 1% aqueous phosphomolybdic acid to reduce fascia autofluorescence. Sections were rinsed again in PBS, and non-specific binding of the primary antibody was blocked using 3% normal goat serum in PBS for 2 hr. After blocking, sections were incubated in primary antibody diluted with PBS in a humidified chamber at 4°C for 18 hr. Sections were then incubated in biotinylated secondary antibody diluted with PBS for 1 hr, then in Alexa Fluor 488-conjugated streptavidin for 45 min, and finally mounted with Vectashield mounting media containing DAPI to visualize cell nuclei. After each application of antibody or streptavidin, sections were rinsed in PBS three times for 15 min. Rat spleen served as a positive control, and sections incubated with PBS in place of the primary antibody served as negative controls. The primary antibodies used in this study were: mouse anti-rat CD163 (1:600, MCA342R, AbD Serotec), rabbit anti-rat CCR7 (1:250, NB110-55678, Novus Biologicals, Littleton, CO), and mouse anti-rat CD31 (1:500, MCA1334GA, AbD Serotec). The biotinylated secondary antibodies used were: horse anti-mouse (1:100, BA-2001, Vector Labs) and goat anti-rabbit (1:200, 111-065-003, Jackson ImmunoResearch Labs).

Semi-quantitative Histologic Analysis

One representative H&E and immunostained section from each rat was semi-quantitatively scored by two blinded, board-certified pathologists (E. Rene Rodriguez, MD and Carmela Tan, MD, Department of Anatomic Pathology, Cleveland Clinic) according to a scoring system adapted from ISO Standard

10993-6 (Table 4.1). H&E sections were scored for the presence of inflammatory cells – lymphocytes, plasma cells, macrophages, and giant cells. The M1 and M2 macrophage phenotypes were scored from sections immunostained for CCR7 and CD163, respectively. Non-inflammatory outcomes such as the presence of fibroblast-like cells and the amount of cellular infiltrate into the graft from the periphery (cellularity) were scored from the H&E sections, and neovascularization was scored from CD31 immunostained sections.

Table 4.1 Histologic scoring system adapted from ISO 10993-6 standard, hpf = high powered field (400x)

	Cell type/response	Score				
		0	1	2	3	4
Inflammatory cell outcomes	Lymphocytes	0	Rare – 1-5/hpf	5-10/hpf	Heavy infiltrate	Packed
	Plasma cells	0	Rare – 1-5/hpf	5-10/hpf	Heavy infiltrate	Packed
	Macrophages	0	Rare – 1-5/hpf	5-10/hpf	Heavy infiltrate	Packed
	Giant cells	0	Rare – 1-2/hpf	3-5/hpf	Heavy infiltrate	Packed
	$CCR7^+$ Pro-inflammatory M1 macrophages	0	Rare – 1-5/hpf	5-10/hpf	Heavy infiltrate	Packed
	$CD163^+$ Pro-remodeling M2 macrophages	0	Rare – 1-5/hpf	5-10/hpf	Heavy infiltrate	Packed
Non-inflammatory outcomes	Total Cellularity	--	< 25%	26-50%	51-75%	> 75%
	Fibroblasts	0	Rare – 100/hpf	100-1000/hpf	Heavy infiltrate	Packed
	$CD31^+$ Endothelial cells (Neovascularization)	0	Minimal capillary proliferation, focal, 1-3 buds	Groups of 4-7 capillaries with supporting fibroblastic structures	Broad band of capillaries with supporting structures	Extensive band of capillaries with supporting fibroblastic structures

Pre and Post-implantation Cross-sectional Area

At the time of implantation, the thickness of each 0.8x1 cm fascia piece was aseptically measured with calipers prior to rehydration. The pre-implantation cross-sectional area of each piece was estimated as the product of the dehydrated thickness times the 1 cm height. Post-implantation cross-sectional area measurements were made by manually tracing the perimeter of the grafts

from H&E stained sections using ImageScope software (Aperio Technologies, Vista, CA).

Statistical Analysis

Two-way ANOVA was performed to examine the effects of treatment and time on HA content, post-implantation cross-sectional area, and all histologic outcomes. One-way ANOVA was performed to examine the effect of treatment on pre-implantation cross-sectional area. When appropriate, multiple comparisons were performed with a Tukey HSD *post-hoc* test. In addition, to compare CD163+ M2 macrophage and CCR7+ M1 macrophage scores, a Wilcoxon signed rank test was performed. Inter-rater reliability between the two pathologists who performed the histologic scoring was evaluated by calculating kappa scores and percent agreement. For all statistical analysis, a p value of ≤ 0.05 was considered significant, and a p value of ≤ 0.10 was indicative of a trend. Results are expressed as mean ± standard deviation or mean (range).

Results

HA Content of Treated Fascia

The HA content of 5x5 cm fascia patches used for these experiments averaged 7.6 ± 2.3 µg/mg for TS-HA treated fascia with cross-linking and 7.8 ± 1.8 µg/mg for treated fascia without cross-linking (Table 4.2). Thus TS-HA constituted ~1% of the tissue weight in the treated groups, which is an order of magnitude higher than the HA content in water treated controls (0.2 ± 0.1 µg/mg).

Table 4.2 HA content (mean ± SD) of treated 5x5 cm fascia grafts at time zero and after the *in vitro* retention (IVR) experiment

Treatment group	Time zero (µg/mg)	IVR (µg/mg)
Water treated control	0.2 ± 0.1	--
TS-HA with cross-linking	7.6 ± 2.3	8.7 ± 2.0 ‡
TS-HA without cross-linking	7.8 ± 1.8 †	2.7 ± 1.5 †,‡

†,‡ Like symbols indicate significant difference ($p<0.001$)
n=8 grafts per group (triplicates data not shown)

In Vitro Retention of TS-HA

The mean HA content of treated fascia without cross-linking decreased by ~65% following the 72 hour retention experiment ($p<0.001$), but there was no decrease from time-zero concentration for treated fascia with cross-linking (Table 4.2).

Distribution of HA in Treated Fascia

HABP staining of treated fascia demonstrated that the exogenously added HA was distributed throughout the fascia matrix, primarily around large fascicle bundles (Figure 4.4).

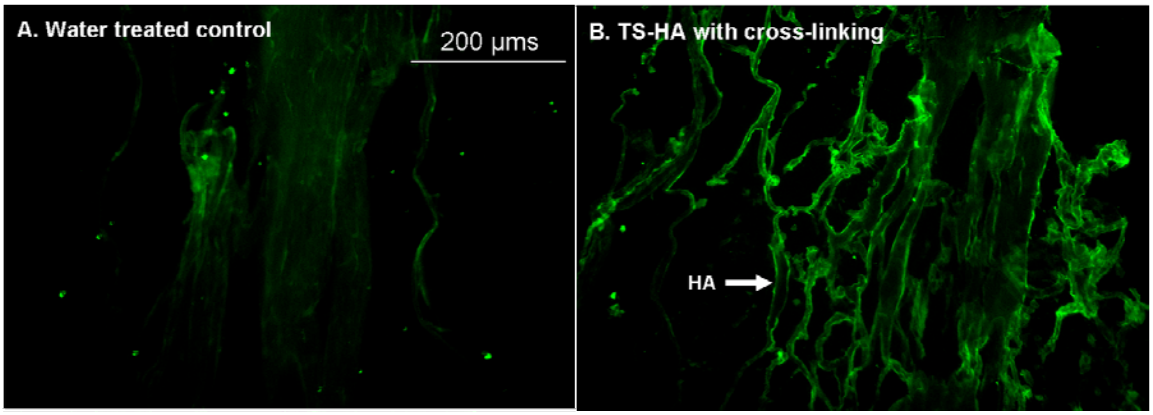

Figure 4.4 Representative images of bHABP stained fascia grafts (A) water treated control and (B) TS-HA treated with cross-linking (100X). The incorporated TS-HA was distributed throughout the fascia matrix, primarily around large fascicle bundles.

Descriptive Histology

Fascia grafts of all experimental groups were still visible and discernable from the underlying muscle at one (Figure 4.5A-C) and three months (Figure 4.6A-C). Remnant fascia architecture was identified as acellular bundles of dense collagen, particularly within the central region of the grafts (Figure 4.5D-I, 4.6D-I). Treated fascia with cross-linking was uniquely characterized by regions of TS-HA hydrogel which stained light blue on H&E sections and were located between collagen bundles throughout the graft (Figure 4.5E, 4.5H, 4.6E, 4.6H). At both time points, fascia in all groups elicited a chronic inflammatory host response predominantly seen at the periphery of the grafts (Figure 4.5D-F, 4.6D-

F). The infiltrates were composed of lymphocytes, macrophages, and a variable number of plasma cells and giant cells (Figure 4.5G-I, 4.6G-I). Of note, there was a persistent, moderate infiltrate of giant cells at three months in treated fascia with cross-linking (Figure 4.6H). Grafts of all groups had variable regions of dense cellularity and disorganized connective tissue, suggestive of matrix remodeling and deposition (Figure 4.5D-F, 4.6D-F). The central region of the grafts showed variable cellularity ranging from completely acellular regions, to regions with a low density of spindle-shaped fibroblast-like cells, to tracks or pockets of dense cellular infiltrate (Figure 4.5G-I, 4.6G-I). Treated fascia without cross-linking tended to show the highest cellularity of the three groups, in part due to infiltration of fibroblast-like cells between collagen bundles (Figure 4.5I, 4.6I). Vascularization was observed within grafts of all groups.

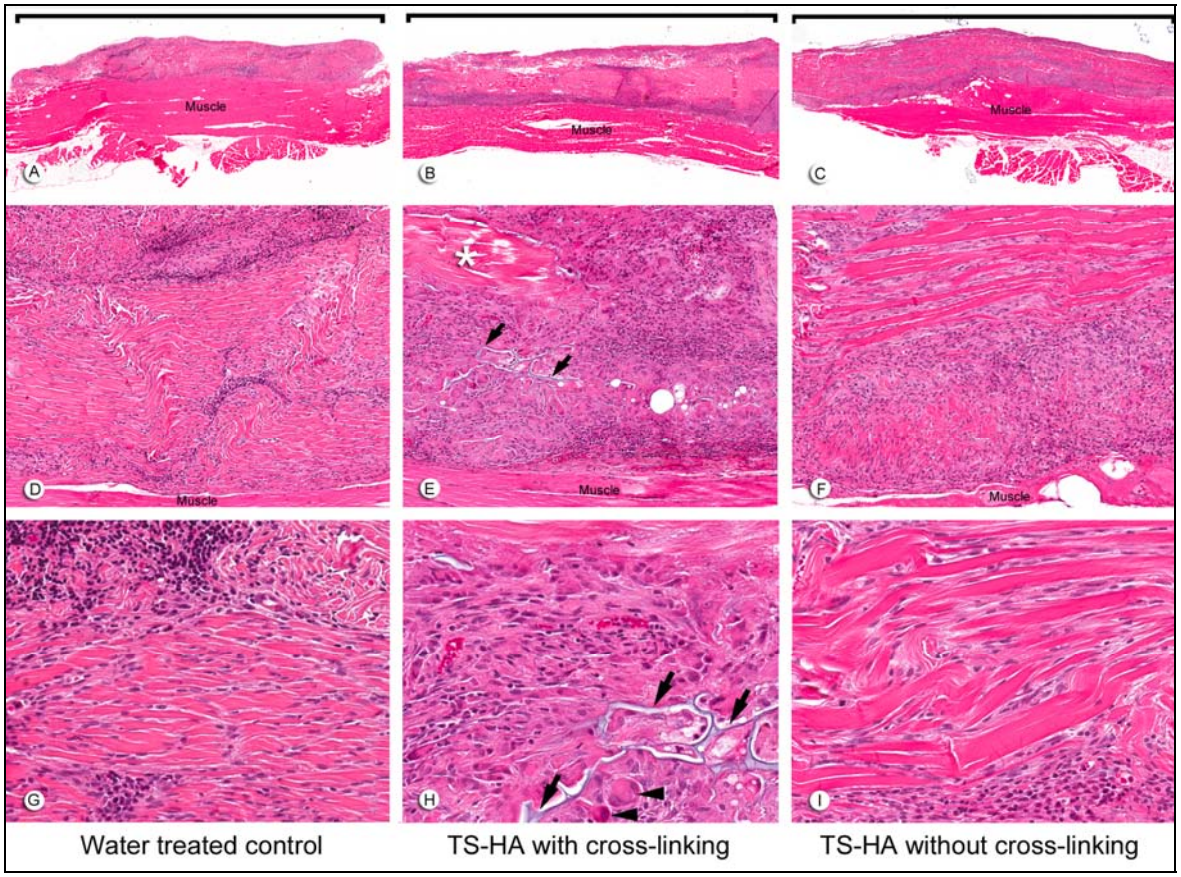

Figure 4.5 Representative H&E images at one month of (A, D, G) water treated control, (B, E, H) TS-HA with cross-linking, and (C, F, I) TS-HA without cross-linking. (A-C, 15x) Fascia grafts (brackets) were still visible and discernable from the underlying abdominal skeletal muscle. (D-F, 100x) Remnant fascia architecture was identifiable as longitudinal, pink, collagenous bands. Grafts exhibited a variable distribution of cellular infiltrates and acellular, collagenous regions (asterisk), as demonstrated in treated fascia with cross-linking (E). (G-I, 400x) Grafts were heavily infiltrated by chronic inflammatory cells, which were predominantly lymphocytes, as demonstrated in water controls (G). In cross-linked treated fascia, TS-HA hydrogel was visible as a light blue material (arrows) surrounded by multinucleated giant cells (H, arrowheads). Spindle-shaped, fibroblast-like cells heavily infiltrated the grafts, often between the collagenous bands, as demonstrated in uncross-linked treated fascia (I).

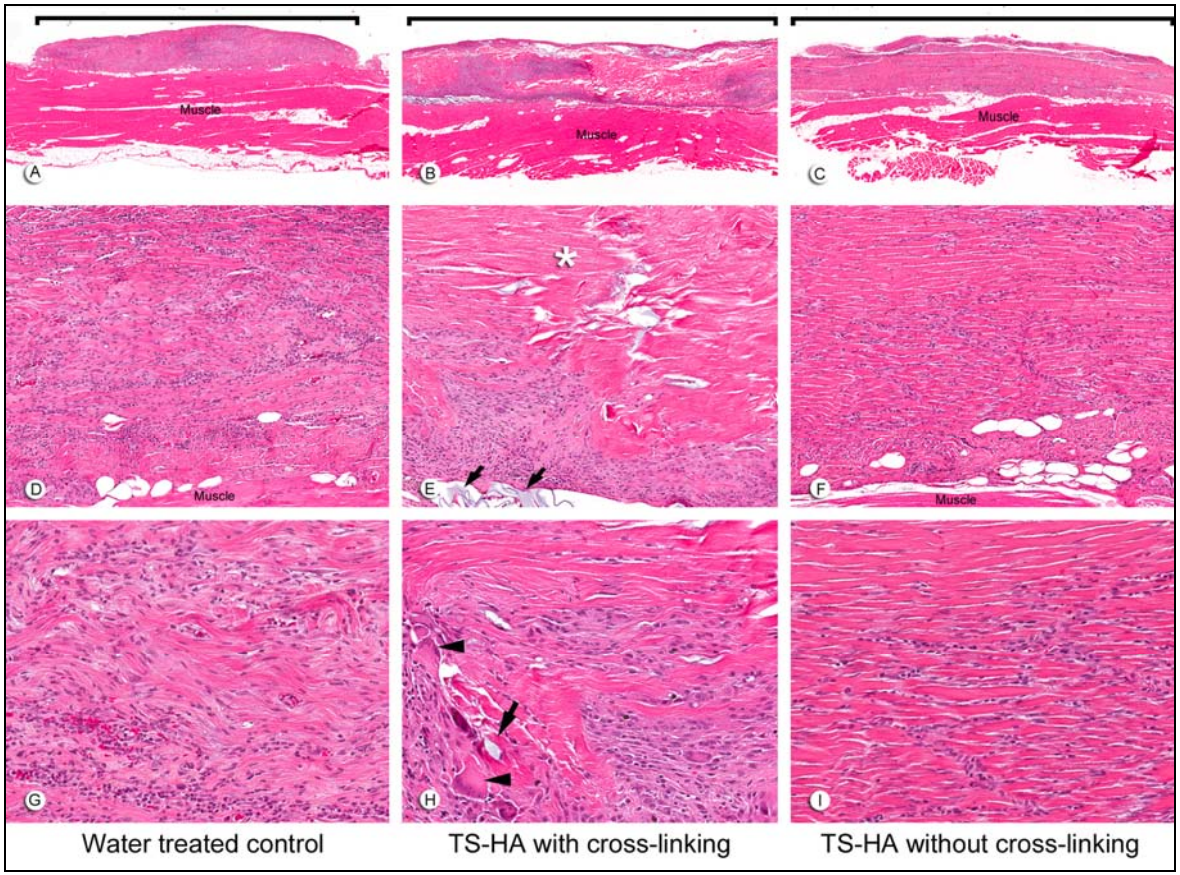

Figure 4.6 Representative H&E images at three months of (A, D, G) water treated control, (B, E, H) TS-HA with cross-linking, and (C, F, I) TS-HA without cross-linking. (A-C, 15x) Fascia grafts (brackets) were still visible and discernable from the underlying abdominal skeletal muscle. (D-F, 100x) A chronic inflammatory response was observed in all grafts at three months, but to a lesser extent than at one month for water control and uncross-linked treated fascia. Cross-linked treated grafts exhibited a variable distribution of cellular infiltrates, acellular regions (asterisk), and TS-HA hydrogel (E, arrows). (G-I, 400x) Fibroblast-like cells and disorganized connective tissue were observed in all groups, as demonstrated in water control grafts (G). In TS-HA with cross-linking grafts, hydrogel (arrows) and giant cells (arrowheads) were observed (H). Spindle-shaped, fibroblast-like cells heavily infiltrated the grafts, often between collagenous bands, as demonstrated in uncross-linked treated fascia (I).

Kappa Scores and Percent Agreement

Histologic scores were assessed for agreement between the two reviewers. Kappa scores for all outcomes ranged from 0.58 to 0.89 and percent agreement was at least 71%, indicating moderate to high agreement. Since inter-rater reliability was acceptable, scores from only one reviewer (ERR) are presented in this dissertation.

Inflammatory Cells

The mean scores for the inflammatory cell outcomes from each group at both time points are presented in Table 4.3. For each histologic outcome, the interaction between experimental group and time was not significant and was, therefore, dropped from the ANOVA model. There were no differences in lymphocyte or plasma cell density between groups at one or three months. Compared to water treated controls, TS-HA treated fascia with cross-linking exhibited significantly more macrophages ($p=0.001$) and giant cells ($p<0.0001$) at one and three months. Similarly, TS-HA treated fascia without cross-linking had significantly more macrophages than water controls ($p=0.001$) at one and three months, but no difference in giant cells. Hence, the only difference in host response between TS-HA treatments was the significantly higher giant cell density in the cross-linked group compared to the uncross-linked group at one and three months ($p<0.0001$). Across all groups, the density of plasma cells ($p=0.02$) and macrophages ($p=0.03$) in fascia grafts significantly decreased with time.

Table 4.3 Mean (range) histologic scores for inflammatory cell outcomes

Time Point	Experimental Group	Inflammatory Cell Outcomes					
		Lymphocytes	**Plasma Cells**	**Macrophages**	**Giant Cells**	**CCR7$^+$ Pro-inflammatory M1 macrophages**	**CD163$^+$ Pro-remodeling M2 macrophages**
1 month	Water treated control	3 (3-3)	2 (1-3)	2.3 [a,b] (1-3)	0.8 [a] (0-1)	1 (1-1)	2.5 (2-3)
	TS-HA with cross-linking	2.5 (1-3)	2.1 (1-4)	3.1 [a] (2-4)	2.8 [a,b] (1-4)	1 (1-1)	2.8 (2-3)
	TS-HA without cross-linking	3 (2-4)	1.5 (1-3)	2.8 [b] (1-4)	1.4 [b] (0-3)	1 (1-1)	2.8 (2-3)
3 month	Water treated control	2.9 (2-3)	0.9 (0-2)	1.5 [c,d] (1-3)	0.8 [c] (0-3)	1 (1-1)	2.3 (2-3)
	TS-HA with cross-linking	2.6 (2-3)	1.8 (0-4)	2.8 [c] (1-4)	2.8 [c,d] (0-4)	1 (1-1)	2.3 (2-3)
	TS-HA without cross-linking	2.6 (2-3)	1.1 (0-2)	2.4 [d] (2-3)	0.6 [d] (0-1)	0.8 (0-1)	2.0 (2-2)

Like letters indicate significant differences for an outcome across experimental groups within each time point ($p \leq 0.001$).
Across all groups, plasma cell ($p=0.02$), macrophage ($p=0.03$), and CD163$^+$ macrophage ($p=0.02$) scores decreased with time.
n=8 per group per time point

In all groups at both time points, the density of CD163+ M2 macrophages was greater than CCR7+ M1 macrophages ($p<0.0001$), indicating that macrophage polarization was dominated by the pro-remodeling phenotype (Table 4.3). Neither CCR7 nor CD163 density was significantly different among experimental groups at either time point. Across all groups, the density of CD163+ M2 macrophages significantly decreased with time ($p=0.02$). CCR7+ M1 macrophages were focally concentrated in small clusters, while CD163+ M2 macrophages were localized at the periphery of the grafts (Figure 4.7).

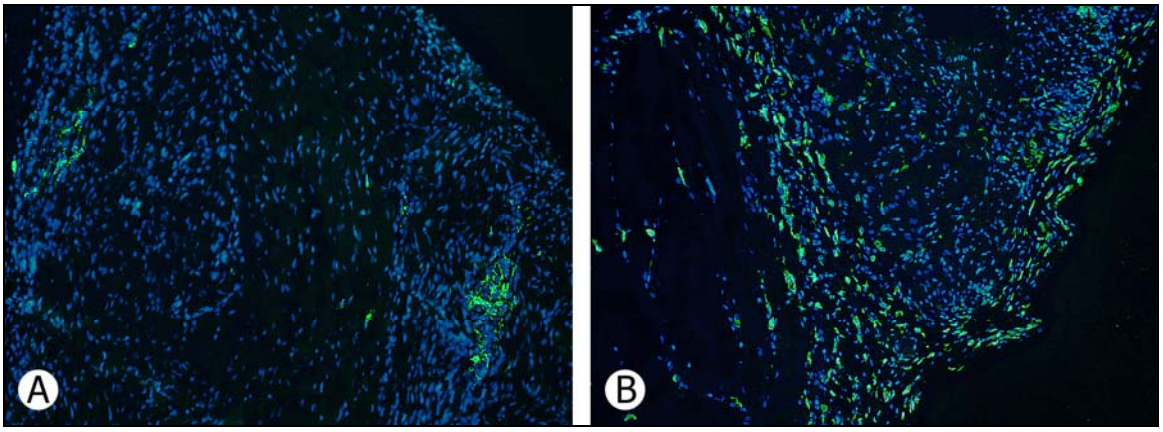

Figure 4.7 Representative immunostaining of (A) CCR7 and (B) CD163 immunostaining at three months of water treated control (200x) CCR7+ M1 macrophages were often focally concentrated in small clusters, and CD163+ M2 macrophages were localized at the periphery of the grafts. CCR7 and CD163 staining was similar for TS-HA treated fascia, with or without cross-linking. Nuclei were stained with DAPI.

Total Cellularity

TS-HA treated fascia without cross-linking demonstrated a trend towards increased cellularity compared to water controls at one and three months (Table 4.4, $p=0.09$).

Table 4.4 Mean (range) histologic scores for non-inflammatory outcomes

Time Point	Experimental Group	Non-inflammatory Outcomes		
		Total Cellularity	Fibroblasts	CD31^{+} Endothelial cells (Neovascularization)
1 month	Water treated control	2.1 † (1-3)	2.9 ^{a} (1-4)	2.3 (2-3)
	TS-HA with cross-linking	2.1 (1-3)	1.4 $^{a, b}$ (0-3)	1.8 (1-2)
	TS-HA without cross-linking	2.5 † (1-4)	2.9 ^{b} (1-4)	2.5 (2-3)
3 month	Water treated control	2 † (1-3)	2.5 ^{c} (2-4)	2.0 (2-2)
	TS-HA with cross-linking	2.5 (1-4)	1.4 $^{c, d}$ (0-3)	1.8 (1-2)
	TS-HA without cross-linking	3.1 † (2-4)	3.3 ^{d} (2-4)	1.8 (1-2)

Like letters indicate significant differences for an outcome across experimental groups within each time point ($p \leq 0.0001$).
†Indicates a trend ($p=0.09$)
CD31^{+} endothelial cells (neovascularization) scores trended toward a decrease with time ($p=0.10$).
n=8 per group per time point

Fibroblast-like Cells

TS-HA treated fascia with cross-linking exhibited a significantly lower density of fibroblast-like cells than water controls ($p<0.0001$) and treated fascia without cross-linking ($p<0.0001$) at one and three months (Table 4.4). TS-HA treated fascia without cross-linking had a similar density of fibroblast-like cells as water controls at both time points.

Vascularity

CD31 scores were not significantly different among experimental groups, but there was a trend towards a decrease with time across all groups (Table 4.4, p=0.10). CD31 staining for neovascularization was predominantly localized at the graft periphery (Figure 4.8).

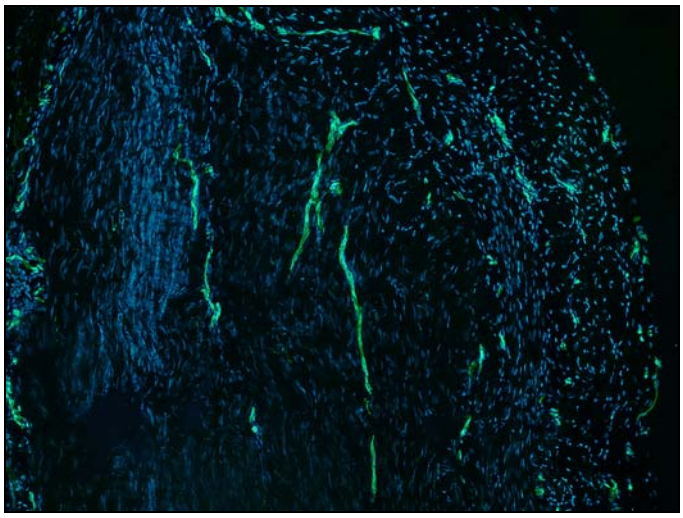

Figure 4.8 Representative CD31 immunostaining for vascularization at three months of water treated control (100x) Capillary vessels are lined with CD31+ endothelial cells. A few longitudinally oriented capillaries are shown in the central area of the graft. Capillary density was higher at the periphery of the graft. CD31 staining was similar for TS-HA treated fascia, with or without cross-linking. Nuclei were stained with DAPI.

Pre- and Post-implantation Cross-sectional Area

TS-HA treated fascia pieces, with (p=0.06) or without cross-linking (p=0.08), trended towards greater pre-implantation cross-sectional area than water controls (Figure 4.9). Post-implantation cross-sectional area significantly decreased from one to three months for all groups (p=0.02). There was no

significant difference in cross-sectional area among groups at either post-implantation time point.

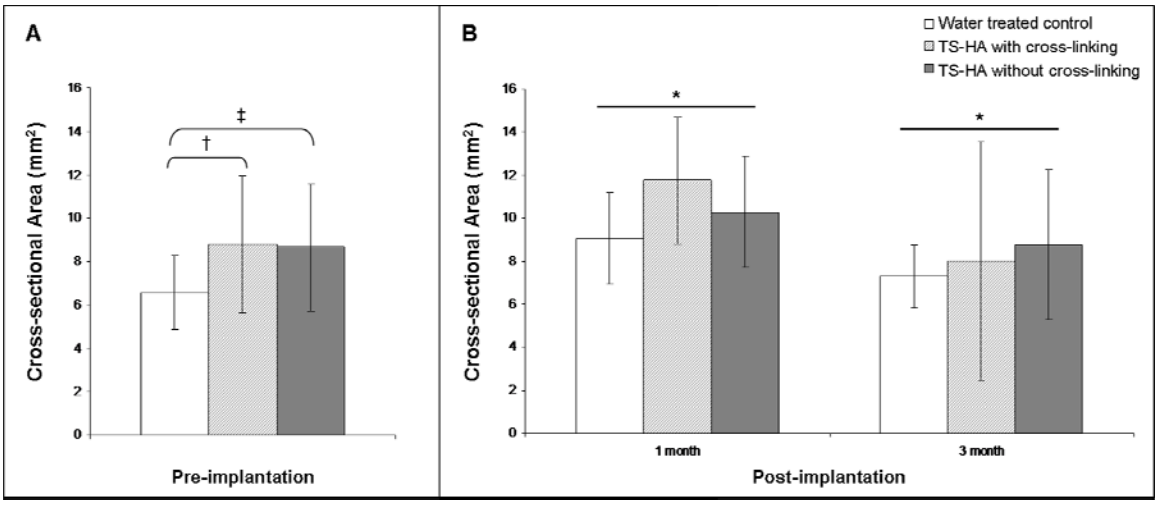

Figure 4.9 (A) Pre-implantation and (B) post-implantation cross-sectional area of water treated control, TS-HA with cross-linking, and TS-HA without cross-linking treated fascia. †, ‡TS-HA treated fascia pieces, with (p=0.06) or without cross-linking (p=0.08), trended towards greater pre-implantation cross-sectional area than water controls. *Post-implantation cross-sectional area significantly decreased from one to three months for all groups (p=0.02). There was no significant difference in cross-sectional area among groups at either post-implantation time point.

Discussion

In this study, a method of TS-HA treatment that increased the amount of HA in fascia by an order of magnitude to approximately 1% tissue weight was demonstrated. Furthermore, the incorporated HA was distributed throughout the tissue and, upon cross-linking, the TS-HA was retained as a hydrogel network. The effectiveness of tyramine cross-linking in immobilizing HA within fascia was validated through an *in vitro* retention experiment. Moreover, this study characterized the host response to TS-HA treated fascia in a rat abdominal wall defect model with the hypothesis that treated fascia with cross-linking would exhibit lower lymphocyte, plasma cell, macrophage and giant cell densities, a higher fibroblast density, and a greater proportion of M2 macrophages than M1 macrophages compared to water treated controls and treated fascia without cross-linking. In contrast, the results showed that TS-HA treated fascia with cross-linking had a similar lymphocyte and plasma cell densities, greater macrophage and giant cell densities, and a lower density of fibroblast-like cells than water treated controls. However, treated fascia with cross-linking did exhibit a predominantly M2 pro-remodeling macrophage profile, similar to water controls and treated fascia without cross-linking.

The water treated controls in this study demonstrate the host response to unmodified, decellularized fascia ECM in a xenogenic implantation model. At three months, water treated fascia supported a heavy population of fibroblast-like cells and a moderate degree of vascularity. A moderate macrophage infiltrate was largely of the pro-remodeling M2 phenotype. Since macrophages are key

mediators of both inflammatory and anti-inflammatory pathways, classification into M1 pro-inflammatory or M2 pro-remodeling phenotypes may serve as a predictive tool for downstream outcomes following graft implantation (107,108). The presence of pro-remodeling macrophages and fibroblast-like cells is suggestive of host repair and remodeling. Water treated fascia was also characterized by a heavy, chronic lymphocyte population, which likely represents an immune reaction to the xenograft.

The host response to an implanted xenograft can differ from an auto- or allograft, as shown in studies using *in vivo* animal models (e.g., intraperitoneal transplantation (151), subcutaneous implantation (113,155,156), and tendon repair (43,152)) and *in vitro* proliferation assays of immune cells after graft exposure (148,157,158). Xenogenic grafts generally elicit a greater number of lymphocytes (specifically T-cells), neutrophils, and monocytes than grafts that are of auto- or allogenic origin (151,158,159).

Allman et al. evaluated the histologic outcomes and cytokine levels of xenogenic rat and allogenic muscle grafts in a mouse subcutaneous model (155). Xenografts demonstrated an acute inflammatory response characterized by the presence of polymorphonuclear leukocytes, followed by an influx of lymphocytes, and eventually necrosis and fibrous encapsulation by 28 days. At seven days, which corresponded to the time of mononuclear cell infiltration, cells within the implanted xenografts expressed both IFN-γ (associated with graft rejection) and IL-4 (associated with graft acceptance). Allografts similarly exhibited an acute inflammatory response, but in contrast to xenogenic muscle, chronic

inflammation was mostly resolved at 10 days, organized collagenous connective tissue was apparent at 28 days, and cells within the muscle allograft expressed IL-4 (associated with graft acceptance) at seven days. As well, the host response to acellularized human dermis appears to differ depending upon the implantation model. When implanted in a rat abdominal wall model, human dermis xenografts exhibited a prominent mononuclear cell population up to 28 days following surgery (112). In contrast, human dermis elicited minimal inflammation with a mild presence of lymphocytes up to 180 days after implantation in a vervet monkey abdominal wall model (156). These results demonstrate that an implanted xenograft can elicit a host response marked by necrosis, fibrous encapsulation, and an increased lymphocytic response when compared to allografts.

In the current study, the chronic lymphocytic response observed for all fascia grafts in the xenogenic rat model may be due specifically to remnant cellular elements (43,62,148) or antibiotic (149,150) that likely remain in the fascia even after processing. Host recognition of the slight molecular differences in the proteoglycans and glycoproteins in tissue from a different species (151,152) or changes to protein structure after processing (153) may have also triggered the adaptive immune system. Thus, fascia ECM would likely elicit less chronic inflammation than seen here, if used as an allograft in human patients.

TS-HA treated fascia, with or without cross-linking, exhibited a heightened macrophage response compared to water controls. The extent to which the mechanism leading to this outcome is the same for both groups is unknown, but

may involve at least some common elements. Because TS-HA treatment tended to increase the cross-sectional area of fascia grafts in both groups, and the added TS-HA was distributed around the fascicle bundles, it was concluded that the inter-fascicular space likely expanded to accommodate the added TS-HA. In the case of treated fascia without cross-linking, TS-HA is presumably leached from these spaces within hours to days after implantation (as supported by the *in vitro* results), allowing for increased cellular infiltration. Further, given that the *in vivo* half-life of HA is on the order of hours (160), the macrophage response in the uncross-linked group may be in part a downstream consequence of a bolus release of HA during the early phases of healing. Any remnant uncross-linked TS-HA may also elicit a macrophage response. In the case of treated fascia with cross-linking, the heightened macrophage response may be a consequence of continued phagocytic activity against the persistent TS-HA hydrogel. Furthermore, CD44-mediated binding of monocytes/macrophages to HA is enhanced upon a covalent association with heavy chains derived from inter-α-inhibitor, a protease inhibitor found in serum (161,162). Binding of monocytes/macrophages to HA has been demonstrated in both *in vitro* and *in vivo* models of inflammation, and could explain the heightened macrophage response observed in this study. Regardless of the mechanism, it is important to note that the heightened macrophage response was not associated with a change in macrophage polarization. TS-HA treated fascia with or without cross-linking was predominantly infiltrated by M2 pro-remodeling macrophages,

suggestive of constructive remodeling by tissue repair and regeneration (107,108).

The observation of giant cells was unique to cross-linked treated fascia, suggesting that regions of the TS-HA hydrogel could not be phagocytosed by macrophages, thereby prompting giant cell formation to breakdown the aggregates by degradative agents. Although graft degradation is expected in the course of host incorporation and tissue remodeling, premature or extensive breakdown of the matrix before host replacement with functional tissue can result in a detrimental loss of mechanical properties (163). The extent to which the giant cell response affects the mechanical properties of TS-HA treated fascia is the subject of ongoing work. Although TS-HA treated fascia with cross-linking was characterized by multinucleated giant cells – the hallmark of the foreign body response – no fibrous capsule was observed at three months. Fibrous encapsulation of TS-HA treated fascia with cross-linking is not expected to occur at later time points, since encapsulation of other ECM grafts such as Permacol (isocyanate-cross-linked porcine dermis) is apparent as early as seven days after implantation (112).

TS-HA treated fascia without cross-linking trended towards an increase in cellularity compared to water treated fascia. As previously mentioned, the expanded inter-fascicular space that becomes devoid of TS-HA after implantation may allow for greater cellular infiltration. This hypothesis is consistent with the finding that treated fascia with cross-linking did not exhibit the same increased cellularity. In fact, cross-linked TS-HA treated fascia had fewer fibroblast-like

cells than water or uncross-linked treated fascia, suggesting that TS-HA hydrogel negatively impacts fibroblast infiltration, adhesion, and/or proliferation. Inhibition of these cell functions may be the result of the impenetrable, smooth nature of a HA hydrogel which is not conducive to fibroblast attachment (164). Further elucidating these mechanisms will aid in the development of TS-HA treated fascia as a scaffold supportive of matrix-producing fibroblasts.

While numerous studies have demonstrated that exogenous, high molecular weight HA can inhibit the infiltration, proliferation, and cytokine production of macrophages (75-80), there is an equally large body of evidence showing that HA can be associated with macrophage activation and adhesion as well as foreign body giant cell response (165-169). It is important to note that previous studies investigated HA in endogenous, soluble, injectable, or pure hydrogel form, in either cell culture or *in vivo* injury models; all of which differ from the form of HA and *in vivo* model system employed in this study. To the best of the author's knowledge, there is no precedent for the investigation of *in vivo* host response to an ECM impregnated with a HA hydrogel, limiting comparison of these results to previous work. However, in one recent study, Brown et al. showed that bladder ECM treated with disulfide cross-linked, thiol-modified HA facilitated and expedited the infiltration of bladder smooth muscle cells into bladder ECM in cell culture (103). Since disulfide cross-linking is reversible and the incorporated HA could be leached or degraded over time (unlike dityramine cross-linking), this result is consistent with the heightened cellularity in TS-HA treated fascia without cross-linking.

Since fascia grafts were not radioactively labeled in this study, the processes of resorption and host tissue deposition could not be distinguished from each other. As a means to estimate the net effect of resorption and deposition over time, post-implantation cross-sectional area at one and three months was measured. The significant decrease in cross-sectional area from one to three months may be a consequence of greater matrix resorption than deposition and/or simply the resolution of an initial edema/swelling. Future work should investigate the effect of TS-HA treatment specifically on the remodeling of the fascia matrix over time.

This study is not without limitations. Although treated fascia patches were selected for implantation based on the criteria that their mean TS-HA content fell within the range of 5-10 μg/mg, the variable nature of the histologic scores within a single experimental group could be attributed to the variability in TS-HA content from one graft to another. Ongoing development of treatment methodologies aims to obtain a more uniform TS-HA concentration within and between treated fascia grafts. Second, the latest implantation time point investigated in this study was three months. Certainly, longer implantation times are necessary to ascertain the extent to which the lymphocyte aggregation clears, the giant cell population diminishes, the TS-HA hydrogel is degraded, and to observe end-stage tissue remodeling. However, three months is sufficient for predicting either a constructive tissue remodeling outcome or a pro-inflammatory (destructive) tissue remodeling outcome (107). Another limitation is that only treated fascia grafts with a mean TS-HA content of 5-10 μg/mg and only one molecular weight

(0.9-1 M Da) were investigated. A dose- or molecular-weight- dependent histologic response to TS-HA amount is certainly possible, and should be further investigated. Lastly, although TS-HA treated fascia was evaluated in a xenogenic implantation model and not at the intended site of clinical use, the rat abdominal wall defect model is an established preclinical tool for comparing the host response to different biomaterials (112,121).

Conclusion

This study is novel in that it characterizes the host response to decellularized fascia ECM and TS-HA treated fascia ECM with or without cross-linking. TS-HA treated fascia with cross-linking had a similar lymphocyte and plasma cell densities, greater macrophage and giant cell densities, and a lower density of fibroblast-like cells than water treated controls. Treated fascia with or without cross-linking exhibited a predominantly M2, pro-remodeling macrophage profile similar to water controls, which is suggestive of constructive tissue remodeling. All grafts exhibited a chronic lymphocytic response that is suggestive of an immune response to the fascia xenograft. These findings suggest that augmentation of an ECM, in particular human fascia lata, with HA can alter the host response to the ECM. This work provides guidance for the ongoing development of HA treated extracellular matrices as scaffolds for augmenting the repair of soft tissues such as tendon. Future work will investigate alternative treatment methods and the dose- and molecular-weight-dependent host response to HA treated fascia ECM.

Chapter 5

Mechanical Properties of Tyramine Substituted-Hyaluronan Enriched Fascia

Introduction

In Chapters 2 and 4, a diffusion-based treatment method by which fascia extracellular matrix (ECM) was enriched with tyramine substituted-hyaluronan (TS-HA) was described. The amount of hyaluronan (HA) in fascia increased by an order of magnitude to approximately 1% tissue weight and the incorporated HA was distributed throughout the tissue. Upon cross-linking, the TS-HA was effectively immobilized within fascia ECM as a hydrogel network. Moreover, the host response to TS-HA treated fascia was evaluated in a rat abdominal wall defect model. Contrary to the hypothesis, cross-linked TS-HA treated fascia exhibited a heightened macrophage and giant cell response compared to water treated control with a predominantly pro-remodeling M2 macrophage phenotype.

Macrophages and giant cells function to phagocytose and degrade implanted biomaterials and do so by secreting reactive oxygen intermediates, acid, and proteolytic enzymes such as matrix metalloproteinases (MMPs) (109,110,132). Since MMP activity has been implicated in the degradation of ECM proteins and a subsequent decrease in matrix mechanical properties (131), the time-zero and post-implantation mechanical properties of TS-HA treated fascia were investigated.

Hence, the objective of this study was to determine changes in the mechanical properties of TS-HA treated fascia after implantation in a rat abdominal wall model. Specifically, load relaxation ratio, load relaxation rate, stiffness of the toe- and linear-regions, elastic modulus of the toe- and linear-regions, and transition strain were determined. Based on the heightened macrophage and giant cell response over water treated control that was observed in the previous histologic study (Chapter 4), TS-HA treated fascia with cross-linking was hypothesized to exhibit a lower load relaxation ratio, a higher load relaxation rate, lower toe- and linear-region stiffness, lower toe- and linear-region moduli, and higher transition strain compared to water treated controls and treated fascia without cross-linking.

Materials and Methods

The preparation and characterization of the water control and TS-HA treated fascia used in this study are described in detail in Chapter 4. Furthermore, the fascia strips used for mechanical testing in this study were implanted into the same rats that were used for the histologic analysis reported previously in Chapter 4.

Experimental Design

Patches of human fascia lata (5x5 cm) treated with water, TS-HA with cross-linking, or TS-HA without cross-linking were used for this study (n=8 patches per group, Figure 5.1). The fascia was derived from the iliotibial tract of donors aged 18-55 years and was donated by the Musculoskeletal Transplant Foundation (Edison, NJ). TS-HA treated patches, both cross-linked and uncross-linked, had a concentration of 5-10 micrograms of TS-HA per milligram of dry weight tissue (μg/mg) as determined in the previous study (Chapter 4). Five mechanical test strips were cut from each fascia patch and were used for mechanical testing at time zero (n=3 per patch) and after one and three months implantation in a rat abdominal wall model (n=1 per patch per time point). A total of 48 rats were used for the *in vivo* implantation study (n=8 per treatment group per time point). Detailed methods are described below.

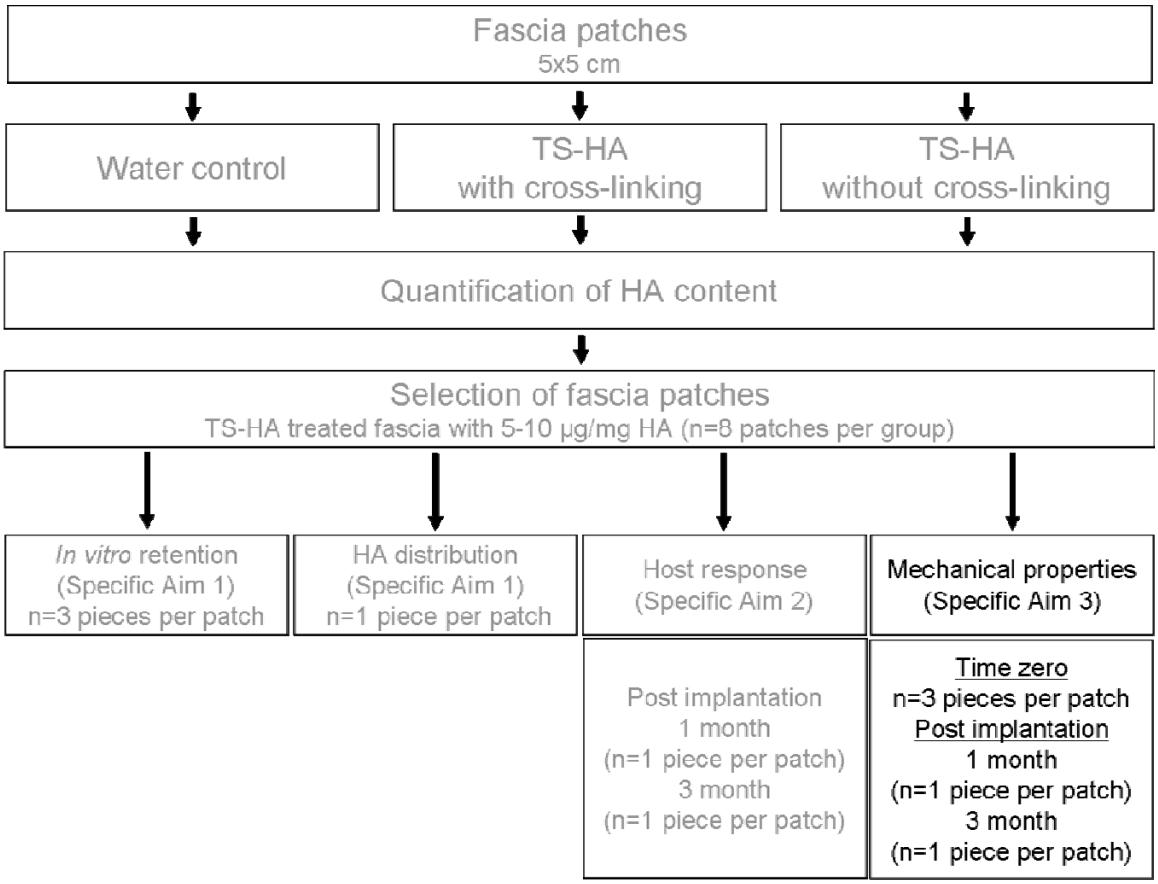

Figure 5.1 Experimental design for the mechanical testing of water controls and TS-HA treated fascia at time zero and post implantation

Rat Abdominal Wall Defect Model

All procedures were performed in accordance with the National Institutes of Health guidelines for care and use of laboratory animals and were approved by the Institutional Animal Care and Use Committee at the Cleveland Clinic.

Forty-eight adult, male Lewis rats were used (450-600 g, Harlan, Indianapolis, IN). Each rat was anesthetized with an intramuscular injection of ketamine, xylazine, and acepromazine (30/6/1 mg/kg). The abdomen was prepared for aseptic surgery. Via a ventral midline incision, a partial-thickness 0.4x4.5 cm defect was created in the anterior sheath adjacent to the linea alba. The anterior sheath was removed, and the underlying rectus muscle,

transversalis fascia, and peritoneum were left intact. One 0.4x4.5 cm fascia strip from each patch was wetted in saline for 10 min, and secured into the defect using four corner sutures of 5-0 Prolene (Figure 5.2). As reported previously, on the contralateral side of the linea alba, a second defect (0.8x1 cm) was created and replaced with a wetted 0.8x1 cm fascia piece from the same patch for semi-quantitative histologic analysis (Chapter 4). The skin incision was closed using 4-0 chromic gut suture, and the rat was allowed to recover from anesthesia under a heating lamp. For analgesia, each rat received 0.15 mg/kg buprenorphine post-operatively, 12 hours later, and thereafter as needed. Rats were housed individually for the duration of the study.

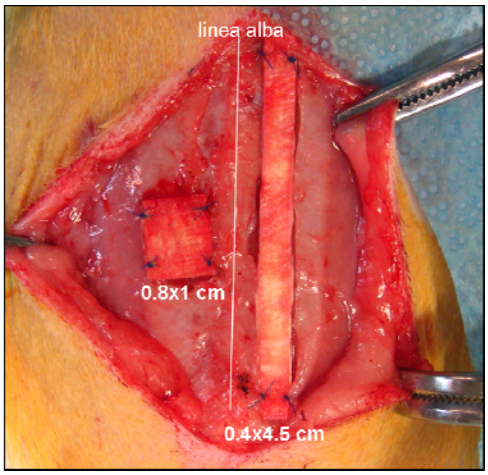

Figure 5.2 The rat abdominal wall defect model. One fascia strip from each patch was secured into a 0.4x4.5 cm defect. On the contralateral side of the linea alba, a second defect (0.8x1 cm) was created and replaced with a fascia piece from the same patch for histologic assessment (previously presented in Chapter 4).

Euthanasia and Tissue Harvest

At one and three months, rats were sacrificed via carbon dioxide asphyxiation (n=8 per group per time point). Fascia grafts and the underlying muscle were harvested and frozen until ready for mechanical testing.

Mechanical Properties Testing

Three 0.4x4.5 cm strips cut from each water control and TS-HA treated fascia patch were used to quantify mechanical properties at time zero. Prior to testing, time-zero test strips were rehydrated for 4 hr in saline. Only a small volume was used (300 µl), to prevent HA leaching from the uncross-linked TS-HA treated fascia. In preparation for mechanical testing, all explanted mechanical test strips were thawed and isolated from the underlying muscle by blunt dissection.

For mechanical testing, samples were gripped in custom clamps under 26 in-oz of torque with superglue and sandpaper, leaving a nominal gauge length of 28 mm. Thickness was determined at five points along the sample length with a linear variable displacement transducer probe under a constant pressure of ~0.001 MPa. Width was determined from optical analysis at three points along a longitudinal image captured with a Leica MZ6 stereomicroscope (Bannockburn, IL). Cross-sectional area was calculated as the product of average thickness and average width. Surface stain lines were placed 5 mm apart on the gage-section, for optical strain analysis and material property determination (62).

All mechanical testing was conducted in 0.9% saline at 37°C on a MTS FlexTest SE electromechanical test system (Eden Prairie, MN) fitted with a 500-N load cell (Honeywell-Sensotec, Columbus, OH). Fascia strips were preconditioned from 0.2 to 2 N for five cycles, immediately elongated 1.2 mm (nominally 4% strain) at 3 mm/sec, and held at that position for 10 min to allow

for relaxation (Figure 5.3). Samples were then returned to a slack position, allowed 5 min to recover (170), and pulled to failure at a rate of 10 mm/min (171).

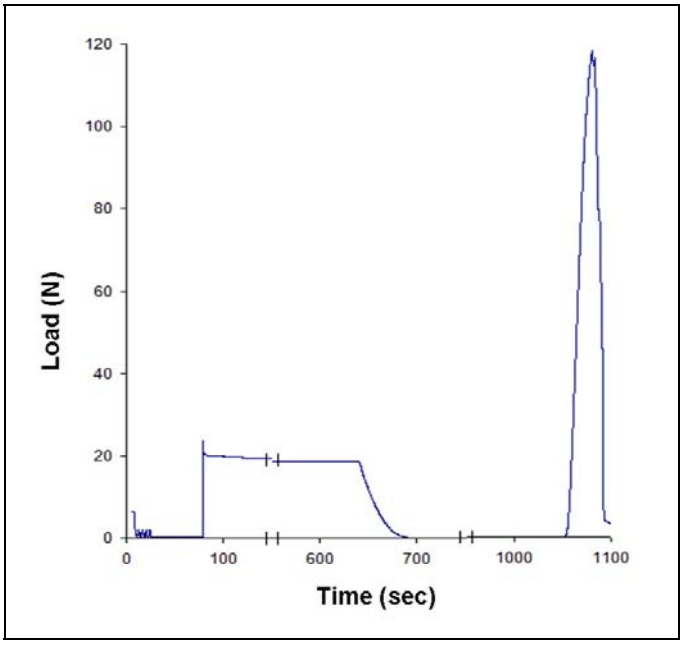

Figure 5.3 Mechanical testing protocol. Fascia strips were preconditioned from 0.2 to 2 N for five cycles, elongated 1.2 mm (nominally 4% strain) at 3 mm/sec, and held at that position for 10 min to allow for relaxation. Samples were returned to a slack position, allowed 5 min to recover, and pulled to failure at a rate of 10 mm/min.

Data Analysis

The load-displacement data from each test was zeroed with 0.2 N load. From the relaxation portion of the test, the load relaxation ratio was computed as the ratio of final to peak load (Figure 5.4A). The load relaxation rate, *n*, was calculated by fitting a power law relationship t^n to the first ten seconds of the load relaxation data (Figure 5.4B) (172).

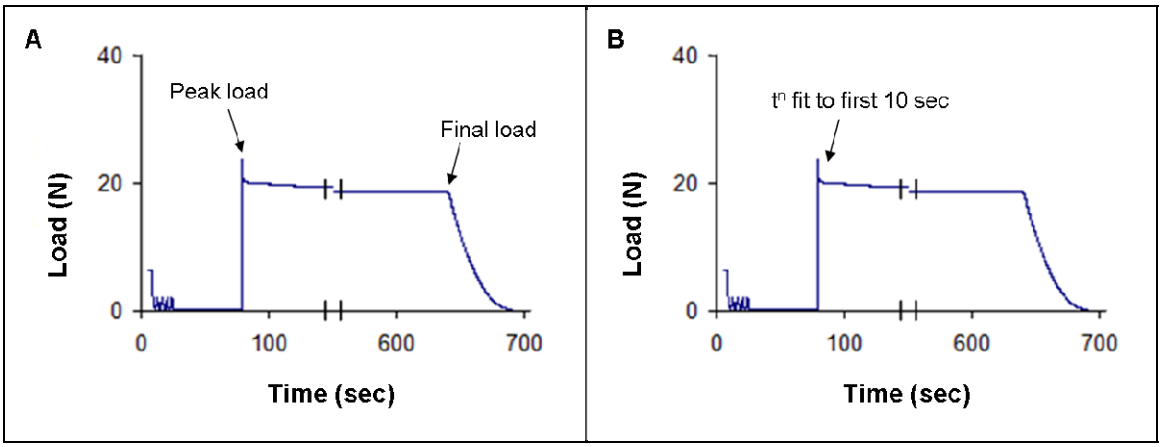

Figure 5.4 Computation of (A) the load relaxation ratio and (B) the load relaxation rate. Load relaxation ratio was computed as the ratio of final to peak load. Load relaxation rate, n, was calculated by fitting a power law relationship t^n to the first ten seconds of the load relaxation data.

From the failure portion of the test, load and local (optical) displacement data were either plotted directly or normalized by cross-sectional area and initial gage length between the stain lines to generate load-displacement or stress-strain curves, respectively. Using the least squares method, a bilinear curvefit was applied to the stress-strain failure data to quantify the elastic moduli from the slopes of the toe- and linear-regions (Figure 5.5A) (137). The strain value corresponding to the transition point of each bilinear fit was also determined. For a small portion of samples, the toe -region was deemed to be non-existent based on the criterion that the toe modulus was greater than 70% of the linear modulus (Figure 5.5B). In these cases, the linear modulus was recalculated as the slope of the entire stress-strain curve, and the transition strain was assigned a value of zero. For another small portion of samples, the data exhibited a significant yield region based on the criterion that the calculated transition strain was negative (Figure 5.5C). In these cases, the yield points were removed, and bilinear curve fitting was reapplied to the remaining data. For the small portion of samples that

exhibited a significant yield region, but not a toe-region, the yield points were removed, the linear modulus was recalculated as the slope of the remaining data, and the transition strain was assigned a value of zero (Figure 5.5D). The toe and linear stiffness were determined in a similar manner. All data analysis was conducted using Matlab software (Mathworks, Natick, MA) and customized Matlab code (Appendix B).

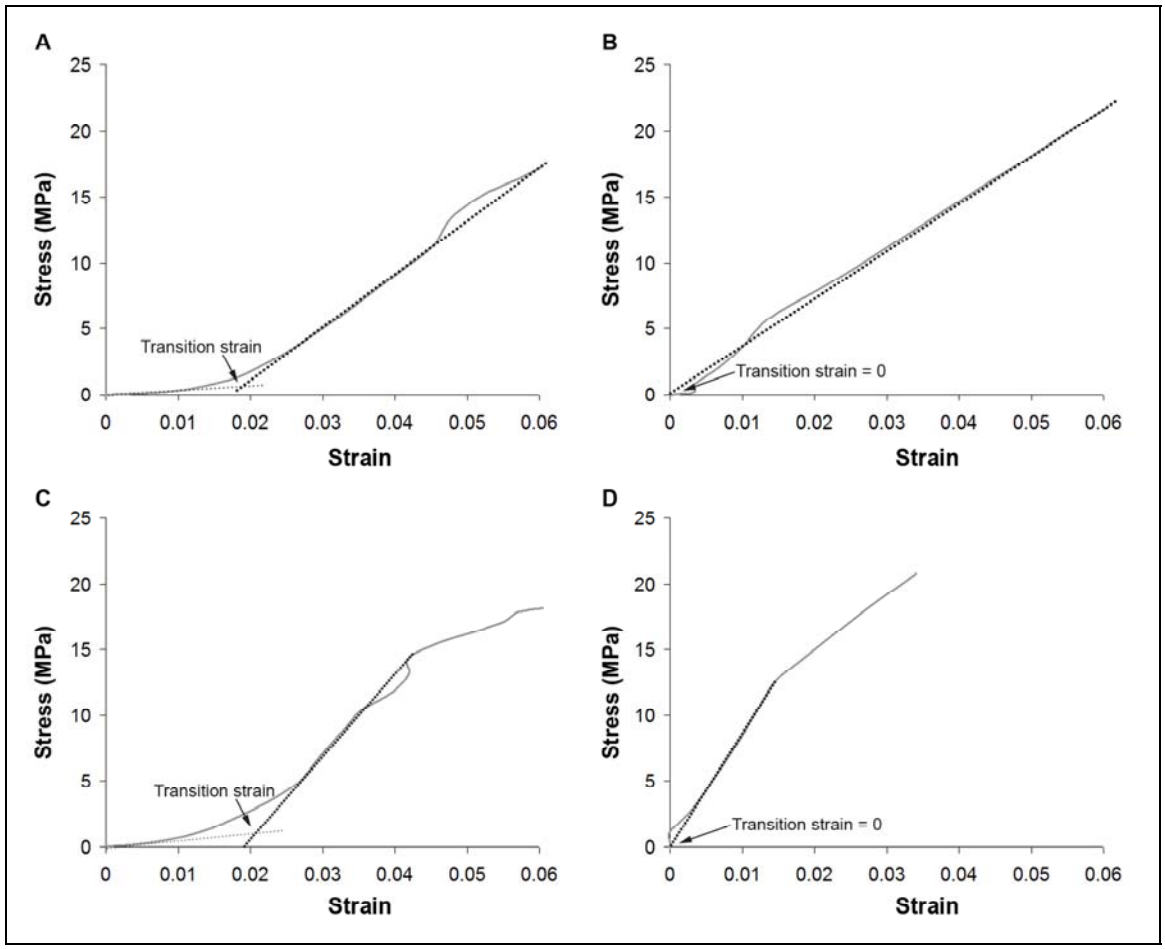

Figure 5.5 Representative stress versus local strain curves demonstrating different mechanical behavior of the samples. (A) Using the least squares method, a bilinear curvefit was applied to quantify toe-region modulus (light dashed line) and linear-region modulus (heavy dashed line). The strain value corresponding to the transition point of each bilinear fit was determined. (B) For a small portion of samples, the toe-region was deemed to be non-existent. Linear modulus was recalculated as the slope of the entire stress-strain curve, and transition strain was assigned a value of zero. (C) For another small portion of samples, the data exhibited a significant yield region. Yield points were removed, and bilinear curve fitting was reapplied to the remaining data. (D) For the small portion of samples that exhibited a significant yield region, but not a toe-region, yield points were removed, linear modulus was recalculated as the slope of the remaining data, and transition strain was assigned a value of zero.

Statistical Analysis

Repeated measures ANOVA was performed to examine the effects of treatment and time on cross-sectional area, load relaxation ratio, load relaxation rate, toe- and linear-region stiffness, toe- and linear-region modulus, and transition strain. When appropriate, multiple comparisons were performed with a

Tukey HSD *post-hoc* test. For all statistical analysis, a p value of ≤ 0.05 was considered significant, and a p value of ≤ 0.10 was indicative of a trend. Results are expressed as mean ± standard deviation.

Results

Gross Observations

At three months, grafts of all groups appeared to have experienced a variable degree of resorption or remodeling. TS-HA with cross-linking test strips occasionally demonstrated extensive or even complete resorption/remodeling (Figure 5.6). In particular, two of the 48 implanted mechanical test strips (one TS-HA with cross-linking at one month and one TS-HA with cross-linking at three months) could not be mechanically tested due to a loss of structural integrity. For two other test strips (both TS-HA with cross-linking at three months), the posterior and anterior ends were extensively resorbed or remodeled and, therefore, were mechanically tested using a shorter grip-to-grip gage length of 15 mm. Because the mechanical integrity of three month fascia strips from all groups was uncertain, three month samples were exempted from viscoelastic testing in order to avoid sub-failure damage prior to the collection of elastic mechanical properties.

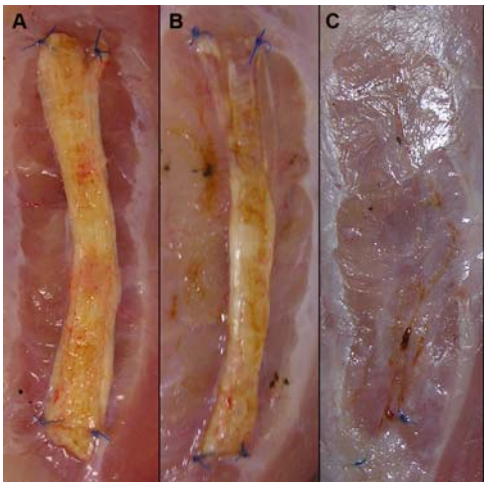

Figure 5.6 Representative images of TS-HA with cross-linking treated fascia strips at explantation at three months. Grafts appeared to have experienced a variable degree of resorption or remodeling, ranging from minimal (A) to extensive (B) to complete (C).

Cross-sectional Area

Two-way ANOVA indicated that only group had a significant effect on cross-sectional area (Figure 5.7, p=0.002), and there was a trend for time (p=0.07). No significant group-time interaction was found. The cross-sectional area of TS-HA treated fascia pieces, with or without cross-linking, was significantly greater than water control. Fascia grafts at three months trended towards a greater cross-sectional area than at one month.

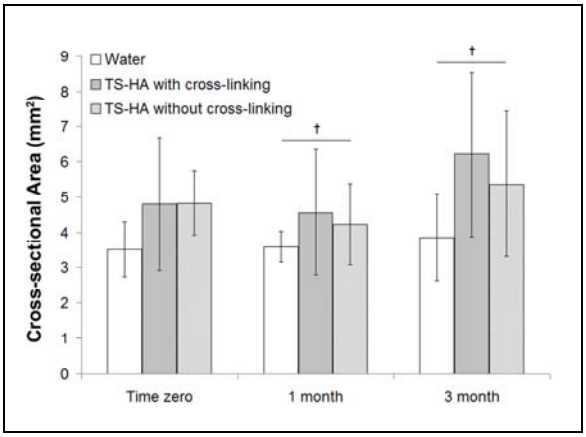

Figure 5.7 Cross-sectional area of water treated control, TS-HA with cross-linking, and TS-HA without cross-linking treated fascia (n=7-8 per group per time point). The cross-sectional area of TS-HA treated fascia pieces, with or without cross-linking, was significantly greater than water control (p=0.002), which is not denoted with symbols because of the manner in which the data are graphically presented here. †Fascia grafts at three months trended towards a greater cross-sectional area than at one month (p=0.07).

Mechanical Properties Testing

The average stress versus local strain curves for water control, TS-HA with cross-linking, and TS-HA without cross-linking treated fascia at all time points are shown in Figure 5.8. Failure is under-represented because all test strips failed at the grips.

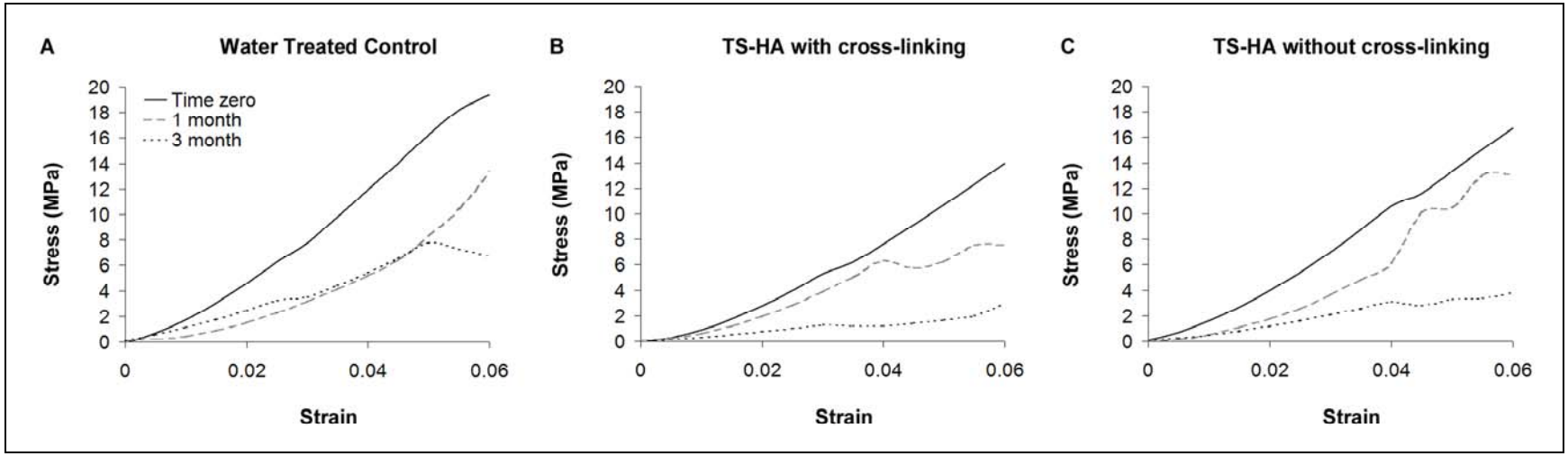

Figure 5.8 Average stress versus local strain curves for water control, TS-HA with cross-linking, and TS-HA without cross-linking test strips at all time points (n= 7-8 per group per time point). The wavy nature of the curves at higher strains is a consequence of including fewer samples in the average as each fails. Also note that failure is under-represented because all test strips failed at the grips.

Viscoelastic Properties

Two-way ANOVA indicated that only time had a significant effect on both load relaxation ratio (Figure 5.9A, $p<0.0001$) and load relaxation rate (Figure 5.9B, $p<0.0001$), and there was no significant group-time interaction. Load relaxation ratio significantly decreased and load relaxation rate significantly increased from time zero to one month.

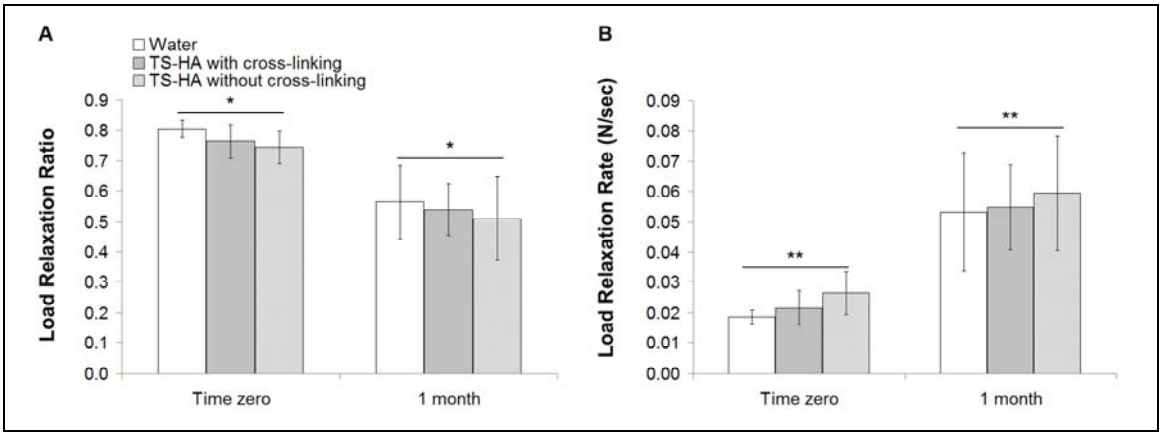

Figure 5.9 (A) Load relaxation ratio and (B) load relaxation rate of water control, TS-HA with cross-linking, and TS-HA without cross-linking treated fascia at time zero and one month (n=7-8 per group per time point). *Load relaxation ratio significantly decreased with time ($p<0.0001$). **Load relaxation rate significantly increased with time ($p<0.0001$).

Elastic Properties

Two-way ANOVA indicated that there was no significant group-time interaction for any of the elastic mechanical properties. Only time had a significant effect on toe-region stiffness, which was greater at time zero than at one month (Figure 5.10A, $p=0.001$). For toe-region elastic modulus, group (Figure 5.10B, $p=0.03$) and time ($p=0.002$) had significant effects. Toe-region modulus was significantly greater at time zero than at one and three months. TS-

HA treated fascia with cross-linking exhibited a significantly lower toe-region elastic modulus than water treated controls.

Only time had a significant effect on linear-region stiffness (Figure 5.10C, $p<0.0001$) and elastic modulus (Figure 5.10D, $p<0.0001$), both of which decreased with time.

Only group had a significant effect on transition strain (Figure 5.10E, $p=0.03$). TS-HA treated fascia with cross-linking had a significantly greater transition strain than treated fascia without cross-linking. Post-hoc multiple comparison testing indicated that treated fascia with cross-linking trended toward a greater transition strain than water treated controls ($p=0.06$).

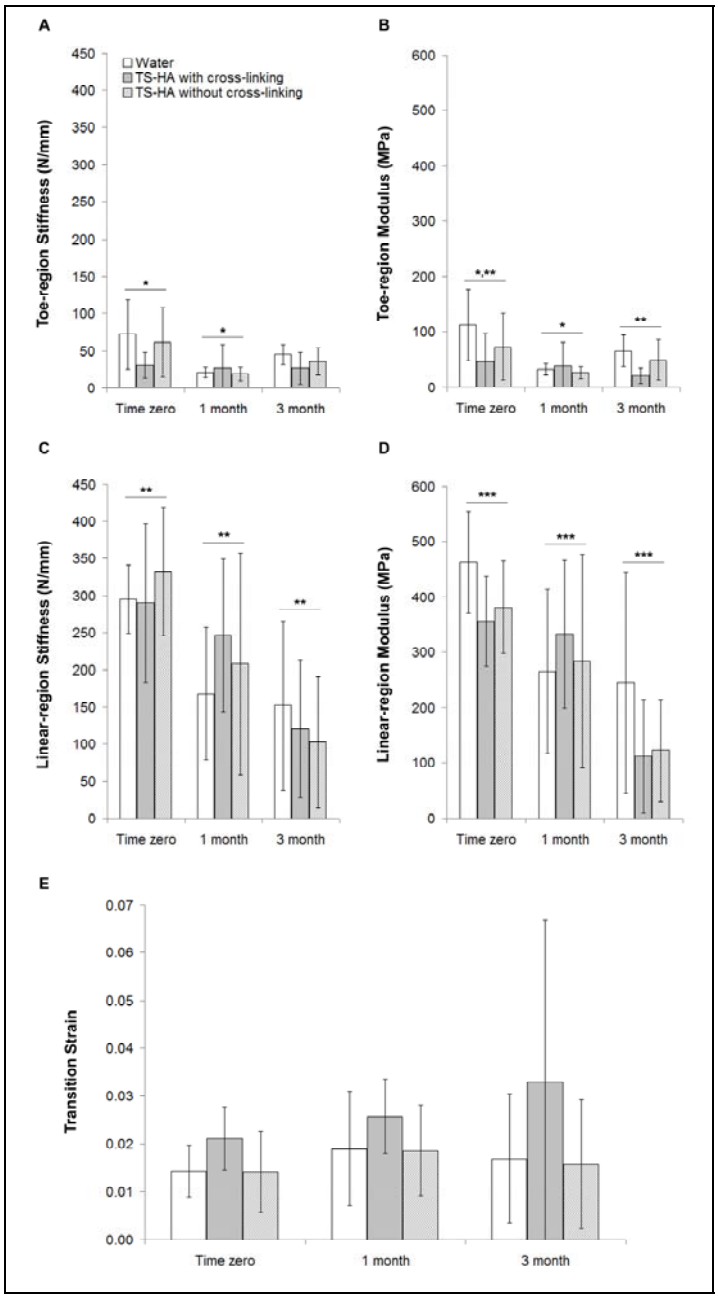

Figure 5.10 Elastic mechanical properties of water control, TS-HA with cross-linking, and TS-HA without cross-linking treated fascia (n=7-8 per group per time point). (A) *Toe-region stiffness was significantly greater at time zero than at one month (p=0.001). (B) For toe-region elastic modulus, group (p=0.03) and time (p=0.002) had significant effects. *,**Toe-region modulus was significantly greater at time zero than at one and three months. TS-HA treated fascia with cross-linking exhibited a significantly lower toe-region elastic modulus than water treated controls, which is not denoted with symbols because of the manner in which the data are graphically presented here. (C) **Linear-region stiffness significantly decreased with time (p<0.0001). (D) ***Linear-region modulus significantly decreased with time (p<0.0001). (E) TS-HA treated fascia with cross-linking had a significantly greater transition strain than treated fascia without cross-linking (p=0.03) and trended toward a greater transition strain than water treated controls (p=0.06). Neither result is denoted with symbols because of the manner in which the data are graphically presented here.

Discussion

The objective of this study was to determine changes in the mechanical properties of water and TS-HA treated fascia after implantation in a rat abdominal wall model. Fascia samples in all groups demonstrated time-dependent decreases in mechanical properties. TS-HA treated fascia with cross-linking exhibited a lower toe-region modulus and trended towards a higher transition strain than water treated controls not only after implantation, as hypothesized, but also at time zero. However, in contrast to the hypothesis, TS-HA treatment, with or without cross-linking, had no significant effect on time-zero or post-implantation load relaxation ratio, load relaxation rate, toe-region stiffness, linear-region stiffness, or linear-region modulus. Hence, the TS-HA treatment employed in this study decreased the low-load elastic mechanical properties of fascia ECM. To consider possible mechanisms for these mechanical property decreases, the results are discussed in light of the host cell response to these materials (Chapter 4).

The elastic properties of water treated fascia – as defined by toe stiffness, toe modulus, linear stiffness, and linear modulus – decreased after implantation. The viscoelastic properties also changed after implantation; load relaxation ratio decreased, while load relaxation rate increased. Previously, it was reported that water treated fascia was infiltrated by a moderate degree of macrophages and a mild degree of giant cells (Chapter 4), both of which are known to secrete the degradative enzymes matrix metalloproteinase (MMP)-1, -2, -9, -12, and -14 (132-134). Because elastin and other non-collagenous ECM proteins are the

main contributors to the mechanical behavior of fascia at low strains (138), it is possible that the decreased toe modulus following implantation is a result of elastase MMP-12 and/or broad spectrum MMP-14 activity. Additionally, the interaction between collagen and other ECM proteins could be physically disrupted by tissue swelling or edema, thus interrupting force transmission through the ground substance and lowering the toe modulus. Swelling and edema could also contribute to the increased stress relaxation of implanted fascia (144).

The mechanical behavior of fascia at higher strains is attributed to collagen fibers that are un-crimped and load-bearing (135-137). Hence, the observed decrease in linear modulus is possibly a result of collagenase (MMP-1, -2, and -9) activity. In support of these proposed mechanisms, it has been shown that MMP activity is a contributing factor in the loss of mechanical properties of ECM grafts following implantation (173,174).

Similar to water controls, both groups of TS-HA treated fascia demonstrated time-dependent decreases in mechanical properties. In addition, TS-HA treated fascia with cross-linking demonstrated an even lower toe modulus at both time zero and post implantation and trended toward a higher transition strain (i.e., longer toe-region) than water controls. Understanding the mechanical behavior of TS-HA treated fascia at low loads is clinically relevant, because normal tendons physiologically operate within the toe-region (i.e. 2-4% strain) (175,176).

The decreased low-load mechanical properties of cross-linked treated fascia at time zero may be attributed to the disruption of the interaction between collagen and other ECM proteins, possibly as a result of increased water uptake (177) during treatment (TS-HA treated fascia with cross-linking was uniquely subjected to a 24 hour rinse in 125 ml of water following the cross-linking reaction to remove any uncross-linked material). As well, the hydrogen peroxide that was used to initiate the cross-linking reaction could have activated endogenous tissue peroxidases, which may have disrupted or degraded ECM proteins involved in low-load mechanical behavior. Both hypothesized mechanisms are supported by the observation that uncross-linked treated fascia, which was not subjected to the 24 hour rinse or the cross-linking reaction, exhibited a similar toe modulus and transition strain as water controls.

Following implantation, the lower toe-modulus of TS-HA treated fascia with cross-linking may simply be a reflection of the decrease in this property at time zero. As well, TS-HA treated fascia with cross-linking was shown to elicit a heightened macrophage and giant cell response compared to water controls (Chapter 4). Hence the potential for increased MMP activity is another possible mechanism for the lower toe-region mechanical properties of cross-linked treated fascia following implantation. However, no difference was seen in high-load (linear region) mechanical properties between TS-HA treated fascia with cross-linking and water controls, suggesting that any increase in MMP activity largely targeted non-collagenous ECM proteins and not the collagen fibers. It is also possible that the cross-linked TS-HA hydrogel network that surrounds the large

fascicle bundles sequesters infiltrating inflammatory cells and mediators (178) or physically shields the collagen from degradative enzymes.

TS-HA treatment, with or without cross-linking, increased the cross-sectional area of fascia compared to water controls at time zero. This finding is consistent with previous results (Chapter 4) and suggests that inter-fascicular spaces expand to accommodate the added TS-HA. Further, the cross-sectional area of all groups tended to increase from one to three months, presumably as a result of tissue swelling, edema, or cellular infiltration. This result may seem to contradict the previous study, in which a decrease in cross-sectional area of fascia grafts from one to three months was reported (Chapter 4). The apparent discrepancy can be explained by noting that the cross-sectional area of mechanical test strips was measured *transversely* in this study, while the cross-sectional area of histologic grafts was measured *longitudinally* in the previous study described in Chapter 4. Hence, remodeling or resorption of the implanted grafts seems to occur from the ends, which is supported by the gross observation of explanted fascia strips.

The time-zero elastic modulus of water treated fascia quantified in this study (463 ± 92 MPa) is similar to the modulus previously reported by the Derwin laboratory (532 ± 106 MPa) (62). Whereas the elastic modulus of fascia following three months implantation in a rabbit vagina model was reported to decrease by 96% (179), a 48% drop is reported here. One explanation for these disparate results may be related to the very different *in vivo* implantation environments between the two studies. In addition, sample geometry and test methods were

different between the two studies (fascia strips in the Walter study had an aspect ratio of 4:1 and the elastic modulus was computed using grip-to-grip strain), so direct comparison of data is difficult. To the author's knowledge, there are no other reports on the post-implantation mechanical properties of fascia at comparable time points to which to compare this work.

The current study is not without limitations. The stress-relaxation test employed in this study involved a single step to 4% strain, which is beyond the toe-region of these materials. Hence viscoelastic differences between groups at low-strains could not be evaluated. Second, all fascia strips explanted at three months were exempted from viscoelastic testing, due to their unknown mechanical integrity. Third, a small number of cross-linked TS-HA treated fascia samples, which experienced extensive remodeling or resorption, could not be mechanically tested. Thus, the mechanical properties of TS-HA treated fascia with cross-linking reported here are likely overestimated, because the mechanically inferior samples were not included. Lastly, the mechanisms responsible for the mechanical property decreases reported herein can only be hypothesized to involve the degradation of collagen or other ECM proteins, as changes to the ECM components were not quantified.

Conclusion

This study is novel in that it characterizes the time-zero and post-implantation mechanical properties of water treated fascia ECM and TS-HA treated fascia with or without cross-linking. TS-HA treated fascia with cross-linking exhibited a lower toe-region modulus and trended towards a higher transition strain than water treated controls at time zero and post implantation. This study, in conjunction with the previous histologic assessment in Chapter 4, evaluates the post-implantation mechanical properties of TS-HA treated fascia in light of histologic outcomes. Together, the results suggest that TS-HA treatment (at the concentration, molecular weight, and tyramine substitution rate used here) adversely affects the elastic mechanical properties and host response to fascia ECM. In general, these findings demonstrate that augmentation of an ECM, in particular human fascia lata, with HA can alter both the mechanical properties and host response to the ECM. This work provides a starting point and guidance for the ongoing development of HA treated ECM scaffolds. Future work will investigate alternative HA treatment strategies with the intent to modulate inflammation within the ECM scaffold, enhance fibroblast infiltration, and consequently promote the regeneration of mechanically functional host tissue.

Chapter 6

Summary and Future Directions

Summary

Despite the increased development and investigation of extracellular matrix (ECM) scaffolds for tendon repair, no commercially-available ECM scaffold has yet demonstrated both the appropriate biological and mechanical properties for rotator cuff repair augmentation. The paucity of clinical studies in published literature includes only a limited number of ECM devices, have mixed patient outcomes, and are difficult to interpret in the absence of proper controls. Hence, there remains a critical need for an ECM scaffold that elicits minimal chronic inflammation, has mechanical properties similar to tendon, and ultimately facilitates the regeneration of a functional tendon-bone bridge. The *objective* of this work is to develop fascia ECM for rotator cuff repair augmentation by incorporating HA to minimize chronic inflammation within the scaffold and by

maintaining fascia's tendon-like mechanical properties. The *central hypothesis* is that HA treatment will decrease chronic inflammation within the scaffold and enhance fibroblast infiltration without decreasing the time-zero or post-implantation mechanical properties of fascia ECM. As described in this dissertation, a method to incorporate and immobilize HA within fascia ECM using tyramine substituted-hyaluronan (TS-HA) was developed. The host inflammatory response and macrophage polarization to TS-HA enriched fascia ECM was evaluated in a rat abdominal wall model. Lastly, the time-zero and post implantation mechanical properties of TS-HA enriched fascia ECM were quantified. A summary of the experimental outcomes associated with each specific aim follows:

Specific Aim 1: Develop an HA treatment of fascia ECM using TS-HA (Chapters 2 and 4)

A method of TS-HA treatment that increased the amount of HA in fascia by an order of magnitude to 5-10 micograms per milligram of dry weight tissue (μg/mg, ~ 1% tissue weight) was demonstrated. Furthermore, the incorporated TS-HA was distributed throughout the tissue and, upon cross-linking, was retained as a hydrogel network. The effectiveness of tyramine cross-linking in immobilizing HA within fascia was validated through an *in vitro* retention experiment, and as hypothesized, treated fascia with cross-linking retained more TS-HA than treated fascia without cross-linking.

Specific Aim 2: Evaluate the extent to which TS-HA treatment minimizes chronic inflammation within fascia ECM (Chapters 3 and 4)

The host inflammatory response to TS-HA treated fascia (5-10 µg/mg HA content) was characterized in a rat abdominal wall defect model with the hypothesis that treated fascia with cross-linking would exhibit lower lymphocyte, plasma cell, and macrophage densities, a higher fibroblast-like cell density, and a greater proportion of M2 pro-remodeling macrophages than M1 pro-inflammatory macrophages compared to water treated controls and treated fascia without cross-linking. In contrast to the hypothesis, TS-HA treated fascia with cross-linking had similar lymphocyte and plasma cell densities, greater macrophage and giant cell densities, and a lower density of fibroblast-like cells than water treated controls. However, cross-linked treated fascia did exhibit a predominantly M2 macrophage profile (suggestive of host repair and remodeling), a moderate degree of vascularization, and no fibrous capsule formation, similar to water controls and treated fascia without cross-linking.

These findings suggest that augmentation of an ECM, in particular human fascia lata, with HA can alter the host response to the ECM. However, the TS-HA treatment – at the particular concentration, molecular weight, and tyramine substitution rate – employed in this study was not effective in minimizing chronic inflammation within the scaffold.

Specific Aim 3: Evaluate the extent to which TS-HA treatment decreases the mechanical properties of fascia ECM (Chapter 5)

The mechanical properties of TS-HA treated fascia were evaluated at time zero and after implantation in a rat abdominal wall model. Specifically, load relaxation ratio, load relaxation rate, stiffness of the toe- and linear-regions, elastic modulus of the toe- and linear-regions, and transition strain were determined. Initially, cross-linked treated fascia was hypothesized to exhibit similar time-zero and post-implantation mechanical properties as water treated controls and uncross-linked treated fascia. However, the hypothesis changed in light of the histologic outcomes obtained from Specific Aim 2 (Chapter 4). Based on the heightened macrophage and giant cell response, it was hypothesized that TS-HA treated fascia with cross-linking would exhibit a lower load relaxation ratio, a higher load relaxation rate, lower toe- and linear-region stiffness, lower toe- and linear-region moduli, and higher transition strain compared to water treated controls and treated fascia without cross-linking.

TS-HA treated fascia with cross-linking demonstrated time-dependent decreases in mechanical properties, similar to water treated controls and treated fascia without cross-linking. The elastic properties of fascia grafts – as defined by toe stiffness, toe modulus, linear stiffness, and linear modulus – decreased after implantation. The viscoelastic properties also changed after implantation; load relaxation ratio decreased, while load relaxation rate increased. Cross-linked treated fascia exhibited a lower toe-region modulus and trended towards a higher transition strain (i.e., longer toe-region) than water treated controls not only after implantation, as hypothesized, but also at time zero. In contrast to the hypothesis, TS-HA treatment with or without cross-linking had no significant

effect on the time-zero or post-implantation load relaxation ratio, load relaxation rate, toe-region stiffness, linear-region stiffness, or linear-region modulus of fascia ECM. Hence, the TS-HA treatment employed in this dissertation decreased only the low-load elastic mechanical properties of fascia ECM.

In conjunction with Specific Aim 2, Specific Aim 3 connects the histologic outcomes of TS-HA treated fascia to post-implantation mechanical properties. Contrary to the intent, TS-HA treated fascia elicited an increased macrophage and giant cell response as well as decreased low-load elastic mechanical properties compared to water treated fascia. These results demonstrate that HA augmentation can alter the host response to an ECM scaffold and consequently affect its post-implantation mechanical properties. However, alternative treatment paradigms should be pursued to minimize the chronic inflammation response to an ECM scaffold, which may consequently mitigate the loss of mechanical properties following implantation.

Future Directions

Although the specific TS-HA treatment developed and evaluated in the preceding chapters did not minimize chronic inflammation as expected, nor did it mitigate the loss of mechanical properties after *in vivo* implantation, this work serves as a starting point from which the Derwin Laboratory will continue to develop TS-HA treated fascia ECM as an augmentation scaffold for rotator cuff repair. Moreover, these findings raised many questions regarding the effect of cross-linked TS-HA on inflammation, the effect of inflammation on ECM mechanical properties, and the underlying mechanisms. Future work will improve on the TS-HA treatment protocol described herein (with respect to approach, TS-HA molecular weight, content, distribution, and tyramine substitution rate) as well as the methods by which TS-HA treated fascia is characterized and assessed. In addition, future studies will attempt to elucidate the mechanisms responsible for the heightened macrophage and giant cell response as well as the decrease in toe-region elastic properties observed for cross-linked TS-HA treated fascia. The following sections provide greater detail on proposed future studies.

Variability in HA Content of Treated Fascia

TS-HA treated fascia patches exhibited patch-to-patch variability in HA content, which may have contributed to the variability seen in the histologic outcomes. Furthermore, inter- and intra-sample variability is undesirable from a manufacturing perspective. The exploration of ways to achieve a more uniform and consistent HA content is necessary and may involve adjustments to the

treatment approach, the TS-HA molecular weight, or the amount of incorporated TS-HA. The diffusion-based treatment method likely allows for a layer of TS-HA with an undefined thickness to cling to the surface of the treated fascia patch, contributing to the variability in HA content. The process of blotting and rinsing to remove excess surface TS-HA could be replaced by a more consistent method such as mechanical scraping that places a pre-set amount of pressure on the scaffold. Furthermore, vacuum or centrifugation methods may prove to be more successful in mechanically forcing the TS-HA through the tissue surface into the inter-fascicular spaces. Complete saturation of these spaces, which is most likely not achieved through a passive diffusion-based protocol, may provide a more homogeneous concentration of HA throughout the tissue. The HA content of treated fascia could be tailored by using TS-HA solutions with different concentrations and/or varying the number of passes with the vacuum or centrifugation methods as previously described in Chapter 2.

Concentration-dependent Host Inflammatory Response

The host inflammatory response to TS-HA treated fascia was characterized for grafts that had an average HA content of 3.5 µg/mg (Chapter 3) as well as those with an HA content of 5-10 µg/mg (Chapter 4). Although the study described in Chapter 3 was preliminary, these findings suggested that cross-linked treated fascia with an HA concentration of 3.5 µg/mg had qualitatively less inflammation than untreated fascia controls. In contrast, cross-linked treated fascia with an HA content of 5-10 µg/mg exhibited a persistent

chronic inflammatory response marked by increased macrophage and giant cell densities over water treated control. Together, these results suggest that cross-linked HA might have a concentration-dependent effect on the host inflammatory response. However, there are no studies in published literature that confirm the possibility that HA, cross-linked or not, has a concentration-dependent effect on inflammatory cell migration, proliferation, or activation. *In vitro* cell culture studies have demonstrated that HA has a concentration-dependent effect on fibroblast proliferation with low concentrations of HA (0.1 mg/ml = 0.01%) being more effective in promoting proliferation than higher concentrations (> 1 mg/ml = 0.1%) (180,181). The dose-effect of cross-linked HA on inflammatory cells could be investigated by evaluating the *in vitro* migration and proliferation of monocytes/macrophages seeded onto cross-linked TS-HA treated fascia of varying concentrations. As well, the host response could be studied in the rat abdominal wall model.

Remodeling of TS-HA Treated Fascia

A method to track the degradation of implanted fascia was not employed in the rat abdominal wall study. Radioactive labeling of collagen with ^{14}C or ^{3}H has been successful in quantifying the degradation rate of implanted ECM scaffolds and determining the fate of their degradation products (expelled as CO_2 or excreted in urine (182)). Incorporation of ^{14}C or ^{3}H into collagen requires continual injections of the radioactive isotope into the developing host animal (182,183). Because the fascia used in this dissertation was procured from human

cadavers, radioactive labeling of the ECM was not possible. Alternatively, fluorescent-labeling of collagen (184,185) prior to implantation is theoretically possible and, similarly, the tyramine adducts on TS-HA could be labeled to monitor degradation of the hydrogel. However, implementation of this idea may be impractical and challenged by photobleaching of the fluorophore, which can generate free radicals that are detrimental to the cell (186). The degradation kinetics of fascia grafts and the fate of degradation products are not of current interest, but labeling techniques such as those discussed here may be pursued in future work.

To distinguish remodeled fascia grafts from underlying native musculature, implanted fascia could be demarcated by running sutures underneath the graft. Identification of the structural components that constitute the remodeled tissue could be accomplished by immunostaining for type I and III collagen (associated with fascia of the anterior sheath) (187) or type I and II myosin (associated with skeletal muscle) (188). However, identifying a rat-specific anti-collagen antibody that does not bind to the human homolog may be difficult, as collagen is highly conserved across species.

Although three months implantation may be a sufficient endpoint for predicting the eventual remodeling fate of TS-HA treated fascia by classification of macrophage polarization, longer time points are necessary to ascertain end-stage outcomes. In particular, resolution of the lymphocyte and giant cell aggregates, degradation of cross-linked TS-HA, and verification of the lack of a fibrous capsule are important results to observe.

Host Response to TS-HA Treated Fascia Allograft

The histologic studies of Chapters 2 and 4 demonstrate the host response to fascia ECM in a xenogenic implantation model. Fascia grafts from all treatment groups, including water controls, were infiltrated by a heavy, chronic lymphocytic population, which likely represented an immune reaction to the xenograft. Hence, this dissertation does not accurately characterize the host response that would result if TS-HA treated fascia were to be used clinically as an allograft. To determine if the lymphocyte population was indeed a response to xenograft implantation, future studies should include rat fascia autograft and/or TS-HA treated rat fascia allograft as controls. However, contracture of rat fascia after surgical release from the abdominal wall would cause the tissue to be difficult to handle, and TS-HA treatment of rat fascia allograft could be challenging. With respect to fascia procurement and TS-HA treatment, implementation of such an allograft implantation study may be more feasible in a large animal model (canine or porcine). Alternatively, the host response to TS-HA treated human fascia could be studied in the athymic rat or primate abdominal wall model. However, these animal models are accompanied with their own set of challenges; athymic mice are high susceptible to infection, and the use of primates raises financial and ethical concerns.

Viscoelastic Mechanical Properties of TS-HA Treated Fascia

The stress-relaxation test described in Chapter 5 involved a single step to 4% strain, which was beyond the toe-region of the fascia samples. Hence,

viscoelastic differences between groups at low-strains could not be evaluated. Only two outcome measures were used to characterize the viscoelastic properties at 4% strain, namely stress-relaxation ratio and rate. With these mechanical testing and analysis methods, no difference between TS-HA treated fascia and water controls were detected, despite the order of magnitude increase in HA concentration of TS-HA treated fascia. Because quantification of stress-relaxation ratio and rate at 4% strain does not fully characterize the viscoelastic behavior of a material, perhaps differences between treated fascia and controls could be detected with more sophisticated methods of analysis. For example, quasi-linear viscoelastic (QLV) theory is often used to model the nonlinear time- and history-dependent viscoelastic behavior of soft tissues, including tendon (189,190). Five parameters describe the elastic response (A and B) and the reduced relaxation function (C, τ_1, and τ_2) (189,190).

Alternatively, future mechanical testing of fascia samples could be accomplished with an incremental stress-relaxation test, during which successive discrete strain increments are applied, each followed by a relaxation period (191). This would allow for evaluation of the relaxation response over a range of different strains, as opposed to only 4% strain, and both viscoelastic (relaxation ratios and rates at different strains) and elastic (peak and equilibrium elastic moduli) mechanical properties could be quantified from the same data set.

Heavy Chain Transfer to Cross-linked TS-HA Treated Fascia

One possible mechanism that could explain the heightened macrophage response exhibited by cross-linked TS-HA treated fascia involves the transfer of heavy chains (HC) from inter-α-inhibitor (IαI), an abundant plasma proteoglycan, to cross-linked HA (161,162). The HC-HA association has been shown to enhance the binding of monocytes/macrophages to HA through a CD44-mediated process (161,162). Future experiments will include immunostaining the histologic sections from the host response study for HCs to visualize their localization on cross-linked TS-HA treated fascia. Western blot analysis of the tissue digest will be conducted to distinguish the transfer of single HCs from those left intact on IαI.

Degradation of Collagen and Other ECM Proteins

In Chapter 5, it was hypothesized that the mechanisms responsible for the mechanical property decreases of implanted fascia grafts may involve the degradation of collagen or other ECM proteins. Future work should include quantifying changes to collagen and GAG in the ECM scaffold after implantation. Decreases in collagen and GAG content would support the hypothesis that their degradation may be responsible for the reduced linear- and toe-region elastic mechanical properties, respectively, of implanted fascia ECM.

Cross-linked TS-HA Coating to Sequester Inflammatory Cells

Day and de la Motte previously proposed that the HC-HA complex may be part of a protective mechanism to regulate inflammation-induced destruction of the ECM (178). By acting as a "sink" for inflammatory cells and mediators, cross-linked HA prevents these cells from forming pro-inflammatory associations with surrounding tissue. The sequestering ability of the HC-HA complex may be exploited by coating only the surface of the fascia scaffold with TS-HA, rather than incorporating the TS-HA throughout the entire matrix. A coating of TS-HA hydrogel could sequester infiltrating macrophages and giant cells away from the underlying fascia scaffold, thereby protecting the bulk matrix from degradative enzymes, acid, and matrix metalloproteinases. Consequently, the loss of mechanical properties observed herein for cross-linked TS-HA treated fascia could be mitigated or reduced. The effects of coating fascia ECM with a TS-HA hydrogel on non-inflammatory cells (i.e., fibroblasts and endothelial cells) are unknown and would require further investigation.

Other Applications of HA Augmentation

TS-HA enriched fascia ECM could potentially serve as a delivery platform for a number of bioactive molecules – including growth factors, therapeutic drugs, and matrix metalloproteinase inhibitors – to enhance tendon healing. This could be accomplished by chemically tethering these molecules to the tyramine adducts of TS-HA or by physically trapping them in the hydrogel upon cross-linking to allow for sustained release of the entrapped molecules. Furthermore,

TS-HA treated fascia could function as a cell culture vehicle, similar to thiol-modified HA. However, issues of oxygen and nutrient diffusion as they relate to cell viability would need to be addressed. HA enriched fascia could also be effective for the surgical reconstruction of other soft tissues, including ligament, bowel, and bladder in the setting of post-surgical repair failure, trauma, and segmental defects. Lastly, HA augmentation could be applied to other ECMs, such as dermis or small intestinal submucosa.

Conclusion

The work described in this dissertation is ***significant*** in that it demonstrates methods to incorporate HA within fascia ECM and characterizes the host response and concomitant mechanical behavior of a novel TS-HA enriched fascia scaffold following *in vivo* implantation. TS-HA treatment (at the concentration, molecular weight, and tyramine substitution rate) described in this dissertation elicited an increased macrophage and giant cell response and decreased low-load elastic mechanical properties compared to water treated control. Hence, the preparation of TS-HA treated fascia described in this dissertation would not be beneficial as an augmentation device for rotator cuff repair. The results, however, suggest that the inflammatory response to an ECM scaffold affects its post-implantation mechanical properties. Therefore, continued work toward a treatment strategy that minimizes chronic inflammation of an ECM scaffold may mitigate the loss of mechanical properties following implantation and should be pursued.

Development of an ECM scaffold that elicits minimal chronic inflammation, has mechanical properties similar to tendon, and ultimately facilitates the regeneration of a functional tendon-bone bridge would ***positively impact*** the repair of torn rotator cuffs and may be beneficial for the augmentation of other soft tissue repairs. HA augmentation is a novel way to influence the host response and concomitant mechanical properties of fascia ECM, but further development is needed. The successful use of TS-HA treated fascia as an

augmentation scaffold for rotator cuff repair would reduce debilitation and alleviate pain, thereby increasing patient quality of life.

Appendix A

Pilot Study: Comparison of Hyaluronic Acid Binding Protein Enzyme-linked Immunosorbent Assay and Hexuronic Acid Assay for the Quantification of Cross-linked Tyramine Substituted-Hyaluronan

Introduction

Hyaluronic acid binding protein enzyme-linked immunosorbent assay (HABP ELISA) is a sandwich protein binding assay that indirectly quantifies hyaluronan (HA) concentration by measuring the intensity of colorimetrically-labeled HABP that binds to uninterrupted oligosaccharides of the hyaluronan (HA) chain. However, this assay may not be appropriate for the quantification of cross-linked tyramine substituted-hyaluronan (TS-HA). The di-tyramine bridges that form upon cross-linking of TS-HA could inhibit HABP from binding to large segments of the HA chain, thereby underestimating the HA concentration.

Hence, the objective of this experiment was to compare the HA concentrations reported by HABP ELISA to hexuronic acid assay (HAA) using solutions containing cross-linked TS-HA. HAA has been routinely used for the quantification of glycosaminoglycans (192,193) and has been shown to equally detect HA and TS-HA (106), as well as uncross-linked TS-HA and cross-linked TS-HA (106). Presumably, the HA adduct bond is cleaved when the sample is heated in concentrated sulfuric acid during the HAA protocol (106). It was hypothesized that HAA would detect a higher HA concentration than ELISA for solutions containing cross-linked TS-HA.

Materials and Methods

The remaining PBS release solutions of the TS-HA treated fascia with cross-linking samples at 48 hours from Pilot Study #2 of Chapter 2 were re-analyzed with HAA (n=10, HA concentrations were previously measured with ELISA). Briefly, 4.4 ml of each solution was dehydrated in a speedvac and reconstituted in 110 µl of PBS (samples were concentrated by a factor of 40 to ensure they would fall on the standard curve). A 100 µl aliquot of each sample was combined with 750 µl of sulfuric acid and heated at 90°C for 5 min. Then, samples were cooled in a water bath for 2 min and mixed with 10 µl hydroxyl phenol. A 250 µl aliquot of each sample was loaded in triplicate on a 96 well plate and absorbance at 532 nm was determined using a SpectraMax Plus spectrophotometer (Molecular Devices Inc., Sunnyvale, CA). HA concentration of

the samples was determined by comparison to a standard curve composed of 640, 320, 200, 80, 40, and 20 nmol/ml of glucuronic acid in ultrapure water.

Results

The HA concentrations of the release solutions containing cross-linked TS-HA were consistently higher when measured with HAA than with ELISA (Table A.1). On average, the HA concentration reported with HAA was 5.5 times greater than ELISA (n=9).

Table A.1 HA concentrations of PBS release solutions containing cross-linked TS-HA as determined by HABP ELISA and HAA

Sample Number	HABP ELISA (ngm/ml)[†]	HAA (ngm/ml)	HAA Fold-increase over ELISA	Average Fold-increase
1	380	6780	17.8	5.5
2	398	1790	4.5	
3	415	1700	4.1	
4	390	1300	3.3	
5	343	1420	4.1	
6	Undetectable	810	---	
7	360	1300	3.6	
8	298	940	3.2	
9	450	1900	4.2	
10	163	730	4.5	

[†]HABP ELISA data from Pilot Study #2 (Chapter 2)

Conclusion

The objective of this experiment was to compare the HA concentrations reported by HABP ELISA to HAA for PBS release solutions containing cross-

linked TS-HA. As hypothesized, HAA detected a (5.5-fold) greater HA concentration than ELISA.

Because this experiment was conducted after the *in vitro* release experiment (Pilot Study #2, Chapter 2) was completed, the PBS release solutions from 1, 6, and 24 hours had already been analyzed with ELISA and were therefore not available for HAA analysis. Hence, a conversion factor of 5.5 was applied to the ELISA data to compare the release solutions of cross-linked TS-HA treated fascia to untreated fascia controls and uncross-linked TS-HA treated fascia. It should be noted that such data analysis was only performed due to the preliminary nature of the experiment. Fluorophore-assisted carbohydrate electrophoresis was used to accurately quantify HA content in TS-HA treated fascia in subsequent experiments (Chapter 4).

Appendix B

Matlab Code

This appendix includes the author-generated Matlab codes used to calculate the mechanical property outcomes presented in Chapter 5.

Code 1: Calculation of viscoelastic and elastic mechanical properties from a mechanical testing protocol that includes both a step relaxation test and a failure test.

Derwin Lab
Date: August 10, 2010
Author: LiKang Chin

This program will read a *.dat data file generated from the MTS FlexTest SE electromechanical test system. This program will generate the following data files:

1. ResultsSummary.xls: toe-region elastic modulus (Elastic Modulus-1), toe-region stiffness (Stiffness-1), the associated r-squared value, linear-region elastic modulus (Elastic Modulus-2), linear-region stiffness (Stiffness-2), the associated r-squared value, strain intercept of the toe- and linear- region lines, load relaxation ratio, delta gage length, load relaxation rate (all data), and load relaxation rate (first 10 seconds of the data).
2. ElasticModulus.xls: Elastic Modulus-1, Elastic Modulus-2, and the associated r-squared values

3. Stiffness.xls: Stiffness-1, Stiffness-2, and the associated r-squared values
4. LoadOpticalDisp.xls: optical displacement and load
5. StressStrain.xls: optical strain and stress
6. Stressrelaxloads.xls: maximum and final loads
7. Gagelength.xls: initial and final gage lengths

Elastic modulus and stiffness are calculated using the following options:

Option 1: User specifies strain limits and the elastic modulus is calculated as the linear portion between these limits from the stress vs. strain curve.
Option 2: The program polyfits the stress vs. strain curve, differentiates the equation, and determines the tangent (elastic modulus) at a strainpoint specified by the user.
Option 3: The program applies a bilinear curve fit to the stress vs. strain curve and determines the intersection of the two lines (strain intercept).

User inputs: The user will be prompted to enter the name of a text file (*.txt) containing the filenames of all the results.csv files (from tc_multi_points) and .dat files to be processed. The format of this file should be an Mx4 matrix where M is the number of data files to process. The first column should be a listing of the result.csv filenames, and the second column should be a listing of the .dat filenames. The third column should be the calibration factor (pixels/mm) of the video capture system; the fourth column should be the first camera frame of the failure portion of the test; the fifth column should be the last camera frame of the failure portion of the test; and the sixth column should be the cross-sectional area of the sample (mm^2).

The user will be asked to input the zero load.

Note well: All *. data files must be sampled at the same frequency. Force data should be recorded in N.

```
**************************************************************************************************
clear
% Ask user for the file containing the filenames of the results.csv files and the .dat files
% This file must be a *.txt file, and you need to type in the *.txt extension
rawfile = input('Enter the name of the file containing the filenames of the results.csv files and .dat
files:  ','s');
% Ask user for zeroload
zeroload = input('Enter the zero load (0.2 N?):  ');
% Read filenames to matrix names
names=[];gage=[];StressStrain=[];maxpt=[];maxstress=[];maxstrain=[];
[A] = textread(rawfile,'%s');
j=1;
for i=1:6:size(A);
   names{j,1}=A{i};
   names(j,2)=A(i+1);
   j=j+1;
end
% Read video calibration factor, first frame, last frame, and cross-sectional area to data
data=[];
data = dlmread(rawfile,'\t',0,2);
totfiles=size(names,1);
for z=1:totfiles;
% Read in raw "results" data file from tc_multi_pts
R = [];
R = csvread(names{z,1},2,0);
totpts=size(R,1);
% Read in raw MTS data file
MTS= [];
```

```
MTS= textread(names{z,2},'','headerlines',5);
totpts2=size(MTS,1);
% Zero the load
zeroedloadvector=[];
zeroedloadvector = MTS(:,3)-zeroload;
% Remove the y value columns from R and save as R1
R1 = [];
R1= [R(:,1),R(:,3),R(:,5),R(:,7)];
% Convert R1 from pixels to mm
R2=[];
R3=[];
for g=1:size(R1,1)
   R2(g,1)=R1(g,1)/data(z,1);
   R2(g,2)=R1(g,2)/data(z,1);
   R3(g,1)=R1(g,3)/data(z,1);
   R3(g,2)=R1(g,4)/data(z,1);
end
% Average the columns of R2 and R3
R4=[];
R5=[];
R4=mean(R2,2);
R5=mean(R3,2);
% Subtract R5 from R4 and make the optical displacement vector
rawdisp=[];
opticaldisp=[];
rawdisp=R5-R4;
MTSframe=[];
MTSvideo=[];
MTSframe=MTS(:,5);
MTSvideo=MTS(:,4);
zeroedloadvector2=[];
k=1;
ttt=0;
for m=data(z,2):data(z,3);
 ttt=0;
   for h=1:totpts2;
      if ttt==0;
   if MTSframe(h)==m;
       if MTSvideo(h)==5;
           zeroedloadvector2(k)=zeroedloadvector(h);
           k=k+1;
           ttt=1;
       end
   end
end
end
end
zeroedloadvector3=[];
rawdisp1=[];
rr=1;
for ss=1:size(zeroedloadvector2,2);
   if zeroedloadvector2(ss)>=0;
       zeroedloadvector3(rr)=zeroedloadvector2(ss);
       rawdisp1(rr)=rawdisp(ss);
       rr=rr+1;
   end
```

```
end
opticaldisp1=[];
opticaldisp1=rawdisp1-(rawdisp1(1));
% Make the stress vector
stress=[];
XSA(z)=data(z,4);
stress=zeroedloadvector3/(data(z,4));
% Make the optical strain vector
opticalstrain=[];
opticalstrain=opticaldisp1/(rawdisp1(1));
rawdisp1(z)=rawdisp1(1);
% Calculate load relaxation ratio
initialgagedisp=[];
kk=1;
lowload = .01;
for t=0:3999;
   if kk==1;
   if zeroedloadvector(4000-t)<lowload;
      if zeroedloadvector(4000-t)>=0;
         if zeroedloadvector(4000-t-20)>.1;
           initialgagedisp=MTS(4000-t,2);
            lowload=zeroedloadvector(4000-t);
            point(z)=t;
            kk=0;
         end
      end
   end
end
end
lowload1=lowload;
yyy=1;
for c=-20:20;
     if zeroedloadvector(4000-point(z)-c)<lowload1;
       if zeroedloadvector(4000-point(z)-c)>=0;
         if zeroedloadvector(4000-point(z)-c-20)>.1;
                  lowload1=zeroedloadvector(4000-point(z)-c);
                   initialgagedisp=[];
                   initialgagedisp=MTS(4000-point(z)-c,2);
                   initialpoint(z)= (4000-point(z)-c);
                end
             end
      end
   end
maxload=[];
[maxload maxloadpt]= max(zeroedloadvector(1:4000));
maxloadtime=MTS(maxloadpt,1);
finalstressrelaxload=[];
jj=1;
for q=1:4000;
   if jj==1;
      if MTS((10000-q),2)>=1;
      if MTS((10000-q),2)==MTS((10000-q-1),2);
         if MTS((10000-q),2)==MTS((10000-q-2),2);
            if MTS((10000-q),2)==MTS((10000-q-3),2);
               if MTS((10000-q),2)==MTS((10000-q-4),2);
                  if MTS((10000-q),2)==MTS((10000-q-5),2);
```

```
                    finalstressrelaxload=zeroedloadvector(10000-q);
                    point2=q;
                    jj=2;
                  end
                end
              end
            end
          end
        end
    end
end
finalgagedisp=[];
stressrelaxationratio= finalstressrelaxload/maxload;
stressrelaxationratiovector(z)=stressrelaxationratio;
% Calculate load relaxation rate (all data and first ten seconds of the
% data)
zeroedtime=[];
logtime=[];
logload=[];
zeroedtime=MTS(maxloadpt:10000-point2,1)-MTS(maxloadpt,1);
logtime=log(zeroedtime(2:size(zeroedtime)));
logload=log(zeroedloadvector(maxloadpt+1:10000-point2));
[rateint, rate, rateR]=regress(logtime, logload);
ratevectorall(z)=rate;
zeroedtime10s=[];
logtime10s=[];
logload10s=[];
zeroedtime10s=MTS(maxloadpt:maxloadpt+100,1)-MTS(maxloadpt,1);
logtime10s=log(zeroedtime10s(2:size(zeroedtime10s)));
logload10s=log(zeroedloadvector(maxloadpt+1:maxloadpt+100));
[rateint10s, rate10s, rateR10s]=regress(logtime10s, logload10s);
ratevector10s(z)=rate10s;
mm=1;
for p=10000:totpts2;
   if mm==1;
     if zeroedloadvector(p)>=0;
        if zeroedloadvector(p+2)>zeroedloadvector(p);
           if zeroedloadvector(p+4)>zeroedloadvector(p+1);
              if zeroedloadvector(p+6)>zeroedloadvector(p+2);
                 if zeroedloadvector(p+8)>zeroedloadvector(p+3);
                    if zeroedloadvector(p+10)>zeroedloadvector(p+4);
                       if zeroedloadvector(p+15)>zeroedloadvector(p+5);
         finalgagedisp=MTS(p,2);
         point3=p;
         mm=2;
      end
   end
end
end
end
end
end
end
deltadisp=finalgagedisp-initialgagedisp;
deltadispvector(z)=deltadisp;
```

```
% Fit the load vs. optical displacement data using a polynomial fit
poly=polyfit(opticaldisp1,zeroedloadvector3,3);
polyfitloadvector=poly(1)*(opticaldisp1.^3)+poly(2)*(opticaldisp1.^2)+poly(3)*(opticaldisp1)+poly(4
);
poly2=polyfit(opticalstrain,stress,3);
polyfitstressvector=poly2(1)*(opticalstrain.^3)+poly2(2)*(opticalstrain.^2)+poly2(3)*(opticalstrain)+
poly2(4);
gage(z)=rawdisp1(1);
% Create Stress vs. optical Strain array
stresstrans=[];
stresstrans=stress';
totptsvector(z)=length(stresstrans);
for gg=1:size(stresstrans,1);
   StressStrain(gg,2*z-1)=stresstrans(gg);
   StressStrain(gg,2*z)=opticalstrain(gg);
end
% Create Load vs. optical Disp array
zeroedloadvector3trans=[];
zeroedloadvector3trans=zeroedloadvector3';
for yy=1:size(zeroedloadvector3trans,1);
   LoadDisp(yy,2*z-1)=zeroedloadvector3trans(yy);
   LoadDisp(yy,2*z)=opticaldisp1(yy);
end
% Create stress-relaxation maximum load and final load array
Maxfinalload(:,2*z-1)=maxload;
Maxfinalload(:,2*z)=finalstressrelaxload;
% Create initial and final gage length array
initialfinalgagedisp(:,2*z-1)=initialgagedisp;
initialfinalgagedisp(:,2*z)=finalgagedisp;
end
%  Write the adjusted StressStrain array to a file called "StressStrain.xls"
fid=fopen('StrainStress.xls','wt');
fprintf(fid,'%s\t\t\t\t\t%s\n','Summary of Stress-Strain Mechanical Testing Data',date);
fprintf(fid,'\n');
for z=1:size(names,1);
   fprintf(fid,'%s\t\t',names{z,2});
end
fprintf(fid,'\n');
for z=1:size(names,1);
   fprintf(fid,'%s\t\%s\t','Stress_MPa','OpticalStrain');
end
fprintf(fid,'\n');
for m=1:size(StressStrain,1);
   for y=1:size(StressStrain,2);
      fprintf(fid,'%f\t',StressStrain(m,y));
   end
   fprintf(fid,'\n');
end
fclose(fid);
fprintf(1,'\n%s\n','The StrainStress.xls file has been successfully generated.');
fprintf(1,'\n');
%Plot stress vs. strain for all files
figure (3)
for s=1:2:size(StressStrain,2);
   hold on
   plot (StressStrain(:,s+1),StressStrain(:,s))
```

```
   title('Stress vs. Optical Strain')
end
%  Write the LoadDisp array to a file called "LoadOpticalDisp.xls"
fid=fopen('LoadOpticalDisp.xls','wt');
fprintf(fid,'%s\t\t\t\t\t%s\n','Summary of Load-Optical Displacement Mechanical Testing
Data',date);
fprintf(fid,'\n');
for z=1:size(names,1);
   fprintf(fid,'%s\t\t',names{z,2});
end
fprintf(fid,'\n');
for z=1:size(names,1);
   fprintf(fid,'%s\t\%s\t','Optical Displacement_mm','Load_N');
end
fprintf(fid,'\n');
for m=1:size(LoadDisp,1);
   for y=1:size(LoadDisp,2);
      fprintf(fid,'%f\t',LoadDisp(m,y));
   end
   fprintf(fid,'\n');
end
fclose(fid);
fprintf(1,'\n%s\n','The LoadOpticalDisp.xls file has been successfully generated.');
fprintf(1,'\n');
%  Write the Maxfinalload array to a file called "Stressrelaxloads.xls"
fid=fopen('Stressrelaxloads.xls','wt');
fprintf(fid,'%s\t\t\t\t\t%s\n','Summary of Stress Relaxation Loads Mechanical Testing Data',date);
fprintf(fid,'\n');
for z=1:size(names,1);
   fprintf(fid,'%s\t\t',names{z,2});
end
fprintf(fid,'\n');
for z=1:size(names,1);
   fprintf(fid,'%s\t\%s\t','MaximumLoad_N','FinalLoad_N');
end
fprintf(fid,'\n');
for m=1:size(Maxfinalload,1);
   for y=1:size(Maxfinalload,2);
      fprintf(fid,'%f\t',Maxfinalload(m,y));
   end
   fprintf(fid,'\n');
end
fclose(fid);
fprintf(1,'\n%s\n','The Stressrelaxloads.xls file has been successfully generated.');
fprintf(1,'\n');
%  Write the initialfinalgagedisp array to a file called "Gagelength.xls"
fid=fopen('Gagelength.xls','wt');
fprintf(fid,'%s\t\t\t\t\t%s\n','Summary of Initial and Final Gage Displacements Mechanical Testing
Data',date);
fprintf(fid,'\n');
for z=1:size(names,1);
   fprintf(fid,'%s\t\t',names{z,2});
end
fprintf(fid,'\n');
for z=1:size(names,1);
   fprintf(fid,'%s\t\%s\t','InitialGageLength_mm','FinalGageLength_mm');
```

```
end
fprintf(fid,'\n');
for m=1:size(initialfinalgagedisp,1);
   for y=1:size(initialfinalgagedisp,2);
      fprintf(fid,'%f\t',initialfinalgagedisp(m,y));
   end
   fprintf(fid,'\n');
end
fclose(fid);
fprintf(1,'\n%s\n','The Gagelength.xls file has been successfully generated.');
fprintf(1,'\n');
fprintf(1,'%s\n','Would you like to specify strain limits for emod? Enter 1.');
fprintf(1,'%s\n','Would you like to take the tangent (emod) at a single point? Enter 2.:  ');
decision3 = input ('Would you like to fit the curve with two linear fits and determine the
intersection? Enter 3.:  ');
fprintf(1,'\n');
if decision3==1;
lowstrain = input('Enter the lower strain limit for computation of elastic modulus:  ');
upstrain = input('Enter the upper strain limit for computation of elastic modulus:  ');
%  Extract emod from stress and strain data in the linear portion (between
%  "lowstrain" and "upstrain") using regress.
fid=fopen('ElasticModulus.xls','wt');
fprintf(fid,'%s\t\t\t\t\t%s\n','Summary of Merlin Mechanical Testing Data',date);
fprintf(fid,'\n\n');
fprintf(fid,'%s\t\t%s\t%s\t\n','Sample_ID','ElasticModulus','R-Squared');
fprintf(fid,'%s\t\t%s\t\t%s\t\t\t\t\t\n','','(MPa)','(MPa)');
for w=1:2:size(StressStrain,2);
Stress2=[];OptStrain=[];k=0;
   for m=1:size(StressStrain,1);
   if StressStrain(m,w+1) > lowstrain;
      if StressStrain(m,w+1) < upstrain;
         k=k+1;
         Stress2(k,1)=StressStrain(m,w);
         OptStrain(k,1)=StressStrain(m,w+1);
         strainpoints(w)=size(OptStrain,1);
      end
   end
   end
   [yint, EMod, RMod] = regress(OptStrain,Stress2);
   EModvector(w)=EMod;
%  Write the modulus data to a summary file called "ElasticModulus.xls"
   l=(w+1)/2;
   fprintf(fid,'%s\t\t%f\t%f\n',names{l,2},EMod,RMod);
end
fclose(fid);
fprintf(1,'\n\n%s\n\n','The ElasticModulus.xls file has been successfully generated (decision 1).');
fid=fopen('Stiffness.xls','wt');
fprintf(fid,'%s\t\t\t\t\t%s\n','Summary of Merlin Mechanical Testing Data',date);
fprintf(fid,'\n\n');
fprintf(fid,'%s\t\t%s\t%s\t\n','Sample_ID','Stiffness','R-Squared');
fprintf(fid,'%s\t\t%s\t\t\t\t\t\t\n','','(N/mm)');
for w=1:2:size(StressStrain,2);
Load=[];Disp=[];k=0;
   for m=1:size(StressStrain,1);
   if StressStrain(m,w+1) > lowstrain;
      if StressStrain(m,w+1) < upstrain;
```

```
            k=k+1;
            Load(k,1)=LoadDisp(m,w);
            Disp(k,1)=LoadDisp(m,w+1);
        end
    end
    end
    [yint, Stiffness, RStiff] = regress(Disp,Load);
    Stiffnessvector(w)=Stiffness;
%  Write the stiffness data to a summary file called "Stiffness.xls"
    l=(w+1)/2;
    fprintf(fid,'%s\t\t%f\t%f\n',names{l,2},Stiffness,RStiff);
    z=z+1;
    tt=0;
    RStiffsaved=.7;
end
fclose(fid);
fprintf(1,'\n\n%s\n\n','The Stiffness.xls file has been successfully generated.');
end
if decision3==2;
    strainpoint = input('Enter strain where you would like to compute the tangent of the stress-
strain curve:  ');
fid=fopen('ElasticModulus.xls','wt');
fprintf(fid,'%s\t\t\t\t\t%s\n','Summary of Merlin Mechanical Testing Data',date);
fprintf(fid,'\n\n');
fprintf(fid,'%s\t\t%s\t\n','Sample_ID','ElasticModulus');
fprintf(fid,'%s\t\t%s\t\t\t\t\t\n','','(MPa)');
%polyfit the stress-strain data, take the derivative of the equation, and
%determine the tangent at the desired strain.
for w=1:totfiles;
Stress2=[];OptStrain=[];k=0;
polyemod=polyfit(StressStrain(1:totptsvector(w),2*w),StressStrain(1:totptsvector(w),2*w-1),3);
tangent=polyder(polyemod);
EMod=tangent(1)*(strainpoint)^2+tangent(2)*(strainpoint)+tangent(3);
strainvector=0:0.005:0.10;
predictedstress=polyemod(1)*(strainvector).^3+polyemod(2)*(strainvector).^2+polyemod(3)*(strai
nvector)+polyemod(4);
predictedstresstrans=predictedstress';
predictedstressmatrix(:,1)=strainvector';
predictedstressmatrix(:,w+1)=predictedstresstrans;
EModvector(w)=EMod;
%plot polyfit data with actual data
polyfitstressvector=[];
polyfitstressvector=polyemod(1)*((StressStrain(1:totptsvector(w),2*w)).^3)+polyemod(2)*((Stress
Strain(1:totptsvector(w),2*w)).^2)+polyemod(3)*(StressStrain(1:totptsvector(w),2*w))+polyemod(4
);
figure (4)
plot (StressStrain(1:totptsvector(w),2*w),StressStrain(1:totptsvector(w),2*w-
1),'b.',StressStrain(1:totptsvector(w),2*w),polyfitstressvector,'rx')
title('Stress vs. Strain, actual data and fit data');
ypred=[];dev=[];SST=[];resid=[];SSE=[];Rsq=[];
ypred=polyval(polyemod,StressStrain(1:totptsvector(w),2*w));
dev=StressStrain(1:totptsvector(w),2*w-1)-mean(StressStrain(1:totptsvector(w),2*w-1));
SST=sum(dev.^2);
resid=StressStrain(1:totptsvector(w),2*w-1)-ypred;
SSE=sum(resid.^2);
Rsq=1-SSE/SST;
```

```
Rsqvector(w)=Rsq;
Rsqlinear2=.5;
yyy=[];
for yyy=1:(length(polyfitstressvector)-3);
[yint, EModlinear, Rsqlinear] =
regress(StressStrain(yyy:yyy+3,2*w),polyfitstressvector(yyy:yyy+3));
if Rsqlinear>=Rsqlinear2;
   Rsqlinear2=Rsqlinear;
   Rsqlinearvector(w)=Rsqlinear;
   startpoint(w)=yyy;
end
end
highpoint(w)=totptsvector(w);
highstrain(w)=StressStrain(totptsvector(w),2*w);
u=0;
qq=[];
for qq=0:((length(polyfitstressvector))-(startpoint(w))-3);
   [yint2, EModlinear2,
Rsqlinear2]=regress(StressStrain(startpoint(w):(startpoint(w)+3+qq),2*w),polyfitstressvector(start
point(w):(startpoint(w)+3+qq)));
  if u==0;
   if Rsqlinear2<0.999;
      highpoint(w)=startpoint(w)+3+qq-1;
      highstrain(w)=StressStrain(highpoint(w),2*w);
      u=1;
   end
end
end
lowpoint(w)=1;
lowstrain(w)=StressStrain(1,2*w);
v=0;
qqq=[];
for qqq=0:(startpoint(w)-1);
   [yint3, EModlinear3, Rsqlinear3]=regress(StressStrain(startpoint(w)-
qqq:(startpoint(w)+3),2*w),polyfitstressvector(startpoint(w)-qqq:(startpoint(w)+3)));
   if v==0;
   if Rsqlinear3<0.999;
      lowpoint(w)=startpoint(w)-qqq+1;
      lowstrain(w)=StressStrain(lowpoint(w),2*w);
      v=1;
   end
end
end
midstrain(w)=highstrain(w)-((highstrain(w)-lowstrain(w))/2);
EModmidstrain(w)=tangent(1)*(midstrain(w))^2+tangent(2)*(midstrain(w))+tangent(3);
EModhighstrain(w)=tangent(1)*(highstrain(w))^2+tangent(2)*(highstrain(w))+tangent(3);
EModlowstrain(w)=tangent(1)*(lowstrain(w))^2+tangent(2)*(lowstrain(w))+tangent(3);
 [yint4, EModlinear4,
Rsqlinear4]=regress(StressStrain(lowpoint(w):highpoint(w),2*w),polyfitstressvector(lowpoint(w):hi
ghpoint(w)));
EModlinear4vector(w)=EModlinear4;
[yint5, Stiffnesslinear5, Rsqlinear5]=regress(LoadDisp(lowpoint(w):highpoint(w),2*w-
1),polyfitstressvector(lowpoint(w):highpoint(w))*XSA(w));
Stiffnesslinear5vector(w)=Stiffnesslinear5;
decision4 = input('Does the fit data represent the actual data? Would you like to continue? Enter
1 for yes, 2 for no.:  ');
```

```
if decision4==1;
%  Write the Merlin modulus data to a summary file called "ElasticModulus.xls"
   l=w;
   fprintf(fid,'%s\t\t%f\n',names{l,2},EMod);
end
end
fclose(fid);
fprintf(1,'\n\n%s\n\n','The ElasticModulus.xls file has been successfully generated (decision 2).');
fid=fopen('Stiffness.xls','wt');
fprintf(fid,'%s\t\t\t\t\t%s\n','Summary of Merlin Mechanical Testing Data',date);
fprintf(fid,'\n\n');
fprintf(fid,'%s\t\t%s\t\n','Sample_ID','Stiffness');
fprintf(fid,'%s\t\t%s\t\t\t\t\t\n','','(N/mm)');
%polyfit the load-disp data, take the derivative of the equation, and
%determine the tangent (stiffness) at the desired strain.
for w=1:totfiles;
Load=[];Disp=[];k=0;
disppoint=strainpoint*gage(w);
disppoint2=midstrain(w)*gage(w);
polyemod2=polyfit(LoadDisp(:,2*w),LoadDisp(:,2*w-1),3);
tangent2=polyder(polyemod2);
Stiffness=tangent2(1)*(disppoint)^2+tangent2(2)*(disppoint)+tangent2(3);
Stiffnessvector(w)=Stiffness;
Stiffnessmidstrain(w)=tangent2(1)*(disppoint2)^2+tangent2(2)*(disppoint2)+tangent2(3);
%  Write the stiffness data to a summary file called "Stiffness.xls"
   l=w;
   fprintf(fid,'%s\t\t%f\n',names{l,2},Stiffness);
end
fclose(fid);
fprintf(1,'\n\n%s\n\n','The Stiffness.xls file has been successfully generated.');
end
if decision3==3;
fid=fopen('ElasticModulus.xls','wt');
fprintf(fid,'%s\t\t\t\t\t%s\n','Summary of Merlin Mechanical Testing Data',date);
fprintf(fid,'\n\n');
fprintf(fid,'%s\t\t%s\t%s\t%s\t%s\t\n','Sample_ID','ElasticModulus-1','R-Squared-','ElasticModulus-
1','R-Squared-2');
fprintf(fid,'%s\t\t%s\t%s\t%s\t%s\t\t\t\t\n','','(MPa)','','(MPa)','');
for w=1:2:size(StressStrain,2);
   yy=(w+1)/2;
Stress2=[];OptStrain=[];
RModmax1=0;
ss=0;
for k=3:1:totptsvector(yy);
   if ss==0;
   Stress2=StressStrain(1:k,w);
   OptStrain=StressStrain(1:k,w+1);
   [yint, EMod, RMod] = regress(OptStrain,Stress2);
       if  RMod >= RModmax1;
           RModmax1=RMod;
           EMod1=EMod;
           yint1=yint;
           lastpt=k;
       end
       if RMod < RModmax1;
          ss=1;
```

```
        end
end
end
end1(yy)=lastpt;
   EMod1vector(yy)=EMod1;
   lastptvector(yy)=lastpt;
   RModmax1vector(yy)=RModmax1;
Stress3=[];OptStrain1=[];
   RModmax2=0;
for k2=3:1:totptsvector(yy)-3;
   Stress3=StressStrain(totptsvector(yy)-k2:totptsvector(yy),w);
   OptStrain1=StressStrain(totptsvector(yy)-k2:totptsvector(yy),w+1);
   [yint2, EMod2, RMod2] = regress(OptStrain1,Stress3);
        if RMod2 > RModmax2;
           RModmax2=RMod2;
           EMod2z=EMod2;
           yint2z=yint2;
             lastpt2=k2;
        end
end
start2(yy)=totptsvector(yy)-lastpt2;
end2(yy)=totptsvector(yy);
   EMod2zvector(yy)=EMod2z;
   RModmax2vector(yy)=RModmax2;
      strainintersect=[];yintersect=[];yvalues1=[];yvalues2=[];
   strainintersect = (yint2z-yint1)/(EMod1-EMod2z);
   strainintersect1(yy) = (yint2z-yint1)/(EMod1-EMod2z);
   strainintersectvector(yy)=strainintersect;
   % D (no toe-region or yield points), B (toe-region and yield points), C (yield points) samples
   if EMod1/EMod2z>0.7 || EMod1/EMod2z<0;
      % B samples (toe-region and yield points)
       if (strainintersect1(yy)>0.10);
          RModmax3=0;
        for k3=3:1:(totptsvector(yy)-lastpt2-2-lastpt-2);
      Stress4=StressStrain((totptsvector(yy)-lastpt2-2-k3):(totptsvector(yy)-lastpt2-2),w);
     OptStrain2=StressStrain((totptsvector(yy)-lastpt2-2-k3):(totptsvector(yy)-lastpt2-2),w+1);
      [yint3, EMod3, RMod3] = regress(OptStrain2,Stress4);
        if RMod3 > RModmax3;
           RModmax3=RMod3;
           RModmax2=RMod3;
           EMod2z=EMod3;
           yint2z=yint3;
          lastpt3=k3;
        end
        end
        start2(yy)=totptsvector(yy)-lastpt2-2-lastpt3;
        end2(yy)=totptsvector(yy)-lastpt2-2;
         strainintersect = (yint2z-yint1)/(EMod1-EMod2z);
   strainintersectvector(yy)=strainintersect;
   % B samples (toe-region and yield points), setting transition strain to 0 if it's negative
   if strainintersect<=0.005;
      strainintersectvector(yy)=0;
      Stress5=StressStrain(1:(totptsvector(yy)-lastpt2-2),w);
      OptStrain5=StressStrain(1:(totptsvector(yy)-lastpt2-2),w+1);
      [yint5, EMod5, RMod5] = regress(OptStrain5,Stress5);
           RModmax2=RMod5;
```

```
            EMod2z=EMod5;
            yint2z=yint5;
            start2(yy)=1;
          end
            % C samples (yield points), setting transition strain to 0
         elseif EMod1/EMod2z>1.20 && EMod1/EMod2z<2;
        Stress4=StressStrain(1:(totptsvector(yy)-lastpt2-2),w);
      OptStrain2=StressStrain(1:(totptsvector(yy)-lastpt2-2),w+1);
        [yint3, EMod3, RMod3] = regress(OptStrain2,Stress4);
            RModmax2=RMod3;
            EMod2z=EMod3;
            yint2z=yint3;
         start2(yy)=1;
         end2(yy)=totptsvector(yy)-lastpt2-2;
         strainintersectvector(yy)=0;
         % D samples (no toe-region or yield points)
        else
        strainintersectvector(yy)=0;
        Stress2b=StressStrain(1:totptsvector(yy),w);
    OptStrain2b=StressStrain(1:totptsvector(yy),w+1);
        [yint2b, EMod2b, RMod2b] = regress(OptStrain2b,Stress2b);
        EMod2z=EMod2b;
        RModmax2=RMod2b;
        yint2z=yint2b;
        start2(yy)=1;
        end2(yy)=totptsvector(yy);
         end
           % Separate B samples (toe-region and yield points) from A samples (toe-region)
    else
        if strainintersect1(yy)<0 && 0<EMod1/EMod2z && EMod1/EMod2z<0.7 && (totptsvector(yy)-
lastpt2-2-lastpt-2) >=3;
k3=[];
RModmax3=0;
          for k3=3:1:(totptsvector(yy)-lastpt2-2-lastpt-2);
        Stress4=StressStrain((totptsvector(yy)-lastpt2-2-k3):(totptsvector(yy)-lastpt2-2),w);
      OptStrain2=StressStrain((totptsvector(yy)-lastpt2-2-k3):(totptsvector(yy)-lastpt2-2),w+1);
        [yint3, EMod3, RMod3] = regress(OptStrain2,Stress4);
          if RMod3 > RModmax3;
            RModmax3=RMod3;
            RModmax2=RMod3;
            EMod2z=EMod3;
            yint2z=yint3;
           lastpt4=k3;
         end
         end
         start2(yy)=totptsvector(yy)-lastpt2-2-lastpt4;
         end2(yy)=totptsvector(yy)-lastpt2-2;
         strainintersect = (yint2z-yint1)/(EMod1-EMod2z);
    strainintersectvector(yy)=strainintersect;
      %B samples (toe-region and yield points), setting transition strain to 0 if it's negative
    if strainintersect<=0;
        strainintersectvector(yy)=0;
        Stress6=StressStrain(1:(totptsvector(yy)-lastpt2-2),w);
        OptStrain6=StressStrain(1:(totptsvector(yy)-lastpt2-2),w+1);
        [yint6, EMod6, RMod6] = regress(OptStrain6,Stress6);
            RModmax2=RMod6;
```

```
            EMod2z=EMod6;
            yint2z=yint6;
            start2(yy)=1;
    end
       end
    end

lastpt2vector(yy)=lastpt2;
  EMod2zvector(yy)=EMod2z;
    RModmax2vector(yy)=RModmax2;
    yintersect = EMod1*(strainintersect)+yint1;
    figure (5)
    yvalues1=EMod1*StressStrain(:,w+1)+yint1;
    yvalues2=EMod2z*StressStrain(:,w+1)+yint2z;
plot
(StressStrain(:,w+1),StressStrain(:,w),'b.',StressStrain(:,w+1),yvalues1,'go',StressStrain(:,w+1),yv
alues2,'k-',strainintersect,yintersect,'rx')
title('Stress vs. Strain, actual data, fit data, and intersect');
decision5 = input('Continue? Enter 1 for yes, 2 for no.:  ');
if decision5==1;
%  Write the modulus data to a summary file called "ElasticModulus.xls"
    l=(w+1)/2;
fprintf(fid,'%s\t\t%f\t%f\t%f\t%f\t%f\n',names{l,2},EMod1,RModmax1,EMod2z,RModmax2,strainint
ersect);
end
end
fclose(fid);
fprintf(1,'\n\n%s\n\n','The ElasticModulus.xls file has been successfully generated (decision 3).');
fid=fopen('Stiffness.xls','wt');
fprintf(fid,'%s\t\t\t\t\t\t%s\n','Summary of Merlin Mechanical Testing Data',date);
fprintf(fid,'\n\n');
fprintf(fid,'%s\t\t%s\t%s\t\n','Sample_ID','Stiffness-1','R-Squared-1','Stiffness-2','R-Squared-2');
fprintf(fid,'%s\t\t%s\t%s\t%s\t\t\t\t\t\t\n','','(N/mm)','','(N/mm)','');
for w=1:2:size(StressStrain,2);
    yy=(w+1)/2;
Load1=[];Disp1=[];
        Load1=LoadDisp(1:end1(yy),w);
        Disp1=LoadDisp(1:end1(yy),w+1);
        [yint, Stiffness, RStiff] = regress(Disp1,Load1);
            RStiffmax1=RStiff;
            Stiffness1=Stiffness;
            yintStiff1=yint;
  Stiffness1vector(yy)=Stiffness1;
    Load2=[];Disp2=[];
       Load2=LoadDisp(start2(yy):end2(yy),w);
        Disp2=LoadDisp(start2(yy):end2(yy),w+1);
        [yint2, Stiffness2, RStiff2] = regress(Disp2,Load2);
          RStiffmax2=RStiff2;
            Stiffness2z=Stiffness2;
            yint2Stiffz=yint2;
    Stiffness2zvector(yy)=Stiffness2z;
%  Write the stiffness data to a summary file called "Stiffness.xls"
    l=(w+1)/2;
    fprintf(fid,'%s\t\t%f\t%f\t%f\t%f\n',names{l,2},Stiffness1,RStiffmax1,Stiffness2z,RStiffmax2);
  end
fclose(fid);
```

```
fprintf(1,'\n\n%s\n\n','The Stiffness.xls file has been successfully generated.');
end
if decision3==3;
fid=fopen('ResultsSummary.xls','wt');
fprintf(fid,'%s\t\t\t\t\t%s\n','Summary of Mechanical Testing Data',date);
fprintf(fid,'\n\n');
fprintf(fid,'%s\t\t%s\t%s\t%s\t%s\t%s\t%s\t%s\t%s\t%s\t%s\t%s\t\n','Sample_ID','EModulus-
1','Stiffness-1','R-squared-1','EModulus-2','Stiffness-2','R-squared-
2','strainintercept','StressRelaxRatio','DeltaGageLength','RelaxRateall','RelaxRate10sec');
fprintf(fid,'%s\t\t%s\t%s\t%s\t%s\t%s\t%s\t%s\t%s\t%s\t%s\t%s\t\t\t\n','','(MPa)','(N/mm)','','(MPa)','
(N/mm)','','','','(mm)','','');
for w=1:totfiles;
%  Write the stiffness data to a summary file called "ResultsSummary.xls"
   l=w;
fprintf(fid,'%s\t\t%f\t%f\t%f\t%f\t%f\t%f\t%f\t%f\t%f\t%f\t%f\n',names{l,2},EMod1vector(l),Stiffness1
vector(l),RModmax1vector(l),EMod2zvector(l),Stiffness2zvector(l),RModmax2vector(l),straininters
ectvector(l),stressrelaxationratiovector(l),deltadispvector(l),ratevectorall(l),ratevector10s(l));
end
fclose(fid);
fprintf(1,'\n\n%s\n\n','The ResultsSummary.xls file has been successfully generated.');
end
if decision3==2;
strainvectortrans=strainvector';
fid=fopen('Predictedstress.xls','wt');
fprintf(fid,'%s\t\t\t\t\t%s\n','Summary of Merlin Mechanical Testing Data',date);
fprintf(fid,'\n');
for z=1:size(names,1);
   fprintf(fid,'%s\t',names{z,2});
end
fprintf(fid,'\n');
fprintf(fid,'%s\t%s\n','Strain','Stress_MPa');
fprintf(fid,'\n');
for m=1:size(predictedstressmatrix,1);
   for y=1:size(predictedstressmatrix,2);
      fprintf(fid,'%f\t',predictedstressmatrix(m,y));
   end
   fprintf(fid,'\n');
end
fclose(fid);
fprintf(1,'\n\n%s\n\n','The Predictedstress.xls file has been successfully generated.');
fid=fopen('ResultsSummary.xls','wt');
fprintf(fid,'%s\t\t\t\t\t%s\n','Summary of Mechanical Testing Data',date);
fprintf(fid,'\n\n');
fprintf(fid,'%s\t\t%s\t%s\t%s\t%s\t%s\t%s\t%s\t%s\t%s\t%s\t%s\t%s\t%s\t%s\t%s\t%s\t\n','Sample
_ID','EModulus','Stiffness','R-
squared','StressRelaxRatio','DeltaGageLength','RelaxRateall','RelaxRate10sec','EModLinearRan
ge','StiffnessLinearRange','EModmidstrain','Stiffnessmidstrain','Emodhighstrain','EModlowstrain','
midstrain','highstrain','lowstrain');
fprintf(fid,'%s\t\t%s\t%s\t%s\t%s\t%s\t%s\t%s\t%s\t%s\t%s\t%s\t%s\t\t\t\t\t\n','','(MPa)','(N/mm
)','','','(mm)','','','MPa','N/mm','MPa','N/mm','MPa','MPa');
for w=1:totfiles;
%  Write the stiffness data to a summary file called "ResultsSummary.xls"
   l=w;
fprintf(fid,'%s\t\t%f\t%f\t%f\t%f\t%f\t%f\t%f\t%f\t%f\t%f\t%f\t%f\t%f\t%f\t%f\t%f\t\n',names{l,2},EMo
dvector(l),Stiffnessvector(l),Rsqvector(l),stressrelaxationratiovector(l),deltadispvector(l),ratevector
```

```
all(l),ratevector10s(l),EModlinear4vector(l),Stiffnesslinear5vector(l),EModmidstrain(l),Stiffnessmid
strain(l),EModhighstrain(l),EModlowstrain(l),midstrain(l),highstrain(l),lowstrain(l));
end
fclose(fid);
fprintf(1,'\n\n%s\n\n','The ResultsSummary.xls file has been successfully generated.');
end
```

Code 2: Calculation of elastic mechanical properties from a mechanical testing protocol that includes only a failure test.

Derwin Lab
Date: August 10, 2010
Author: LiKang Chin

This program will read a *.dat data file generated from the MTS FlexTest SE electromechanical test system. This program will generate the following data files:

1. ResultsSummary.xls: toe-region elastic modulus (Elastic Modulus-1), toe-region stiffness (Stiffness-1), the associated r-squared value, linear-region elastic modulus (Elastic Modulus-2), linear-region stiffness (Stiffness-2), the associated r-squared value, strain intercept of the toe- and linear- region lines, and delta gage length.
2. ElasticModulus.xls: Elastic Modulus-1, Elastic Modulus-2, and the associated r-squared values
3. Stiffness.xls: Stiffness-1, Stiffness-2, and the associated r-squared values
4. LoadOpticalDisp.xls: optical displacement and load
5. StressStrain.xls: optical strain and stress
7. Gagelength.xls: initial and final gage lengths

Elastic modulus and stiffness are calculated using the following options:

Option 1: User specifies strain limits and the elastic modulus is calculated as the linear portion between these limits from the stress vs. strain curve.
Option 2: The program polyfits the stress vs. strain curve, differentiates the equation, and determines the tangent (elastic modulus) at a strainpoint specified by the user.
Option 3: The program applies a bilinear curve fit to the stress vs. strain curve and determines the intersection of the two lines (strain intercept).

User inputs: The user will be prompted to enter the name of a text file (*.txt) containing the filenames of all the results.csv files (from tc_multi_points) and .dat files to be processed. The format of this file should be an Mx4 matrix where M is the number of data files to process. The first column should be a listing of the result.csv filenames, and the second column should be a listing of the .dat filenames. The third column should be the calibration factor (pixels/mm) of the video capture system; the fourth column should be the first camera frame of the failure portion of the test; the fifth column should be the last camera frame of the failure portion of the test; and the sixth column should be the cross-sectional area of the sample (mm^2).

The user will be asked to input the zero load.

Note well: All *. data files must be sampled at the same frequency. Force data should be recorded in N.

```
**************************************************************************************************
clear
 % Ask user for the file containing the filenames of the DAT files and *.xls* files.
% This file must be a *.txt file, and you need to type in the *.txt extension.
rawfile = input('Enter the name of the file containing the filenames of the *. files and *.xls files:
','s');
% Ask user for zeroload.
zeroload = input('Enter the zero load:  ');
% Read filenames to matrix "names".
names=[];gage=[];StressStrain=[];maxpt=[];maxstress=[];maxstrain=[];
```

```
[A] = textread(rawfile,'%s');
j=1;
for i=1:6:size(A);
   names{j,1}=A{i};
   names(j,2)=A(i+1);
   j=j+1;
end
% Read video calibration factor, first frame, last frame, and cross-sectional area to matrix "data".
data=[];
data = dlmread(rawfile,'\t',0,2);
totfiles=size(names,1);
for z=1:totfiles;
% Read in raw "results" data file from tc_multi_pts.
R = [];
R = csvread(names{z,1},2,0);
totpts=size(R,1);
% Read in raw MTS data file.
MTS= [];
MTS= textread(names{z,2},'','headerlines',5);
totpts2=size(MTS,1);
%convert gm force to Newton
zeroedloadvector1=[];
zeroedloadvector1=MTS(:,3)*.00980665;
%zero the load
zeroedloadvector=[];
zeroedloadvector = zeroedloadvector1-zeroload;
%remove the y value columns from R1
R1 = [];
R1= [R(:,1),R(:,3),R(:,5),R(:,7)];
%convert R1 from pixels to mm
R2=[];
R3=[];
for g=1:size(R1,1)
   R2(g,1)=R1(g,1)/data(z,1);
   R2(g,2)=R1(g,2)/data(z,1);
   R3(g,1)=R1(g,3)/data(z,1);
   R3(g,2)=R1(g,4)/data(z,1);
end
%average of columns of R2 and R3
R4=[];
R5=[];
R4=mean(R2,2);
R5=mean(R3,2);
%subtract R5 from R4 and make optical displacement vector
rawdisp=[];
opticaldisp=[];
rawdisp=R5-R4;
%opticaldisp= rawdisp-(rawdisp(1));
MTSframe=[];
MTSvideo=[];
MTSframe=MTS(:,5);
MTSvideo=MTS(:,4);
zeroedloadvector2=[];
k=1;
ttt=0;
for m=data(z,2):data(z,3);
```

```
ttt=0;
   for h=1:totpts2;
      if ttt==0;
   if MTSframe(h)==m;
       if MTSvideo(h)==5;
          zeroedloadvector2(k)=zeroedloadvector(h);
          k=k+1;
          ttt=1;
       end
   end
end
end
end
zeroedloadvector3=[];
rawdisp1=[];
rr=1;
for ss=1:size(zeroedloadvector2,2);
   if zeroedloadvector2(ss)>=0;
       zeroedloadvector3(rr)=zeroedloadvector2(ss);
       rawdisp1(rr)=rawdisp(ss);
       rr=rr+1;
   end
end
opticaldisp1=[];
opticaldisp1=rawdisp1-(rawdisp1(1));
% Stress vector
stress=[];
XSA(z)=data(z,4);
stress=zeroedloadvector3/(data(z,4));
% Optical strain vector
opticalstrain=[];
opticalstrain=opticaldisp1/(rawdisp1(1));
finalgagedisp=[];
mm=1;
for p=550:totpts2;
   if mm==1;
      if zeroedloadvector(p)>=0;
         if zeroedloadvector(p+2)>zeroedloadvector(p);
            if zeroedloadvector(p+4)>zeroedloadvector(p+1);
               if zeroedloadvector(p+6)>zeroedloadvector(p+2);
                  if zeroedloadvector(p+8)>zeroedloadvector(p+3);
                     if zeroedloadvector(p+10)>zeroedloadvector(p+4);
                        if zeroedloadvector(p+15)>zeroedloadvector(p+5);
          finalgagedisp=MTS(p,2);
          point3=p;
          mm=2;
       end
   end
end
end
end
end
end
end
end
finalgagedispvector(z)=finalgagedisp;
```

```
%fit the load vs. optical displacement data using a polynomial fit
poly=polyfit(opticaldisp1,zeroedloadvector3,3);
%plot polyfit data with actual data
polyfitloadvector=poly(1)*(opticaldisp1.^3)+poly(2)*(opticaldisp1.^2)+poly(3)*(opticaldisp1)+poly(4
);
poly2=polyfit(opticalstrain,stress,3);
%plot polyfit data with actual data
polyfitstressvector=poly2(1)*(opticalstrain.^3)+poly2(2)*(opticalstrain.^2)+poly2(3)*(opticalstrain)+
poly2(4);
gage(z)=rawdisp1(1);
% Create Stress vs. optical Strain array
stresstrans=[];
stresstrans=stress';
totptsvector(z)=length(stresstrans);
for gg=1:size(stresstrans,1);
   StressStrain(gg,2*z-1)=stresstrans(gg);
   StressStrain(gg,2*z)=opticalstrain(gg);
end
% Create Load vs. optical Disp array
zeroedloadvector3trans=[];
zeroedloadvector3trans=zeroedloadvector3';
for yy=1:size(zeroedloadvector3trans,1);
   LoadDisp(yy,2*z-1)=zeroedloadvector3trans(yy);
   LoadDisp(yy,2*z)=opticaldisp1(yy);
end
initialfinalgagedisp(:,2*z-1)=finalgagedisp;
end
%  Write the adjusted StressStrain array to a file called "StressStrain.xls"
fid=fopen('StrainStress.xls','wt');
fprintf(fid,'%s\t\t\t\t\t%s\n','Summary of Stress-Strain Mechanical Testing Data',date);
fprintf(fid,'\n');
for z=1:size(names,1);
   fprintf(fid,'%s\t\t',names{z,2});
end
fprintf(fid,'\n');
for z=1:size(names,1);
   fprintf(fid,'%s\t\%s\t','Stress_MPa','OpticalStrain');
end
fprintf(fid,'\n');
for m=1:size(StressStrain,1);
   for y=1:size(StressStrain,2);
      fprintf(fid,'%f\t',StressStrain(m,y));
   end
   fprintf(fid,'\n');
end
fclose(fid);
fprintf(1,'\n%s\n','The StrainStress.xls file has been successfully generated.');
fprintf(1,'\n');
%Plot stress vs. strain for all files
figure (3)
for s=1:2:size(StressStrain,2);
   hold on
   plot (StressStrain(:,s+1),StressStrain(:,s))
   title('Stress vs. Optical Strain')
end
%  Write the LoadDisp array to a file called "LoadOpticalDisp.xls"
```

```
fid=fopen('LoadOpticalDisp.xls','wt');
fprintf(fid,'%s\t\t\t\t\t%s\n','Summary of Load-Optical Displacement Mechanical Testing
Data',date);
fprintf(fid,'\n');
for z=1:size(names,1);
   fprintf(fid,'%s\t\t',names{z,2});
end
fprintf(fid,'\n');
for z=1:size(names,1);
   fprintf(fid,'%s\t\%s\t','Optical Displacement_mm','Load_N');
end
fprintf(fid,'\n');
for m=1:size(LoadDisp,1);
   for y=1:size(LoadDisp,2);
      fprintf(fid,'%f\t',LoadDisp(m,y));
   end
   fprintf(fid,'\n');
end
fclose(fid);
fprintf(1,'\n%s\n','The LoadOpticalDisp.xls file has been successfully generated.');
fprintf(1,'\n');
%  Write the initialfinalgagedisp array to a file called "Gagelength.xls"
fid=fopen('Gagelength.xls','wt');
fprintf(fid,'%s\t\t\t\t\t%s\n','Summary of Initial and Final Gage Displacements Mechanical Testing
Data',date);
fprintf(fid,'\n');
for z=1:size(names,1);
   fprintf(fid,'%s\t\t',names{z,2});
end
fprintf(fid,'\n');
for z=1:size(names,1);
   fprintf(fid,'%s\t','FinalGageLength_mm');
end
fprintf(fid,'\n');
for m=1:size(initialfinalgagedisp,1);
   for y=1:size(initialfinalgagedisp,2);
      fprintf(fid,'%f\t',initialfinalgagedisp(m,y));
   end
   fprintf(fid,'\n');
end
fclose(fid);
fprintf(1,'\n%s\n','The Gagelength.xls file has been successfully generated.');
fprintf(1,'\n');
fprintf(1,'%s\n','Would you like to specify strain limits for emod? Enter 1.');
fprintf(1,'%s\n','Would you like to take the tangent (emod) at a single point? Enter 2.:  ');
decision3 = input ('Would you like to fit the curve with two linear fits and determine the
intersection? Enter 3.:  ');
fprintf(1,'\n');
if decision3==1;
lowstrain = input('Enter the lower strain limit for computation of elastic modulus:  ');
upstrain = input('Enter the upper strain limit for computation of elastic modulus:  ');
%  Extract emod from stress and strain data in the linear portion (between
%  "lowstrain" and "upstrain") using regress.
fid=fopen('ElasticModulus.xls','wt');
fprintf(fid,'%s\t\t\t\t\t%s\n','Summary of Merlin Mechanical Testing Data',date);
fprintf(fid,'\n\n');
```

```
fprintf(fid,'%s\t\t%s\t%s\t\n','Sample_ID','ElasticModulus','R-Squared');
fprintf(fid,'%s\t\t%s\t\t%s\t\t\t\t\t\n','','(MPa)','(MPa)');
for w=1:2:size(StressStrain,2);
Stress2=[];OptStrain=[];k=0;
   for m=1:size(StressStrain,1);
   if StressStrain(m,w+1) > lowstrain;
      if StressStrain(m,w+1) < upstrain;
         k=k+1;
         Stress2(k,1)=StressStrain(m,w);
         OptStrain(k,1)=StressStrain(m,w+1);
         strainpoints(w)=size(OptStrain,1);
      end
   end
   end
   [yint, EMod, RMod] = regress(OptStrain,Stress2);
   EModvector(w)=EMod;
%  Write the modulus data to a summary file called "ElasticModulus.xls"
   l=(w+1)/2;
   fprintf(fid,'%s\t\t%f\t%f\n',names{l,2},EMod,RMod);
end
fclose(fid);
fprintf(1,'\n\n%s\n\n','The ElasticModulus.xls file has been successfully generated (decision 1).');
fid=fopen('Stiffness.xls','wt');
fprintf(fid,'%s\t\t\t\t\t%s\n','Summary of Merlin Mechanical Testing Data',date);
fprintf(fid,'\n\n');
fprintf(fid,'%s\t\t%s\t%s\t\n','Sample_ID','Stiffness','R-Squared');
fprintf(fid,'%s\t\t%s\t\t\t\t\t\t\n','','(N/mm)');
for w=1:2:size(StressStrain,2);
Load=[];Disp=[];k=0;
   for m=1:size(StressStrain,1);
   if StressStrain(m,w+1) > lowstrain;
      if StressStrain(m,w+1) < upstrain;
         k=k+1;
         Load(k,1)=LoadDisp(m,w);
         Disp(k,1)=LoadDisp(m,w+1);
      end
   end
   end
   [yint, Stiffness, RStiff] = regress(Disp,Load);
   Stiffnessvector(w)=Stiffness;
%  Write the stiffness data to a summary file called "Stiffness.xls"
   l=(w+1)/2;
   fprintf(fid,'%s\t\t%f\t%f\n',names{l,2},Stiffness,RStiff);
   z=z+1;
   tt=0;
   RStiffsaved=.7;
end
fclose(fid);
fprintf(1,'\n\n%s\n\n','The Stiffness.xls file has been successfully generated.');
end
if decision3==2;
   strainpoint = input('Enter strain where you would like to compute the tangent of the stress-
strain curve:  ');
fid=fopen('ElasticModulus.xls','wt');
fprintf(fid,'%s\t\t\t\t\t%s\n','Summary of Merlin Mechanical Testing Data',date);
fprintf(fid,'\n\n');
```

```
fprintf(fid,'%s\t\t%s\t\n','Sample_ID','ElasticModulus');
fprintf(fid,'%s\t\t%s\t\t\t\t\t\n','','(MPa)');
for w=1:totfiles;
Stress2=[];OptStrain=[];k=0;
polyemod=polyfit(StressStrain(1:totptsvector(w),2*w),StressStrain(1:totptsvector(w),2*w-1),3);
tangent=polyder(polyemod);
EMod=tangent(1)*(strainpoint)^2+tangent(2)*(strainpoint)+tangent(3);
strainvector=0:0.005:0.10;
predictedstress=polyemod(1)*(strainvector).^3+polyemod(2)*(strainvector).^2+polyemod(3)*(strai
nvector)+polyemod(4);
predictedstresstrans=predictedstress';
predictedstressmatrix(:,1)=strainvector';
predictedstressmatrix(:,w+1)=predictedstresstrans;
EModvector(w)=EMod;
%plot polyfit data with actual data
polyfitstressvector=[];
polyfitstressvector=polyemod(1)*((StressStrain(1:totptsvector(w),2*w)).^3)+polyemod(2)*((Stress
Strain(1:totptsvector(w),2*w)).^2)+polyemod(3)*(StressStrain(1:totptsvector(w),2*w))+polyemod(4
);
figure (4)
plot (StressStrain(1:totptsvector(w),2*w),StressStrain(1:totptsvector(w),2*w-
1),'b.',StressStrain(1:totptsvector(w),2*w),polyfitstressvector,'rx')
title('Stress vs. Strain, actual data and fit data');
ypred=[];dev=[];SST=[];resid=[];SSE=[];Rsq=[];
ypred=polyval(polyemod,StressStrain(1:totptsvector(w),2*w));
dev=StressStrain(1:totptsvector(w),2*w-1)-mean(StressStrain(1:totptsvector(w),2*w-1));
SST=sum(dev.^2);
resid=StressStrain(1:totptsvector(w),2*w-1)-ypred;
SSE=sum(resid.^2);
Rsq=1-SSE/SST;
Rsqvector(w)=Rsq;
Rsqlinear2=.5;
yyy=[];
for yyy=1:(length(polyfitstressvector)-3);
[yint, EModlinear, Rsqlinear] =
regress(StressStrain(yyy:yyy+3,2*w),polyfitstressvector(yyy:yyy+3));
if Rsqlinear>=Rsqlinear2;
   Rsqlinear2=Rsqlinear;
   Rsqlinearvector(w)=Rsqlinear;
   startpoint(w)=yyy;
end
end
highpoint(w)=totptsvector(w);
highstrain(w)=StressStrain(totptsvector(w),2*w);
u=0;
qq=[];
for qq=0:((length(polyfitstressvector))-(startpoint(w))-3);
   [yint2, EModlinear2,
Rsqlinear2]=regress(StressStrain(startpoint(w):(startpoint(w)+3+qq),2*w),polyfitstressvector(start
point(w):(startpoint(w)+3+qq)));
  if u==0;
   if Rsqlinear2<0.999;
      highpoint(w)=startpoint(w)+3+qq-1;
      highstrain(w)=StressStrain(highpoint(w),2*w);
      u=1;
   end
```

```
end
end
lowpoint(w)=1;
lowstrain(w)=StressStrain(1,2*w);
v=0;
qqq=[];
for qqq=0:(startpoint(w)-1);
   [yint3, EModlinear3, Rsqlinear3]=regress(StressStrain(startpoint(w)-
qqq:(startpoint(w)+3),2*w),polyfitstressvector(startpoint(w)-qqq:(startpoint(w)+3)));
   if v==0;
   if Rsqlinear3<0.999;
      lowpoint(w)=startpoint(w)-qqq+1;
      lowstrain(w)=StressStrain(lowpoint(w),2*w);
      v=1;
   end
end
end
midstrain(w)=highstrain(w)-((highstrain(w)-lowstrain(w))/2);
EModmidstrain(w)=tangent(1)*(midstrain(w))^2+tangent(2)*(midstrain(w))+tangent(3);
EModhighstrain(w)=tangent(1)*(highstrain(w))^2+tangent(2)*(highstrain(w))+tangent(3);
EModlowstrain(w)=tangent(1)*(lowstrain(w))^2+tangent(2)*(lowstrain(w))+tangent(3);
 [yint4, EModlinear4,
Rsqlinear4]=regress(StressStrain(lowpoint(w):highpoint(w),2*w),polyfitstressvector(lowpoint(w):hi
ghpoint(w)));
EModlinear4vector(w)=EModlinear4;
[yint5, Stiffnesslinear5, Rsqlinear5]=regress(LoadDisp(lowpoint(w):highpoint(w),2*w-
1),polyfitstressvector(lowpoint(w):highpoint(w))*XSA(w));
Stiffnesslinear5vector(w)=Stiffnesslinear5;
decision4 = input('Does the fit data represent the actual data? Would you like to continue? Enter
1 for yes, 2 for no.:  ');
if decision4==1;
%  Write the Merlin modulus data to a summary file called "ElasticModulus.xls"
   l=w;
   fprintf(fid,'%s\t\t%f\n',names{l,2},EMod);
end
end
fclose(fid);
fprintf(1,'\n\n%s\n\n','The ElasticModulus.xls file has been successfully generated (decision 2).');
fid=fopen('Stiffness.xls','wt');
fprintf(fid,'%s\t\t\t\t\t\t%s\n','Summary of Merlin Mechanical Testing Data',date);
fprintf(fid,'\n\n');
fprintf(fid,'%s\t\t%s\t\n','Sample_ID','Stiffness');
fprintf(fid,'%s\t\t%s\t\t\t\t\t\t\n','','(N/mm)');
%polyfit the load-disp data, take the derivative of the equation, and
%determine the tangent (stiffness) at the desired strain.
for w=1:totfiles;
Load=[];Disp=[];k=0;
disppoint=strainpoint*gage(w);
disppoint2=midstrain(w)*gage(w);
polyemod2=polyfit(LoadDisp(:,2*w),LoadDisp(:,2*w-1),3);
tangent2=polyder(polyemod2);
Stiffness=tangent2(1)*(disppoint)^2+tangent2(2)*(disppoint)+tangent2(3);
Stiffnessvector(w)=Stiffness;
Stiffnessmidstrain(w)=tangent2(1)*(disppoint2)^2+tangent2(2)*(disppoint2)+tangent2(3);
%  Write the stiffness data to a summary file called "Stiffness.xls"
   l=w;
```

```
   fprintf(fid,'%s\t\t%f\n',names{l,2},Stiffness);
end
fclose(fid);
fprintf(1,'\n\n%s\n\n','The Stiffness.xls file has been successfully generated.');
end
if decision3==3;
fid=fopen('ElasticModulus.xls','wt');
fprintf(fid,'%s\t\t\t\t\t%s\n','Summary of Merlin Mechanical Testing Data',date);
fprintf(fid,'\n\n');
fprintf(fid,'%s\t\t%s\t%s\t%s\t%s\t\n','Sample_ID','ElasticModulus-1','R-Squared-
1','ElasticModulus-1','R-Squared-2');
fprintf(fid,'%s\t\t%s\t%s\t%s\t%s\t\t\t\t\n','','(MPa)','','(MPa)','');
for w=1:2:size(StressStrain,2);
   yy=(w+1)/2;
Stress2=[];OptStrain=[];
RModmax1=0;
ss=0;
for k=3:1:totptsvector(yy);
   if ss==0;
   Stress2=StressStrain(1:k,w);
   OptStrain=StressStrain(1:k,w+1);
   [yint, EMod, RMod] = regress(OptStrain,Stress2);
       if  RMod >= RModmax1;
           RModmax1=RMod;
           EMod1=EMod;
           yint1=yint;
           lastpt=k;
       end
       if RMod < RModmax1;
          ss=1;
       end
end
end
end1(yy)=lastpt;
   EMod1vector(yy)=EMod1;
   lastptvector(yy)=lastpt;
   RModmax1vector(yy)=RModmax1;
Stress3=[];OptStrain1=[];
   RModmax2=0;
for k2=3:1:totptsvector(yy)-3;
   Stress3=StressStrain(totptsvector(yy)-k2:totptsvector(yy),w);
   OptStrain1=StressStrain(totptsvector(yy)-k2:totptsvector(yy),w+1);
   [yint2, EMod2, RMod2] = regress(OptStrain1,Stress3);
        if RMod2 > RModmax2;
           RModmax2=RMod2;
           EMod2z=EMod2;
           yint2z=yint2;
             lastpt2=k2;
        end
end
start2(yy)=totptsvector(yy)-lastpt2;
end2(yy)=totptsvector(yy);
   EMod2zvector(yy)=EMod2z;
   RModmax2vector(yy)=RModmax2;
      strainintersect=[];yintersect=[];yvalues1=[];yvalues2=[];
```

```
strainintersect = (yint2z-yint1)/(EMod1-EMod2z);
strainintersect1(yy) = (yint2z-yint1)/(EMod1-EMod2z);
strainintersectvector(yy)=strainintersect;
%D (no toe-region or yield points), B (toe-region and yield points), C (yield points) samples
if EMod1/EMod2z>0.7 || EMod1/EMod2z<0;
    %B samples (toe-region and yield points)
     if (strainintersect1(yy)>0.10);
        RModmax3=0;
      for k3=3:1:(totptsvector(yy)-lastpt2-2-lastpt-2);
    Stress4=StressStrain((totptsvector(yy)-lastpt2-2-k3):(totptsvector(yy)-lastpt2-2),w);
  OptStrain2=StressStrain((totptsvector(yy)-lastpt2-2-k3):(totptsvector(yy)-lastpt2-2),w+1);
    [yint3, EMod3, RMod3] = regress(OptStrain2,Stress4);
      if RMod3 > RModmax3;
         RModmax3=RMod3;
         RModmax2=RMod3;
         EMod2z=EMod3;
         yint2z=yint3;
        lastpt3=k3;
      end
      end
      start2(yy)=totptsvector(yy)-lastpt2-2-lastpt3;
      end2(yy)=totptsvector(yy)-lastpt2-2;
       strainintersect = (yint2z-yint1)/(EMod1-EMod2z);
strainintersectvector(yy)=strainintersect;
%B samples (toe-region and yield points), setting transition strain to 0 if it's negative
if strainintersect<=0.005;
    strainintersectvector(yy)=0;
    Stress5=StressStrain(1:(totptsvector(yy)-lastpt2-2),w);
    OptStrain5=StressStrain(1:(totptsvector(yy)-lastpt2-2),w+1);
    [yint5, EMod5, RMod5] = regress(OptStrain5,Stress5);
         RModmax2=RMod5;
         EMod2z=EMod5;
         yint2z=yint5;
         start2(yy)=1;
end
        % C samples (yield points), setting transition strain to 0
     elseif EMod1/EMod2z>1.20 && EMod1/EMod2z<2;
    Stress4=StressStrain(1:(totptsvector(yy)-lastpt2-2),w);
  OptStrain2=StressStrain(1:(totptsvector(yy)-lastpt2-2),w+1);
    [yint3, EMod3, RMod3] = regress(OptStrain2,Stress4);
         RModmax2=RMod3;
         EMod2z=EMod3;
         yint2z=yint3;
      start2(yy)=1;
      end2(yy)=totptsvector(yy)-lastpt2-2;
      strainintersectvector(yy)=0;
      %D samples (no toe-region or yield points)
     else
    strainintersectvector(yy)=0;
    Stress2b=StressStrain(1:totptsvector(yy),w);
OptStrain2b=StressStrain(1:totptsvector(yy),w+1);
    [yint2b, EMod2b, RMod2b] = regress(OptStrain2b,Stress2b);
    EMod2z=EMod2b;
    RModmax2=RMod2b;
    yint2z=yint2b;
    start2(yy)=1;
```

```
        end2(yy)=totptsvector(yy);
        end
          %B samples (toe-region and yield points) from A samples
          %(toe-region)
    else
        if strainintersect1(yy)<0 && 0<EMod1/EMod2z && EMod1/EMod2z<0.7 && (totptsvector(yy)-
lastpt2-2-lastpt-2) >=3;
k3=[];
RModmax3=0;
         for k3=3:1:(totptsvector(yy)-lastpt2-2-lastpt-2);
        Stress4=StressStrain((totptsvector(yy)-lastpt2-2-k3):(totptsvector(yy)-lastpt2-2),w);
      OptStrain2=StressStrain((totptsvector(yy)-lastpt2-2-k3):(totptsvector(yy)-lastpt2-2),w+1);
        [yint3, EMod3, RMod3] = regress(OptStrain2,Stress4);
          if RMod3 > RModmax3;
              RModmax3=RMod3;
              RModmax2=RMod3;
              EMod2z=EMod3;
              yint2z=yint3;
             lastpt4=k3;
          end
          end
          start2(yy)=totptsvector(yy)-lastpt2-2-lastpt4;
          end2(yy)=totptsvector(yy)-lastpt2-2;
          strainintersect = (yint2z-yint1)/(EMod1-EMod2z);
    strainintersectvector(yy)=strainintersect;
       %B samples (toe-region and yield points), setting transition strain to 0 if it's negative
    if strainintersect<=0;
        strainintersectvector(yy)=0;
        Stress6=StressStrain(1:(totptsvector(yy)-lastpt2-2),w);
        OptStrain6=StressStrain(1:(totptsvector(yy)-lastpt2-2),w+1);
        [yint6, EMod6, RMod6] = regress(OptStrain6,Stress6);
              RModmax2=RMod6;
              EMod2z=EMod6;
              yint2z=yint6;
              start2(yy)=1;
    end
        end
    end
lastpt2vector(yy)=lastpt2;
  EMod2zvector(yy)=EMod2z;
    RModmax2vector(yy)=RModmax2;
    yintersect = EMod1*(strainintersect)+yint1;
    figure (5)
    yvalues1=EMod1*StressStrain(:,w+1)+yint1;
    yvalues2=EMod2z*StressStrain(:,w+1)+yint2z;
plot
(StressStrain(:,w+1),StressStrain(:,w),'b.',StressStrain(:,w+1),yvalues1,'go',StressStrain(:,w+1),yv
alues2,'k-',strainintersect,yintersect,'rx')
title('Stress vs. Strain, actual data, fit data, and intersect');
decision5 = input('Continue? Enter 1 for yes, 2 for no.:  ');
if decision5==1;
%  Write the modulus data to a summary file called "ElasticModulus.xls"
    l=(w+1)/2;
fprintf(fid,'%s\t\t%f\t%f\t%f\t%f\t%f\n',names{l,2},EMod1,RModmax1,EMod2z,RModmax2,strainint
ersect);
end
```

```
end
fclose(fid);
fprintf(1,'\n\n%s\n\n','The ElasticModulus.xls file has been successfully generated (decision 3).');
fid=fopen('Stiffness.xls','wt');
fprintf(fid,'%s\t\t\t\t\t\t%s\n','Summary of Merlin Mechanical Testing Data',date);
fprintf(fid,'\n\n');
fprintf(fid,'%s\t\t%s\t%s\t\n','Sample_ID','Stiffness-1','R-Squared-1','Stiffness-2','R-Squared-2');
fprintf(fid,'%s\t\t%s\t%s\t%s\t\t\t\t\t\t\n','','(N/mm)','','(N/mm)','');
for w=1:2:size(StressStrain,2);
   yy=(w+1)/2;
Load1=[];Disp1=[];
      Load1=LoadDisp(1:end1(yy),w);
      Disp1=LoadDisp(1:end1(yy),w+1);
      [yint, Stiffness, RStiff] = regress(Disp1,Load1);
         RStiffmax1=RStiff;
         Stiffness1=Stiffness;
         yintStiff1=yint;
   Stiffness1vector(yy)=Stiffness1;
   Load2=[];Disp2=[];
      Load2=LoadDisp(start2(yy):end2(yy),w);
      Disp2=LoadDisp(start2(yy):end2(yy),w+1);
      [yint2, Stiffness2, RStiff2] = regress(Disp2,Load2);
         RStiffmax2=RStiff2;
         Stiffness2z=Stiffness2;
         yint2Stiffz=yint2;
   Stiffness2zvector(yy)=Stiffness2z;
%  Write the stiffness data to a summary file called "Stiffness.xls"
   l=(w+1)/2;
   fprintf(fid,'%s\t\t%f\t%f\t%f\t%f\n',names{l,2},Stiffness1,RStiffmax1,Stiffness2z,RStiffmax2);
 end
fclose(fid);
fprintf(1,'\n\n%s\n\n','The Stiffness.xls file has been successfully generated.');
end
if decision3==3;
fid=fopen('ResultsSummary.xls','wt');
fprintf(fid,'%s\t\t\t\t\t\t%s\n','Summary of Mechanical Testing Data',date);
fprintf(fid,'\n\n');
fprintf(fid,'%s\t\t%s\t%s\t%s\t%s\t%s\t%s\t%s\t%s\t%s\t%s\t%s\t%s\t%s\t\n','Sample_ID','EModulus-
1','Stiffness-1','R-squared-1','EModulus-2','Stiffness-2','R-squared-
2','strainintercept','StressRelaxRatio','DeltaGageLength','RelaxRateall','RelaxRate10sec');
fprintf(fid,'%s\t\t%s\t%s\t%s\t%s\t%s\t%s\t%s\t%s\t%s\t%s\t%s\t%s\t%s\t%s\t\t\t\n','','(MPa)','(N/mm)','','(MPa)','
(N/mm)','','','','(mm)','','');
%polyfit the load-disp data, take the derivative of the equation, and
%determine the tangent (stiffness) at the desired strain.
for w=1:totfiles;
%  Write the stiffness data to a summary file called "Stiffness.xls"
   l=w;
fprintf(fid,'%s\t\t%f\t%f\t%f\t%f\t%f\t%f\t%f\t%f\t\n',names{l,2},EMod1vector(l),Stiffness1vector(l),RMo
dmax1vector(l),EMod2zvector(l),Stiffness2zvector(l),RModmax2vector(l),strainintersectvector(l));
end
fclose(fid);
fprintf(1,'\n\n%s\n\n','The ResultsSummary.xls file has been successfully generated.');
end
if decision3==2;
strainvectortrans=strainvector';
fid=fopen('Predictedstress.xls','wt');
```

```
fprintf(fid,'%s\t\t\t\t\t%s\n','Summary of Merlin Mechanical Testing Data',date);
fprintf(fid,'\n');
for z=1:size(names,1);
   fprintf(fid,'%s\t',names{z,2});
end
fprintf(fid,'\n');
fprintf(fid,'%s\t%s\n','Strain','Stress_MPa');
fprintf(fid,'\n');
for m=1:size(predictedstressmatrix,1);
   for y=1:size(predictedstressmatrix,2);
      fprintf(fid,'%f\t',predictedstressmatrix(m,y));
   end
   fprintf(fid,'\n');
end
fclose(fid);
fprintf(1,'\n\n%s\n\n','The Predictedstress.xls file has been successfully generated.');
fid=fopen('ResultsSummary.xls','wt');
fprintf(fid,'%s\t\t\t\t\t%s\n','Summary of Mechanical Testing Data',date);
fprintf(fid,'\n\n');
fprintf(fid,'%s\t\t%s\t%s\t%s\t%s\t%s\t%s\t%s\t%s\t%s\t%s\t%s\t%s\t%s\t%s\t\n','Sample_ID','EModulus','S
tiffness','R-
squared','EModLinearRange','StiffnessLinearRange','EModmidstrain','Stiffnessmidstrain','Emodhi
ghstrain','EModlowstrain','midstrain','highstrain','lowstrain');
fprintf(fid,'%s\t\t%s\t%s\t%s\t%s\t%s\t%s\t%s\t%s\t%s\t%s\t\t\t\t\t\n','','(MPa)','(N/mm)','','MPa','(N/mm)'
,'MPa','(N/mm)','MPa','MPa');
%polyfit the load-disp data, take the derivative of the equation, and
%determine the tangent (stiffness) at the desired strain.
for w=1:totfiles;
%  Write the stiffness data to a summary file called "ResultsSummary.xls"
   l=w;
fprintf(fid,'%s\t\t%f\t%f\t%f\t%f\t%f\t%f\t%f\t%f\t%f\t%f\t%f\t%f\t%f\t\n',names{l,2},EModvector(l),Stiffne
ssvector(l),Rsqvector(l),EModlinear4vector(l),Stiffnesslinear5vector(l),EModmidstrain(l),Stiffness
midstrain(l),EModhighstrain(l),EModlowstrain(l),midstrain(l),highstrain(l),lowstrain(l));
end
fclose(fid);
fprintf(1,'\n\n%s\n\n','The ResultsSummary.xls file has been successfully generated.');
end
```

Bibliography

1. Vitale MA, Vitale MG, Zivin JG, Braman JP, Bigliani LU, Flatow EL. Rotator cuff repair: an analysis of utility scores and cost-effectiveness. J Shoulder Elbow Surg 2007 Mar;16(2):181-7.

2. American Academy Orthopaedic Surgery. Number of Patients, Number of Procedures, Average Patient Age, Average Length of Stay -National Hospital Discharge Survey 1998- 2005. Data obtained from U.S.Department of Health and Human Services, Centers for Disease Control and Prevention, National Center for Health Statistics http://www.aaos.org/Research/stats/Rotator%20Cuff%20Repair.pdf. 2008.

3. Meislin RJ, Sperling JW, Stitik TP. Persistent shoulder pain: epidemiology, pathophysiology, and diagnosis. Am J Orthop (Belle Mead NJ) 2005 Dec;34(12 Suppl):5-9.

4. Tempelhof S. Age-related prevalance of rotator cuff tears in asymptomatic shoulders. J Shoulder Elbow Surg 1999;8(4):296-9.

5. Reilly P, Macleod I, Macfarlane R, Windley J, Emery RJ. Dead men and radiologists don't lie: a review of cadaveric and radiological studies of rotator cuff tear prevalence. Ann R Coll Surg Engl 2006 Mar;88(2):116-21.

6. Mehta S, Gimbel JA, Soslowsky LJ. Etiologic and pathogenetic factors for rotator cuff tendinopathy. [Review] [68 refs]. Clin Sports Med 2003 Oct;22(4):791-812.

7. Fukuda H. The Management of Partial-thickness Tears of the Rotator Cuff. The Journal of Bone and Joint Surgery 2003;85(B):3-11.

8. Rees JD, Wilson AM, Wolman RL. Current concepts in the management of tendon disorders. Rheumatology (Oxford) 2006 May;45(5):508-21.

9. Matava MJ, Purcell DB, Rudzki JR. Partial-thickness rotator cuff tears. Am J Sports Med 2005 Sep;33(9):1405-17.

10. Bartolozzi A, Andreychik D, Ahmad S. Determinants of outcome in the treatment of rotator cuff disease. Clin Orthop Rel Res 1994 Nov;308:90-7.

11. Cofield RH, Parvizi J, Hoffmeyer PJ, Lanzer WL, Ilstrup DM, Rowland CM. Surgical repair of chronic rotator cuff tears. A prospective long-term study. J Bone Jt Surg [Am] 2001 Jan;83-A(1):71-7.

12. Goutallier D, Postel JM, Gleyze P, Leguilloux P, Van Driessche S. Influence of cuff muscle fatty degeneration on anatomic and functional outcomes after simple suture of full-thickness tears. J Shoulder Elbow Surg 2003 Nov;12(6):550-4.

13. Hamada K, Tomonaga A, Gotoh M, Yamakawa H, Fukuda H. Intrinsic healing capacity and tearing process of torn supraspinatus tendons: in situ hybridization study of alpha 1 (I) procollagen mRNA. J Orthop Res 1997 Jan;15(1):24-32.

14. Iannotti JP. Full Thickness Rotator Cuff Tears: Factors Affecting Surgical Outcome. J Am Acad Orthop Surg 1994;2:87-95.

15. Riley GP, Harrall RL, Constant CR, Chard MD, Cawston TE, Hazleman BL. Tendon degeneration and chronic shoulder pain: changes in the collagen composition of the human rotator cuff tendons in rotator cuff tendinitis. Ann Rheum Dis 1994;53(6):359-66.

16. Romeo AA, Hang DW, Bach BR, Jr., Shott S. Repair of full thickness rotator cuff tears. Gender, age, and other factors affecting outcome. Clin Orthop Rel Res 1999 Oct;367:243-55.

17. Thomopoulos S, Soslowsky LJ, Flanagan CL, Tun S, Keefer CC, Mastaw J, et al. The effect of fibrin clot on healing rat supraspinatus tendon defects. J Shoulder Elbow Surg 2002;11(3):239-47.

18. Uhthoff HK, Trudel G, Himori K. Relevance of pathology and basic research to the surgeon treating rotator cuff disease. J Orthop Sci 2003;8(3):449-56.

19. Adams JE, Zobitz ME, Reach JS, Jr., An KN, Steinmann SP. Rotator cuff repair using an acellular dermal matrix graft: an in vivo study in a canine model. Arthroscopy 2006;22(7):700-9.

20. Coons DA, Alan BF. Tendon graft substitutes-rotator cuff patches. Sports Med Arthrosc 2006 Sep;14(3):185-90.

21. Derwin KA, Baker AR, Spragg RK, Leigh DR, Iannotti JP. Commercial extracellular matrix scaffolds for rotator cuff tendon repair. Biomechanical, biochemical, and cellular properties. J Bone Joint Surg [Am] 2006;88(12):2665-72.

22. Hodde J. Extracellular matrix as a bioactive material for soft tissue reconstruction. ANZ J Surg 2006 Dec;76(12):1096-100.

23. Whitlock PW, Smith TL, Poehling GG, Shilt JS, Van DM. A naturally derived, cytocompatible, and architecturally optimized scaffold for tendon and ligament regeneration. Biomaterials 2007 Oct;28(29):4321-9.

24. Barber FA, Aziz-Jacobo J. Biomechanical testing of commercially available soft-tissue augmentation materials. Arthroscopy 2009 Nov;25(11):1233-9.

25. Yokoya S, Mochizuki Y, Nagata Y, Deie M, Ochi M. Tendon-bone insertion repair and regeneration using polyglycolic acid sheet in the rabbit rotator cuff injury model. Am J Sports Med 2008 Jul;36(7):1298-309.

26. Moffat KL, Kwei AS, Spalazzi JP, Doty SB, Levine WN, Lu HH. Novel nanofiber-based scaffold for rotator cuff repair and augmentation. Tissue Eng Part A 2009 Jan;15(1):115-26.

27. Aoki M, Miyamoto S, Okamura K, Yamashita T, Ikada Y, Matsuda S. Tensile properties and biological response of poly(L-lactic acid) felt graft: an experimental trial for rotator-cuff reconstruction. J Biomed Mater Res B Appl Biomater 2004;71(2):252-9.

28. Derwin KA, Baker AR, Iannotti JP, McCarron JA. Pre-clinical models for translating regenerative medicine therapies for rotator cuff repair. Tissue Eng. In press 2009.

29. Koh JL, Szomor Z, Murrell GA, Warren RF. Supplementation of rotator cuff repair with a bioresorbable scaffold. Am J Sports Med 2002 May;30(3):410-3.

30. MacGillivray JD, Fealy S, Terry MA, Koh JL, Nixon AJ, Warren RF. Biomechanical evaluation of a rotator cuff defect model augmented with a bioresorbable scaffold in goats. J Shoulder Elbow Surg 2006 Sep;15(5):639-44.

31. Kimura A, Aoki M, Fukushima S, Ishii S, Yamakoshi K. Reconstruction of a defect of the rotator cuff with polytetrafluoroethylene felt graft. Recovery of tensile strength and histocompatibility in an animal model. J Bone Jt Surg [Br] 2003;85(2):282-7.

32. Funakoshi T, Majima T, Suenaga N, Iwasaki N, Yamane S, Minami A. Rotator cuff regeneration using chitin fabric as an acellular matrix. J Shoulder Elbow Surg 2006;15(1):112-8.

33. Funakoshi T, Majima T, Iwasaki N, Suenaga N, Sawaguchi N, Shimode K, et al. Application of tissue engineering techniques for rotator cuff regeneration using a chitosan-based hyaluronan hybrid fiber scaffold. Am J Sports Med 2005;33(8):1193-201.

34. Chen JM, Willers C, Xu J, Wang A, Zheng MH. Autologous tenocyte therapy using porcine-derived bioscaffolds for massive rotator cuff defect in rabbits. Tissue Eng 2007 Jul;13(7):1479-91.

35. Dejardin LM, Arnoczky SP, Clarke RB. Use of small intestinal submucosal implants for regeneration of large fascial defects: an experimental study in dogs. J Biomed Mater Res 1999 Aug;46(2):203-11.

36. Dejardin LM, Arnoczky SP, Ewers BJ, Haut RC, Clarke RB. Tissue-engineered rotator cuff tendon using porcine small intestine submucosa. Histologic and mechanical evaluation in dogs. Am J Sports Med 2001;29(2):175-84.

37. McAdams TR, Knudsen KR, Yalamanchi N, Chang J, Goodman SB. Deltoid flap combined with fascia lata autograft for rotator cuff defects: a histologic study. Knee Surg Sports Traumatol Arthrosc 2007 Sep;15(9):1144-9.

38. Nicholson GP, Breur GJ, Van SD, Yao JQ, Kim J, Blanchard CR. Evaluation of a cross-linked acellular porcine dermal patch for rotator cuff repair augmentation in an ovine model. J Shoulder Elbow Surg 2007 Sep;16(5 Suppl):S184-S190.

39. Perry SM, Gupta RR, Kleunen JV, Ramsey ML, Soslowsky LJ, Glaser DL. Use of small intestine submucosa in a rat model of acute and chronic rotator cuff tear. J Shoulder Elbow Surg 2007 Jul 11;15(5 Suppl):179-83.

40. Sano H, Kumagai J, Sawai T. Experimental fascial autografting for the supraspinatus tendon defect: remodeling process of the grafted fascia and the insertion into bone. J Shoulder Elbow Surg 2002;11(2):166-73.

41. Schlegel TF, Hawkins RJ, Lewis CW, Motta T, Turner AS. The effects of augmentation with Swine small intestine submucosa on tendon healing under tension: histologic and mechanical evaluations in sheep. Am J Sports Med 2006 Feb;34(2):275-80.

42. Zalavras CG, Gardocki R, Huang E, Stevanovic M, Hedman T, Tibone J. Reconstruction of large rotator cuff tendon defects with porcine small intestinal submucosa in an animal model. J Shoulder Elbow Surg 2006 Mar;15(2):224-31.

43. Zheng MH, Chen J, Kirilak Y, Willers C, Xu J, Wood D. Porcine small intestine submucosa (SIS) is not an acellular collagenous matrix and contains porcine DNA: possible implications in human implantation. J Biomed Mater Res B Appl Biomater 2005;73(1):61-7.

44. Derwin KA, Badylak SF, Steinmann SP, Iannotti JP. Extracellular matrix scaffold devices for rotator cuff repair. J Shoulder Elbow Surg 2010 Apr;19(3):467-76.

45. "How X-Repair Works." Synthasome. Web. 2009. 29 Nov 2010. http://www.synthasome.com/xRepair-technology.php

46. Badylak SF. The extracellular matrix as a scaffold for tissue reconstruction. Semin Cell Dev Biol 2002;13(5):377-83.

47. Hodde JP, Ernst DM, Hiles MC. An investigation of the long-term bioactivity of endogenous growth factor in OASIS Wound Matrix. J Wound Care 2005;14(1):23-5.

48. Hodde JP, Record RD, Liang HA, Badylak SF. Vascular endothelial growth factor in porcine-derived extracellular matrix. Endothelium 2001;8(1):11-24.

49. McDevitt CA, Wildey GM, Cutrone RM. Transforming growth factor-beta1 in a sterilized tissue derived from the pig small intestine submucosa. J Biomed Mater Res A 2003;67(2):637-40.

50. Reing JE, Zhang L, Myers-Irvin J, Cordero KE, Freytes DO, Heber-Katz E, et al. Degradation products of extracellular matrix affect cell migration and proliferation. Tissue Eng Part A 2009 Mar;15(3):605-14.

51. Voytik-Harbin SL, Brightman AO, Kraine MR, Waisner B, Badylak SF. Identification of extractable growth factors from small intestinal submucosa. J Cell Biochem 1997;67(4):478-91.

52. Metcalf MH, Savoie FH, III, Kellum B. Surgical technique for xenograft (SIS) augmentation of rotator-cuff repairs. Operative Techniques Orthop 2002;12(3):204-8.

53. Sclamberg SG, Tibone JE, Itamura JM, Kasraeian S. Six-month magnetic resonance imaging follow-up of large and massive rotator cuff repairs reinforced with porcine small intestinal submucosa. J Shoulder Elbow Surg 2004 Sep;13(5):538-41.

54. Iannotti JP, Codsi MJ, Kwon YW, Derwin K, Ciccone J, Brems JJ. Porcine small intestine submucosa augmentation of surgical repair of chronic two-tendon rotator cuff tears. A randomized, controlled trial. J Bone Jt Surg [Am] 2006 Jun;88(6):1238-44.

55. Walton JR, Bowman NK, Khatib Y, Linklater J, Murrell GA. Restore orthobiologic implant: not recommended for augmentation of rotator cuff repairs. J Bone Jt Surg [Am] 2007;89(4):786-91.

56. Malcarney HL, Bonar F, Murrell GA. Early inflammatory reaction after rotator cuff repair with a porcine small intestine submucosal implant: a report of 4 cases. Am J Sports Med 2005 Jun;33(6):907-11.

57. Dopirak R, Bond JL, Snyder SJ. Arthroscopic total rotator cuff replacement with an acellular human dermal allograft matrix. Intl J Shoulder Surg 2007;1(1):7-15.

58. Burkhead WZ, Schiffern SC, Krishnan SG. Use of GraftJacket as an augmentation for massive rotator cuff tears. Semin Arthoplasty 2007;(18):11-8.

59. Bond JL, Dopirak RM, Higgins J, Burns J, Snyder SJ. Arthroscopic replacement of massive, irreparable rotator cuff tears using a GraftJacket allograft: technique and preliminary results. Arthroscopy 2008 Apr;24(4):403-9.

60. Badhe SP, Lawrence TM, Smith FD, Lunn PG. An assessment of porcine dermal xenograft as an augmentation graft in the treatment of extensive rotator cuff tears. J Shoulder Elbow Surg 2008;17:35S-9S.

61. Soler JA, Gidwani S, Curtis MJ. Early complications from the use of porcine dermal collagen implants (Permacol) as bridging constructs in the repair of massive rotator cuff tears. A report of 4 cases. Acta Orthop Belg 2007 Aug;73(4):432-6.

62. Derwin KA, Baker AR, Spragg RK, Leigh DR, Farhat W, Iannotti JP. Regional variability, processing methods, and biophysical properties of human fascia lata extracellular matrix. J Biomed Materials Res, Part A 2008 Feb;84(2):500-7.

63. Aurora A, McCarron J, Iannotti JP, Derwin K. Commercially available extracellular matrix materials for rotator cuff repairs: state of the art and future trends. J Shoulder Elbow Surg 2007 Sep;16(5 Suppl):S171-S178.

64. Sikka RS, Neault M, Guanche CA. Reconstruction of the pectoralis major tendon with fascia lata allograft. Orthopedics 2005 Oct;28(10):1199-201.

65. Zielaskowski LA, Pontious J. Extensor hallucis longus tendon rupture repair using a fascia lata allograft. J Am Podiatr Med Assoc 2002 Sep;92(8):467-70.

66. Haas F, Seibert FJ, Koch H, Hubmer M, Moshammer HE, Pierer G, et al. Reconstruction of combined defects of the Achilles tendon and the overlying soft tissue with a fascia lata graft and a free fasciocutaneous lateral arm flap. Ann Plast Surg 2003 Oct;51(4):376-82.

67. Truncale KG, Depaula CA, Cartmell JS, Gocke DJ, Syring C, Von Versen R. Soft Tissue Processing. USA Patent Application 101885. 28 Sep 2006.

68. Fraser JR, Laurent TC, Laurent UB. Hyaluronan: its nature, distribution, functions and turnover. J Intern Med 1997 Jul;242(1):27-33.

69. Parkkinen JJ, Hakkinen TP, Savolainen S, Wang C, Tammi R, Agren UM, et al. Distribution of hyaluronan in articular cartilage as probed by a biotinylated binding region of aggrecan. Histochem Cell Biol 1996 Mar;105(3):187-94.

70. Tammi MI, Day AJ, Turley EA. Hyaluronan and homeostasis: a balancing act. Journal of Biological Chemistry 2002 Feb 15;277(7):4581-4.

71. Toole BP, Gross J. The extracellular matrix of the regenerating newt limb: synthesis and removal of hyaluronate prior to differentiation. Dev Biol 1971 May;25(1):57-77.

72. Cantor JO, Nadkarni PP. Hyaluronan: the Jekyll and Hyde molecule. Inflamm Allergy Drug Targets 2006 Dec;5(4):257-60.

73. Noble PW. Hyaluronan and its catabolic products in tissue injury and repair. Matrix Biol 2002;21(1):25-9.

74. Darr A, Calabro A. Synthesis and characterization of tyramine-based hyaluronan hydrogels. J Mater Sci Mater Med 2009 Jan;20(1):33-44.

75. Schimizzi AL, Massie JB, Murphy M, Perry A, Kim CW, Garfin SR, et al. High-molecular-weight hyaluronan inhibits macrophage proliferation and cytokine release in the early wound of a preclinical postlaminectomy rat model. Spine J 2006 Sep;6(5):550-6.

76. Nakamura K, Yokohama S, Yoneda M, Okamoto S, Tamaki Y, Ito T, et al. High, but not low, molecular weight hyaluronan prevents T-cell-mediated liver injury by reducing proinflammatory cytokines in mice. J Gastroenterol 2004;39(4):346-54.

77. Proctor M, Proctor K, Shu XZ, McGill LD, Prestwich GD, Orlandi RR. Composition of hyaluronan affects wound healing in the rabbit maxillary sinus. Am J Rhinol 2006 Mar;20(2):206-11.

78. Yasuda T. Hyaluronan inhibits cytokine production by lipopolysaccharide-stimulated U937 macrophages through down-regulation of NF-kappaB via ICAM-1. Inflamm Res 2007 Jun;56(6):246-53.

79. Sheehan KM, DeLott LB, West RA, Bonnema JD, DeHeer DH. Hyaluronic acid of high molecular weight inhibits proliferation and induces cell death in U937 macrophage cells. Life Sci 2004 Nov 12;75(26):3087-102.

80. Yasuda T. Hyaluronan inhibits prostaglandin E2 production via CD44 in U937 human macrophages. Tohoku J Exp Med 2010;220(3):229-35.

81. Akatsuka M, Yamamoto Y, Tobetto K, Yasui T, Ando T. In vitro effects of hyaluronan on prostaglandin E2 induction by interleukin-1 in rabbit articular chondrocytes. Agents Actions 1993 Jan;38(1-2):122-5.

82. Santangelo KS, Johnson AL, Ruppert AS, Bertone AL. Effects of hyaluronan treatment on lipopolysaccharide-challenged fibroblast-like synovial cells. Arthritis Res Ther 2007;9(1):R1.

83. Bernanke DH, Markwald RR. Effects of hyaluronic acid on cardiac cushion tissue cells in collagen matrix cultures. Tex Rep Biol Med 1979;39:271-85.

84. Docherty R, Forrester JV, Lackie JM, Gregory DW. Glycosaminoglycans facilitate the movement of fibroblasts through three-dimensional collagen matrices. J Cell Sci 1989 Feb;92 (Pt 2):263-70.

85. Goueffic Y, Guilluy C, Guerin P, Patra P, Pacaud P, Loirand G. Hyaluronan induces vascular smooth muscle cell migration through RHAMM-mediated PI3K-dependent Rac activation. Cardiovasc Res 2006 Nov 1;72(2):339-48.

86. Yagi M, Sato N, Mitsui Y, Gotoh M, Hamada T, Nagata K. Hyaluronan modulates proliferation and migration of rabbit fibroblasts derived from flexor tendon epitenon and endotenon. J Hand Surg Am 2010 May;35(5):791-6.

87. Tolg C, Hamilton SR, Nakrieko KA, Kooshesh F, Walton P, McCarthy JB, et al. Rhamm-/- fibroblasts are defective in CD44-mediated ERK1,2

motogenic signaling, leading to defective skin wound repair. J Cell Biol 2006 Dec 18;175(6):1017-28.

88. Chen WY, Abatangelo G. Functions of hyaluronan in wound repair. Wound Repair Regen 1999 Mar;7(2):79-89.

89. Kutty JK, Cho E, Soo LJ, Vyavahare NR, Webb K. The effect of hyaluronic acid incorporation on fibroblast spreading and proliferation within PEG-diacrylate based semi-interpenetrating networks. Biomaterials 2007 Nov;28(33):4928-38.

90. Longaker MT, Chiu ES, Adzick NS, Stern M, Harrison MR, Stern R. Studies in fetal wound healing. V. A prolonged presence of hyaluronic acid characterizes fetal wound fluid. Ann Surg 1991 Apr;213(4):292-6.

91. Goldberg VM, Buckwalter JA. Hyaluronans in the treatment of osteoarthritis of the knee: evidence for disease-modifying activity. Osteoarthritis Cartilage 2005 Mar;13(3):216-24.

92. Hagberg L, Gerdin B. Sodium hyaluronate as an adjunct in adhesion prevention after flexor tendon surgery in rabbits. J Hand Surg [Am] 1992 Sep;17(5):935-41.

93. Moro-oka T, Miura H, Mawatari T, Kawano T, Nakanishi Y, Higaki H, et al. Mixture of hyaluronic acid and phospholipid prevents adhesion formation on the injured flexor tendon in rabbits. J Orthop Res 2000 Sep;18(5):835-40.

94. Shu XZ, Ahmad S, Liu Y, Prestwich GD. Synthesis and evaluation of injectable, in situ crosslinkable synthetic extracellular matrices for tissue engineering. J Biomed Mater Res A 2006 Dec 15;79(4):902-12.

95. Hu M, Sabelman EE, Cao Y, Chang J, Hentz VR. Three-dimensional hyaluronic acid grafts promote healing and reduce scar formation in skin incision wounds. J Biomed Mater Res B Appl Biomater 2003 Oct 15;67(1):586-92.

96. Prestwich GD. Simplifying the extracellular matrix for 3-D cell culture and tissue engineering: a pragmatic approach. J Cell Biochem 2007 Aug 15;101(6):1370-83.

97. Allemann F, Mizuno S, Eid K, Yates KE, Zaleske D, Glowacki J. Effects of hyaluronan on engineered articular cartilage extracellular matrix gene expression in 3-dimensional collagen scaffolds. J Biomed Mater Res 2001 Apr;55(1):13-9.

98. Allison DD, Grande-Allen KJ. Review. Hyaluronan: a powerful tissue engineering tool. Tissue Eng 2006 Aug;12(8):2131-40.

99. Shu XZ, Liu Y, Luo Y, Roberts MC, Prestwich GD. Disulfide cross-linked hyaluronan hydrogels. Biomacromolecules 2002 Nov;3(6):1304-11.

100. Prestwich GD, Kuo JW. Chemically-modified HA for therapy and regenerative medicine. Curr Pharm Biotechnol 2008 Aug;9(4):242-5.

101. Tang S, Vickers SM, Hsu HP, Spector M. Fabrication and characterization of porous hyaluronic acid-collagen composite scaffolds. J Biomed Mater Res A 2007 Aug;82(2):323-35.

102. de WT, de PD, Tra WM, Rakhorst HA, van Osch GJ, Hovius SE, et al. Auto-crosslinked hyaluronic acid gel accelerates healing of rabbit flexor tendons in vivo. J Orthop Res 2009 Mar;27(3):408-15.

103. Brown AL, Srokowski EM, Shu XZ, Prestwich GD, Woodhouse KA. Development of a model bladder extracellular matrix combining disulfide cross-linked hyaluronan with decellularized bladder tissue. Macromol Biosci 2006 Aug 7;6(8):648-57.

104. Brown AL, Farhat W, Merguerian PA, Wilson GJ, Khoury AE, Woodhouse KA. 22 week assessment of bladder acellular matrix as a bladder augmentation material in a porcine model. Biomaterials 2002 May;23(10):2179-90.

105. Roth CC, Mondalek FG, Kibar Y, Ashley RA, Bell CH, Califano JA, et al. Bladder regeneration in a canine model using hyaluronic acid-poly(lactic-co-glycolic-acid) nanoparticle modified porcine small intestinal submucosa. BJU Int 2010 Oct 13.

106. Darr AB. Development of Tyramine-based Hyaluronan Hydrogels for the Repair of Focal Articular Cartilage Injuries. PhD Dissertation. Case Western Reserve University, Cleveland" ProQuest, 2008.

107. Brown BN, Valentin JE, Stewart-Akers AM, McCabe GP, Badylak SF. Macrophage phenotype and remodeling outcomes in response to biologic scaffolds with and without a cellular component. Biomaterials 2009 Mar;30(8):1482-91.

108. Badylak SF, Valentin JE, Ravindra AK, McCabe GP, Stewart-Akers AM. Macrophage Phenotype as a Determinant of Biologic Scaffold Remodeling. Tissue Eng Part A 2008 Nov;14(11):1835-42.

109. Anderson JM, Rodriguez A, Chang DT. Foreign body reaction to biomaterials. Semin Immunol 2008 Apr;20(2):86-100.

110. Anderson JM. Biological Responses to Materials. Annu Rev Mater Res 2001;31:81-110.

111. Snyder SJ, Arnoczky SP, Bond JL, Dopirak R. Histologic evaluation of a biopsy specimen obtained 3 months after rotator cuff augmentation with GraftJacket Matrix. Arthroscopy 2009 Mar;25(3):329-33.

112. Valentin JE, Badylak JS, McCabe GP, Badylak SF. Extracellular matrix bioscaffolds for orthopaedic applications. A comparative histologic study. J Bone Joint Surg [Am] 2006;88(12):2673-86.

113. Sandor M, Xu H, Connor J, Lombardi J, Harper JR, Silverman RP, et al. Host Response to Implanted Porcine-Derived Biologic Materials in a Primate Model of Abdominal Wall Repair. Tissue Eng Part A 2008 Jul 25.

114. Mantovani A, Sica A, Locati M. Macrophage polarization comes of age. Immunity 2005 Oct;23(4):344-6.

115. Mills CD, Kincaid K, Alt JM, Heilman MJ, Hill AM. M-1/M-2 macrophages and the Th1/Th2 paradigm. J Immunol 2000 Jun 15;164(12):6166-73.

116. Mosser DM. The many faces of macrophage activation. J Leukoc Biol 2003 Feb;73(2):209-12.

117. Mantovani A, Sica A, Sozzani S, Allavena P, Vecchi A, Locati M. The chemokine system in diverse forms of macrophage activation and polarization. Trends Immunol 2004 Dec;25(12):677-86.

118. Stout RD, Jiang C, Matta B, Tietzel I, Watkins SK, Suttles J. Macrophages sequentially change their functional phenotype in response to changes in microenvironmental influences. J Immunol 2005 Jul 1;175(1):342-9.

119. Stout RD, Suttles J. Immunosenescence and macrophage functional plasticity: dysregulation of macrophage function by age-associated microenvironmental changes. Immunol Rev 2005 Jun;205:60-71.

120. Badylak S, Kokini K, Tullius B, Simmons-Byrd A, Morff R. Morphologic study of small intestinal submucosa as a body wall repair device. J Surg Res 2002;103(2):190-202.

121. Cook JL, Fox DB, Kuroki K, Jayo M, De Deyne PG. In vitro and in vivo comparison of five biomaterials used for orthopedic soft tissue augmentation. Am J Vet Res 2008 Jan;69(1):148-56.

122. Konstantinovic ML, Lagae P, Zheng F, Verbeken EK, De RD, Deprest JA. Comparison of host response to polypropylene and non-cross-linked porcine small intestine serosal-derived collagen implants in a rat model. BJOG 2005 Nov;112(11):1554-60.

123. Thomsen P, Bjursten LM, Ericson LE. Implants in the abdominal wall of the rat. Scand J Plast Reconstr Surg 1986;20(2):173-82.

124. Zheng F, Lin Y, Verbeken E, Claerhout F, Fastrez M, De RD, et al. Host response after reconstruction of abdominal wall defects with porcine dermal collagen in a rat model. Am J Obstet Gynecol 2004 Dec;191(6):1961-70.

125. Kidd KR, Dal Ponte DB, Kellar RS, Williams SK. A comparative evaluation of the tissue responses associated with polymeric implants in the rat and mouse. J Biomed Mater Res 2002 Mar 15;59(4):682-9.

126. Laschke MW, Haufel JM, Thorlacius H, Menger MD. New experimental approach to study host tissue response to surgical mesh materials in vivo. J Biomed Mater Res A 2005 Sep 15;74(4):696-704.

127. Petillo O, Peluso G, Ambrosio L, Nicolais L, Kao WJ, Anderson JM. In vivo induction of macrophage Ia antigen (MHC class II) expression by biomedical polymers in the cage implant system. J Biomed Mater Res 1994 May;28(5):635-46.

128. Marchant RE. The cage implant system for determining in vivo biocompatibility of medical device materials. Fundam Appl Toxicol 1989 Aug;13(2):217-27.

129. Peron JM, Danjoux M, Kamar N, Missoury R, Poirson H, Vinel JP, et al. Liver histology in patients with sporadic acute hepatitis E: a study of 11 patients from South-West France. Virchows Arch 2007 Apr;450(4):405-10.

130. ISO10993-6. Biological evaluation of medical devices-Part 6:Tests for local effects after implantation. Arlington, VA:, American National Standards Institute.

131. Arnoczky SP, Lavagnino M, Egerbacher M, Caballero O, Gardner K. Matrix metalloproteinase inhibitors prevent a decrease in the mechanical properties of stress-deprived tendons: an in vitro experimental study. Am J Sports Med 2007 May;35(5):763-9.

132. Webster NL, Crowe SM. Matrix metalloproteinases, their production by monocytes and macrophages and their potential role in HIV-related diseases. J Leukoc Biol 2006 Nov;80(5):1052-66.

133. MacLauchlan S, Skokos EA, Meznarich N, Zhu DH, Raoof S, Shipley JM, et al. Macrophage fusion, giant cell formation, and the foreign body response require matrix metalloproteinase 9. J Leukoc Biol 2009 Apr;85(4):617-26.

134. Colombat M, Caudroy S, Lagonotte E, Mal H, Danel C, Stern M, et al. Pathomechanisms of cyst formation in pulmonary light chain deposition disease. Eur Respir J 2008 Nov;32(5):1399-403.

135. Woo SLY, An KN, Frank CB, Livesay GA, Ma CB, Zeminski J, et al. Anatomy, Biology, and Biomechanics of Tendon and Ligament. In: Buckwalter J, Einhorn T, Simon S, editors. Orthopaedic Basic Science: Biology and Biomechanics of the Musculoskeletal System. 2nd ed. Rosemont, IL: American Academy of Orthopaedic Surgeons; 2000. p. 581-616.

136. Hansen KA, Weiss JA, Barton JK. Recruitment of tendon crimp with applied tensile strain. J Biomech Engin 2002;124(1):72-7.

137. Lake SP, Miller KS, Elliott DM, Soslowsky LJ. Effect of fiber distribution and realignment on the nonlinear and inhomogeneous mechanical properties of human supraspinatus tendon under longitudinal tensile loading. J Orthop Res 2009 Dec;27(12):1596-602.

138. Eshel H, Lanir Y. Effects of strain level and proteoglycan depletion on preconditioning and viscoelastic responses of rat dorsal skin. Ann Biomed Eng 2001 Feb;29(2):164-72.

139. Screen HR, Chhaya VH, Greenwald SE, Bader DL, Lee DA, Shelton JC. The influence of swelling and matrix degradation on the microstructural integrity of tendon. Acta Biomater 2006 Sep;2(5):505-13.

140. Elden HR. Hydration of connective tissue and tendon elasticity. Biochim Biophys Acta 1964 May 25;79:592-9.

141. Netti P, 'Amore A, Ronca D, Ambrosio L, Nicolais L. Structure-mechanical properties relationship of natural tendons and ligaments. Journal of Materials Science: Materials in Medicine 1996;7:525-30.

142. Nettelbladt O, Bergh J, Schenholm M, Tengblad A, Hallgren R. Accumulation of hyaluronic acid in the alveolar interstitial tissue in bleomycin-induced alveolitis. Am Rev Respir Dis 1989 Mar;139(3):759-62.

143. Bjermer L, Engstrom-Laurent A, Lundgren R, Rosenhall L, Hallgren R. Hyaluronate and type III procollagen peptide concentrations in bronchoalveolar lavage fluid as markers of disease activity in farmer's lung. Br Med J (Clin Res Ed) 1987 Oct 3;295(6602):803-6.

144. Atkinson TS, Ewers BJ, Haut RC. The tensile and stress relaxation responses of human patellar tendon varies with specimen cross-sectional area. J Biomech 1999 Sep;32(9):907-14.

145. Calabro A, Benavides M, Tammi M, Hascall VC, Midura RJ. Microanalysis of enzyme digests of hyaluronan and chondroitin/dermatan sulfate by fluorophore-assisted carbohydrate electrophoresis (FACE). Glycobiology 2000;10(3):273-81.

146. Rost FWD. Fluorescence microscopy. Cambridge: Cambridge University Press; 1995.

147. Lin W, Shuster S, Maibach HI, Stern R. Patterns of hyaluronan staining are modified by fixation techniques. J Histochem Cytochem 1997 Aug;45(8):1157-63.

148. Bayrak A, Tyralla M, Ladhoff J, Schleicher M, Stock UA, Volk HD, et al. Human immune responses to porcine xenogeneic matrices and their extracellular matrix constituents in vitro. Biomaterials 2010 May;31(14):3793-803.

149. Shirley SF, Little JR. Immunopotentiating effects of amphotericin B. II. Enhanced in vitro proliferative responses of murine lymphocytes. J Immunol 1979 Dec;123(6):2883-9.

150. Vonk AG, Netea MG, Denecker NE, Verschueren IC, van der Meer JW, Kullberg BJ. Modulation of the pro- and anti-inflammatory cytokine balance by amphotericin B. J Antimicrob Chemother 1998 Oct;42(4):469-74.

151. Fox A, Harrison LC. Innate immunity and graft rejection. Immunol Rev 2000 Feb;173:141-7.

152. Tauro JC, Parsons JR, Ricci J, Alexander H. Comparison of bovine collagen xenografts to autografts in the rabbit. Clin Orthop Rel Res 1991 May;(266):271-84.

153. Badylak SF, Gilbert TW. Immune response to biologic scaffold materials. Semin Immunol 2008 Apr;20(2):109-16.

154. Tammi MI, Day AJ, Turley EA. Hyaluronan and homeostasis: a balancing act. J Biol Chem 2002 Feb 15;277(7):4581-4.

155. Allman AJ, McPherson TB, Badylak SF, Merrill LC, Kallakury B, Sheehan C, et al. Xenogeneic extracellular matrix grafts elicit a TH2-restricted immune response. Transplantation 2001;71(11):1631-40.

156. Xu H, Wan H, Sandor M, Qi S, Ervin F, Harper JR, et al. Host Response to Human Acellular Dermal Matrix Transplantation in a Primate Model of Abdominal Wall Repair. Tissue Eng Part A 2008 Jul 1.

157. Pinkowski JL, Reiman PR, Chen SL. Human lymphocyte reaction to freeze-dried allograft and xenograft ligamentous tissue. Am J Sports Med 1989 Sep;17(5):595-600.

158. Dorling A, Lombardi G, Binns R, Lechler RI. Detection of primary direct and indirect human anti-porcine T cell responses using a porcine dendritic cell population. Eur J Immunol 1996 Jun;26(6):1378-87.

159. Yang YG, Sykes M. Xenotransplantation: current status and a perspective on the future. Nat Rev Immunol 2007 Jul;7(7):519-31.

160. Lindholm A, Roneus B, Lindblad G, Jones B. Hyaluronan turnover in the synovial fluid in metacarpophalangeal--and middle carpal joints in standardbred horses. Acta Vet Scand 1996;37(2):147-51.

161. Lauer ME, Fulop C, Mukhopadhyay D, Comhair S, Erzurum SC, Hascall VC. Airway smooth muscle cells synthesize hyaluronan cable structures independent of inter-alpha-inhibitor heavy chain attachment. J Biol Chem 2009 Feb 20;284(8):5313-23.

162. Zhuo L, Kanamori A, Kannagi R, Itano N, Wu J, Hamaguchi M, et al. SHAP potentiates the CD44-mediated leukocyte adhesion to the hyaluronan substratum. J Biol Chem 2006 Jul 21;281(29):20303-14.

163. Badylak SF, Freytes DO, Gilbert TW. Extracellular matrix as a biological scaffold material: Structure and function. Acta Biomater 2009 Jan;5(1):1-13.

164. Shu XZ, Ghosh K, Liu Y, Palumbo FS, Luo Y, Clark RA, et al. Attachment and spreading of fibroblasts on an RGD peptide-modified injectable hyaluronan hydrogel. J Biomed Mater Res A 2004 Feb 1;68(2):365-75.

165. Wallet MA, Wallet SM, Guiulfo G, Sleasman JW, Goodenow MM. IFNgamma primes macrophages for inflammatory activation by high molecular weight hyaluronan. Cell Immunol 2010;262(2):84-8.

166. Savani RC, Hou G, Liu P, Wang C, Simons E, Grimm PC, et al. A role for hyaluronan in macrophage accumulation and collagen deposition after bleomycin-induced lung injury. Am J Respir Cell Mol Biol 2000 Oct;23(4):475-84.

167. Jokela TA, Lindgren A, Rilla K, Maytin E, Hascall VC, Tammi RH, et al. Induction of hyaluronan cables and monocyte adherence in epidermal keratinocytes. Connect Tissue Res 2008;49(3):115-9.

168. Lemperle G, Morhenn V, Charrier U. Human histology and persistence of various injectable filler substances for soft tissue augmentation. Aesthetic Plast Surg 2003 Sep;27(5):354-66.

169. Al-Shraim M, Jaragh M, Geddie W. Granulomatous reaction to injectable hyaluronic acid (Restylane) diagnosed by fine needle biopsy. J Clin Pathol 2007 Sep;60(9):1060-1.

170. Flatow EL, Nasser P, Lee L, Schaffler MB, Jepsen KL. Overestimation of the Degradation State in Fatigue Loaded Tendon due to Transient Effects [abstract]. In: Proceedings of the 48th Annual Meeting of the Orthopaedic Research Society; 2002 Feb 10-12; Dallas. Poster No 621.

171. Lin TW, Cardenas L, Soslowsky LJ. Tendon properties in interleukin-4 and interleukin-6 knockout mice. J Biomech 2005 Jan;38(1):99-105.

172. Duenwald SE, Vanderby R, Jr., Lakes RS. Viscoelastic relaxation and recovery of tendon. Ann Biomed Eng 2009 Jun;37(6):1131-40.

173. Roberts JM, Goldstrohm GL, Brown TD, Mears DC. Comparison of unrepaired, primarily repaired, and polyglactin mesh-reinforced Achilles tendon lacerations in rabbits. Clin Orthop Relat Res 1983 Dec;(181):244-9.

174. Yildirim Y, Kara H, Cabukoglu C, Esemenli T. Suture holding capacity of the Achilles tendon during the healing period: an in vivo experimental study in rabbits. Foot Ankle Int 2006 Feb;27(2):121-4.

175. Bey MJ, Ramsey ML, Soslowsky LJ. Intratendinous strain fields of the supraspinatus tendon: effect of a surgically created articular-surface rotator cuff tear. Journal of Shoulder & Elbow Surgery 2002 Nov;11(6):562-9.

176. Maganaris CN, Paul JP. In vivo human tendon mechanical properties. J Physiol 1999 Nov 15;521 Pt 1:307-13.

177. Comper WD, Laurent TC. Physiological function of connective tissue polysaccharides. Physiol Rev 1978 Jan;58(1):255-315.

178. Day AJ, De La Motte CA. Hyaluronan cross-linking: a protective mechanism in inflammation? Trends Immunol 2005 Dec;26(12):637-43.

179. Walter AJ, Morse AN, Leslie KO, Zobitz ME, Hentz JG, Cornella JL. Changes in tensile strength of cadaveric human fascia lata after implantation in a rabbit vagina model. J Urol 2003 May;169(5):1907-10.

180. Akmal M, Singh A, Anand A, Kesani A, Aslam N, Goodship A, et al. The effects of hyaluronic acid on articular chondrocytes. J Bone Joint Surg Br 2005 Aug;87(8):1143-9.

181. Kawasaki K, Ochi M, Uchio Y, Adachi N, Matsusaki M. Hyaluronic acid enhances proliferation and chondroitin sulfate synthesis in cultured chondrocytes embedded in collagen gels. J Cell Physiol 1999 May;179(2):142-8.

182. Gilbert TW, Stewart-Akers AM, Badylak SF. A quantitative method for evaluating the degradation of biologic scaffold materials. Biomaterials 2007 Jan;28(2):147-50.

183. Klein L, Lewis JA. Simultaneous quantification of 3 H-collagen loss and 1 H-collagen replacement during healing of rat tendon grafts. J Bone Joint Surg Am 1972 Jan;54(1):137-46.

184. O'Grady RL, Nethery A, Hunter N. A fluorescent screening assay for collagenase using collagen labeled with 2-methoxy-2,4-diphenyl-3(2H)-furanone. Anal Biochem 1984 Aug 1;140(2):490-4.

185. Bergdoll AS, Song F, Windor LJ. Media and Cell Mediated Fluorescent Collagen Degradation [abstract]. In: Proceedings of the 85th General Session and Exhibition of the International Association for Dental Research; 2007 Mar 21-24; New Orleans. Abstract No 678.

186. Semwogerere D, Weeks ER. Confocal Microscopy. In: Encyclopedia of Bf Biomaterials and Biomedical Engineering. Bowlin GL, Wnek G, editors. Abingdon: Taylor & Francis; 2005.

187. Klinge U, Si ZY, Zheng H, Schumpelick V, Bhardwaj RS, Klosterhalfen B. Collagen I/III and matrix metalloproteinases (MMP) 1 and 13 in the fascia of patients with incisional hernias. J Invest Surg 2001 Jan;14(1):47-54.

188. Valentin JE, Turner NJ, Gilbert TW, Badylak SF. Functional skeletal muscle formation with a biologic scaffold. Biomaterials 2010 Oct;31(29):7475-84.

189. Abramowitch SD, Woo SL. An improved method to analyze the stress relaxation of ligaments following a finite ramp time based on the quasi-linear viscoelastic theory. J Biomech Eng 2004 Feb;126(1):92-7.

190. Abramowitch SD, Woo SL, Clineff TD, Debski RE. An evaluation of the quasi-linear viscoelastic properties of the healing medial collateral ligament in a goat model. Ann Biomed Eng 2004 Mar;32(3):329-35.

191. Abreu EL, Leigh D, Derwin KA. Effect of altered mechanical load conditions on the structure and function of cultured tendon fascicles. J Orthop Res 2008 Mar;26(3):364-73.

192. Cesaretti M, Luppi E, Maccari F, Volpi N. A 96-well assay for uronic acid carbazole reaction. Carbohydrate Polymers 2003;54:59-61.

193. Blumenkrantz N, Asboe-Hansen G. New method for quantitative determination of uronic acids. Anal Biochem 1973 Aug;54(2):484-9.